

Characterization of a Full-Length TTP Family Member Association with RNA Sequence  
Elements

by

Onica Leigh Washington

Department of Biochemistry  
Duke University

Date: \_\_\_\_\_

Approved:

\_\_\_\_\_  
Perry Blackshear, Co-Supervisor

\_\_\_\_\_  
Richard Brennan, Co-Supervisor

\_\_\_\_\_  
Andrew Alspaugh

\_\_\_\_\_  
Michael Been

\_\_\_\_\_  
Arno Greenleaf

\_\_\_\_\_  
Kenneth Kreuzer

Dissertation submitted in partial fulfillment of  
the requirements for the degree of Doctor  
of Philosophy in the Department of  
Biochemistry in the Graduate School  
of Duke University

2016

ABSTRACT

Characterization of a Full-Length TTP Family Member Association with RNA Sequence Elements

by

Onica Leigh Washington

Department of Biochemistry  
Duke University

Date: \_\_\_\_\_

Approved:

\_\_\_\_\_  
Perry Blackshear, Chair

\_\_\_\_\_  
Richard Brennan, Co-Chair

\_\_\_\_\_  
Andrew Alspaugh

\_\_\_\_\_  
Michael Been

\_\_\_\_\_  
Arno Greenleaf

\_\_\_\_\_  
Kenneth Kreuzer

An abstract of a dissertation submitted in partial fulfillment of the requirements for the degree of Doctor of Philosophy in the Department of Biochemistry in the Graduate School of Duke University

2016

Copyright by  
Onica Leigh Washington  
2016

## Abstract

Post-transcriptional regulation of cytoplasmic mRNAs is an efficient mechanism of regulating the amounts of active protein within a eukaryotic cell. RNA sequence elements located in the untranslated regions of mRNAs can influence transcript degradation or translation through associations with RNA-binding proteins. Tristetraprolin (TTP) is the best known member of a family of CCCH zinc finger proteins that targets adenosine-uridine rich element (ARE) binding sites in the 3' untranslated regions (UTRs) of mRNAs, promoting transcript deadenylation through the recruitment of deadenylases. More specifically, TTP has been shown to bind AREs located in the 3'-UTRs of transcripts with known roles in the inflammatory response. The mRNA-binding region of the protein is the highly conserved CCCH tandem zinc finger (TZF) domain. Studies have shown that TTP binds to the minimal 7-mer binding site, UAUUUAU. The synthetic TTP TZF domain has been shown to bind with high affinity to the 13-mer sequence of UUUUAUUUAUUUU. However, the binding affinities of full-length TTP family members to the same sequence and its variants are unknown. Furthermore, the distance needed between two overlapping or neighboring UUAUUUAUU 9-mers for tandem binding events of a full-length TTP family member to a target transcript has not been explored. To address these questions, we recombinantly expressed and purified the full-length *C. albicans* TTP family member Zfs1. Using full-

length Zfs1, tagged at the N-terminus with maltose binding protein (MBP), we determined the binding affinities of the protein to the optimal TTP binding sequence, UUAUUUAUU. Fluorescence anisotropy experiments determined that the binding affinities of MBP-Zfs1 to non-canonical AREs were influenced by ionic buffer strength, suggesting that transcript selectivity may be affected by intracellular conditions. Furthermore, electrophoretic mobility shift assays (EMSAs) revealed that separation of two core AUUUA sequences by two uridines (or two 7-mer binding sites separated by no uridines) is sufficient for tandem binding of MBP-Zfs1. Finally, we found evidence for tandem binding of MBP-Zfs1 to a 27-base RNA oligonucleotide containing only a single ARE-binding site, and showed that this was concentration and RNA length dependent; this phenomenon had not been seen previously. These data suggest that the association of the TTP TZF domain and the TZF domains of other species, to ARE-binding sites is highly conserved. Domains outside of the TZF domain may mediate transcript selectivity in changing cellular conditions, and promote protein-RNA interactions not associated with the ARE-binding TZF domain.

In summary, the evidence presented here suggests that Zfs1-mediated decay of mRNA targets may require additional interactions, in addition to ARE-TZF domain associations, to promote transcript destabilization and degradation. These studies further our understanding of post-transcriptional steps in gene regulation.



## **Dedication**

I dedicate this thesis to all those on whose shoulders I stand. I also dedicate this thesis to my loving family and to my wonderful husband, Matt.

# Contents

Abstract .....	iv
Contents.....	viii
List of Tables.....	xiii
List of Figures .....	xiv
List of Abbreviations .....	xvi
Acknowledgements .....	xviii
1. Introduction.....	1
1.1 mRNA Turnover as a Regulatory Mechanism of Gene Expression in Eukaryotes .....	1
1.2 Mechanisms of mRNA Turnover .....	2
1.3 Notable 3'-UTR RNA-Binding Proteins and Their Effects on mRNA Stability..	5
1.4 Characterization of 3'-UTR Adenosine-Uridine Rich Elements (AREs).....	9
1.5 The Tristetraprolin Family .....	11
1.6 Fungal TTP Family Members.....	16
1.6.1. <i>S. pombe</i> 's TTP family member, Zfs1 .....	17
1.6.2. <i>S. cerevisiae</i> 's TTP family members, Cth1 and Cth2 .....	19
1.7 The TZF Domain and Its High-Affinity Binding to Target Binding Sites .....	24
1.7.1 The TZF Domain is Functionally Conserved .....	30
1.7.2 Characteristics of Target Binding Sites Within AREs .....	32
1.8 Aim of Research.....	37

2. Post-transcriptional Regulation of Transcript Abundance by a Conserved Member of the Tristetraprolin Family in <i>C. albicans</i> .....	39
2.1 Introduction.....	39
2.2 Materials and Methods .....	43
2.2.1 Plasmid Construction and Protein Purification of Recombinant MBP-tagged Full-Length Zfs1 .....	43
2.2.2 Preparation of RNA Substrates for Biochemical Assays .....	44
2.2.3 RNA Electrophoretic Mobility Gel Shift (EMSA) .....	45
2.2.4 Fluorescence Anisotropy.....	45
2.3 Results .....	47
2.3.1 Expression and Purification of Recombinant MBP-tagged Full-Length Zfs1... ..	47
2.3.2 Characteristics of Binding of MBP-tagged Full-Length Zfs1 to an RNA Oligonucleotide Containing a Single Binding Site .....	49
2.4 Discussion.....	52
3. Full-length <i>C. albicans</i> Tristetraprolin Family Member, Zfs1, Binds to Non-Canonical AREs.....	55
3.1 Introduction.....	55
3.2 Materials and Methods .....	58
3.2.1 Plasmid Construction and Protein Purification.....	58
3.2.1.A. Double selection of high-expressing clones for optimal protein expression .....	58
3.2.2 Preparation of RNA Substrates for Biochemical Assays .....	59
3.2.3 RNA Electrophoretic Mobility Gel Shift (EMSA) .....	59

3.2.4	Fluorescence Anisotropy.....	59
3.3	Results .....	61
3.3.1	Binding Affinities of MBP-Zfs1 to Non-Canonical TTP Family Member Binding Sites are Affected by Buffer Ionic Salt Concentrations.....	61
3.4	Discussion.....	64
4.	Characteristics of Binding of MBP-tagged, <i>Candida albicans</i> Full-Length Zfs1 to RNA Probes Containing Double and Overlapping ARE-Binding Sites.....	67
4.1	Introduction.....	67
4.2	Materials and Methods.....	72
4.2.1	Preparation of RNA Substrates for Biochemical Assays .....	73
4.2.2	Plasmid Construction and Protein Purification.....	73
4.2.3	RNA Electrophoretic Mobility Gel Shift (EMSA).....	73
4.2.3.A.	EMSA quantification .....	73
4.2.4	Fluorescence Anisotropy.....	74
4.3	Results .....	74
4.3.1	Transition from One to Two Binding Events of MBP-Zfs1 to RNA Oligonucleotides Containing TTP Family Member Binding Sites Determined by EMSAs.....	74
4.4	Discussion.....	82
5.	Evidence for Binding of Two Molecules of MBP-Zfs1 to Oligonucleotides Containing a Single 9-mer Binding Site.....	85
5.1	Introduction.....	85
5.2	Materials and Methods.....	88
5.2.1	Expression and Purification of MBP-tagged Full-Length Zfs1.....	88

5.2.2	RNA Electrophoretic Mobility Gel Shift (EMSA) .....	88
5.2.3	Analytical Gel Filtration .....	88
5.2.4	Size Exclusion Chromatography Coupled to Multi-Angle Light Scattering (SEC-MALS) .....	90
5.3	Results .....	91
5.3.1	The Binding of MBP-Zfs1 to a 27-mer Oligonucleotide Containing One ARE-Binding Site and a 13-mer Oligonucleotide Containing One ARE-Binding Site Generates Two Protein: RNA Complexes.....	91
5.3.2	Size Exclusion Chromatography and SEC-MALS Assays Report Dimerization of MBP-Zfs1 in the Presence of a 27-mer RNA Oligonucleotide Containing a Single ARE-Binding Site .....	93
5.4	Discussion.....	100
6.	Conclusion.....	103
	Appendix.....	105
7.	Crystallographic Determination of the <i>Candida albicans</i> Zfs1-RNA complex and the use of Biochemical Studies to Help Elucidate Zfs1 Protein Partners.....	105
7.1	Introduction.....	105
7.2	Materials and methods .....	107
7.2.1	Expression and Purification of MBP tagged Full-Length Zfs1 and MBP tagged Zfs1 TZF domain .....	107
7.2.1.A.	Plasmid construction and protein purification of MBP tagged full-length Zfs1	107
7.2.1.B.	Plasmid construction and purification of <i>C. albicans</i> MBP-Zfs1-TZF domain.....	107
7.2.1.C.	Plasmid construction and protein purification of 6xHis-Zfs1 .....	109
7.2.2	Setup of Protein Crystallization Experiments .....	110

7.2.3	Production and Testing of Antibodies to 6xHis-Zfs1.....	110
7.2.4	Pull-Down Assays using MBP-Zfs1 and <i>C. albicans</i> Clarified Lysates .....	111
7.3	Results .....	113
7.3.1	Crystallization Trials of MBP-Zfs1 and MBP-Zfs1-TZF domain.....	113
7.3.2	Determination of Zfs1 Protein Partners .....	115
7.4	Discussion.....	119
8.	Deviation of Equation 1 (Chapter 3) .....	122
	References .....	123
	Biography.....	136

## List of Tables

<b>Table 1. Equilibrium Binding of MBP-Zfs1 to Variant Class I AREs as Compared to the TTP TZF domain Synthetic Peptide (TTP73) (68) .....</b>	<b>62</b>
<b>Table 2. Biotinylated Probes Containing One, Overlapping, and Two Separated ARE Sites.....</b>	<b>75</b>
<b>Table 3. Binding Constants and Hill Coefficients of MBP-Zfs1 bound to RNA containing a single or two binding sites. ....</b>	<b>79</b>
<b>Table 4. Equilibrium Binding Constants MBP-Zfs1 to RNA Oligonucleotides Containing One, Overlapping, and Two Separated ARE Sites .....</b>	<b>81</b>
<b>Table 5. SEC-MALS Calculated Molecular Weights of Protein-RNA Complexes .....</b>	<b>100</b>

## List of Figures

<b>Figure 1. mRNA Steady-State Levels Reflect a Balance of Synthesis and Degradation of Transcripts</b> .....	3
<b>Figure 2. The Stabilizing and Destabilizing Effects of ARE-binding Proteins on mRNA</b> .....	11
<b>Figure 3. TTP and its Family Members Contain a Novel Zinc Finger Domain.</b> .....	12
<b>Figure 4. Sequence Alignment of Fungal TTP Family Members</b> .....	23
<b>Figure 5. Sequence Alignment of the TZF Domains from TTP and other Mammalian and Non-Mammalian TTP Family Members</b> .....	25
<b>Figure 6. Structure of the TZF domain of ZFP36L2 associated with a 9-mer RNA containing a single binding site (65)</b> .....	27
<b>Figure 7. EMSA Demonstrates the Minimal Binding Sequence Needed for the TTP TZF Domain</b> .....	35
<b>Figure 8. Purified MBP-tagged Full-Length Zfs1 at Amounts of 2, 4, and 8 µg</b> .....	49
<b>Figure 9. Measurement of MBP-Zfs1 RNA-Binding Affinity Using Fluorescence Anisotropy</b> .....	51
<b>Figure 10. EMSA Demonstrates Transition from Single to Tandem Binding Events of MBP-Zfs1 to ARE-Binding Sites Containing Overlapping UUAUUUAUU (9-mer) Sequences</b> .....	76
<b>Figure 11. Fluorescent Anisotropy Studies Reveals No Cooperative Binding of MBP-Zfs1 to Probes Containing One or Two Binding Sites</b> .....	78
<b>Figure 12. Calibration Curve of Superdex 200 10/30 Using Standard Proteins</b> .....	89
<b>Figure 13. Detection of Multiple MBP-Zfs1:RNA Species Using EMSAs</b> .....	92
<b>Figure 14. MBP-Zfs1 Does Not Bind to a 27-mer RNA Oligonucleotide Containing a Poly(U) Sequence</b> .....	93



## List of Abbreviations

AREs	AU-Rich elements, adenosine-uridine rich elements
cryo-EM	Cryo-electron microscopy
EMSA	Electrophoretic mobility shift assay
GM-CSF	Granulocyte Macrophage-Colony Stimulating Factor
ITC	Isothermal Titration Calorimetry
MBP	Maltose Binding Protein
mRNA	Messenger Ribonucleic Acid
miRNAs	Micro Ribonucleic Acids
MWCO	Molecular weight cut off
NMD	Nonsense-mediated decay
NMR	Nuclear Magnetic Resonance
nt	Nucleotide
PARN	Poly(A)-specific exoribonuclease
SAXS	Small-angle X-ray scattering
SEC-MALS	Size Exclusion Chromatography coupled to Multi-Angle Light Scattering
TNF $\alpha$	Tumor Necrosis Factor alpha
TTP	Tristetraprolin
TZF domain	Tandem Zinc Finger Domain

UTR

Untranslated Region

## Acknowledgements

First, I would like to thank my advisor, Perry Blackshear, for his mentorship and guidance. Perry has trained me to think critically and to be able to more effectively communicate my scientific ideas to those around me. Also, I would like to thank my wonderful committee: Dr. Richard Brennan, Dr. Michael Been, Dr. Andrew Alspaugh, Dr. Arno Greenleaf, and Dr. Kenneth Kreuzer. They all have guided me in my thesis project, and helped me develop into a more confident scientist.

I am truly grateful for the help and guidance of all Blackshear lab members, past and present. I especially want to acknowledge Dr. Stephanie Hicks and Dr. Melissa Wells for their support, mentorship, and helping me through the “awkward” graduate student phase. I am truly a wiser person because of Steph and Melissa. To Wi Lai, Lianqun Qui, Sonika Patial, Franzi Bollmann, Debbie Stumpo, and Timothy Gingerich, for all of their scientific advice and for making the lab fun.

I am grateful for several wonderful people at the National Institute of Environmental Health Sciences. I would like to thank Dr. Ron Cannon of the National Institutes of Environmental Health Sciences for all his insightful advice on my project and for his advice. To Dr. Lars Pedersen and Dr. Andrea Moon (NIEHS) for their help in my crystallization experiments and providing the pMALx vector that made my project possible. Thank you to Dr. Robin Stanley, Dr. Traci Hall, and their groups for the help

they provided for size exclusion chromatography and multi-angle light scattering experiments. I also want to thank, Dr. Lalith Perea (NIEHS), for his modeling work of my protein.

Finally, I would like to thank my family and friends. Thank you, Mommy, Daddy, and Olivia, for all your love and support. Thank you, Dad (Mr. Moore) and Mike for accepting me into your family, and for all your love and support as well. Thanks to my girlfriends, Pamela Mosley, Shanen Sherrer, Tammi Wood, and Shonda Carson, for all the good times and good memories. I want to especially thank my first science mentors, my Father, Mrs. Nancy James, Dr. Pamela Riggs-Gelasco, and Dr. Michelle Brooks for fostering my love of science. Thank you to my very best friend, Matthew Moore, for all of your love, laughter, and for making me your wife. I love you all so much and thank you.

# 1. Introduction

## 1.1 *mRNA Turnover as a Regulatory Mechanism of Gene Expression in Eukaryotes*

Gene expression, a highly regulated process in all living organisms, can be modulated at the DNA, RNA, and protein levels. Regulation of transcription, RNA processing, and translation ensures production of essential enzymes, structural proteins, and DNA- and RNA-binding proteins required for survival. Regulation of gene expression through control of mRNA turnover has been shown to be one mechanism for the control of protein biosynthesis. Control of mRNA decay allows for flexibility in the regulation of translation of transcripts in response to homeostatic conditions and cellular signals. RNA-binding proteins can directly influence mRNA turnover by mediating transcript stability or instability. The vertebrate protein tristetraprolin (TTP) and its family members are tandem CCCH zinc finger proteins that bind sites within AU-rich elements (AREs) located in the 3' untranslated region (UTR). RNA-binding activity through the tandem zinc finger (TZF) domain has been shown to destabilize target transcripts and promote their deadenylation, leading to mRNA decay. The goal of this thesis is to present novel data describing the interactions of the TTP family member found in *C. albicans*, *Zfs1*, to RNA sequence elements in an effort to understand the mechanisms of ARE-binding selectivity in eukaryotes.

## **1.2 Mechanisms of mRNA Turnover**

As the link between transcription and translation, mRNA serves as the conduit for gene expression in the cell. mRNA degradation has an integral role in gene expression since control of steady-state levels of mRNA are achieved through a balance of synthesis and decay of transcripts (Figure 1). The decay rates of transcripts in different cell types vary extensively, with half-lives ranging from seconds to days. The half-lives of transcripts can also fluctuate in response to external and internal stimuli, providing flexibility for gene expression. mRNAs can be targeted through several different pathways: micro RNA-mediated (miRNA) decay, nonsense-mediated decay, and adenosine-uridine rich element-mediated decay (discussed more in section 1.4).

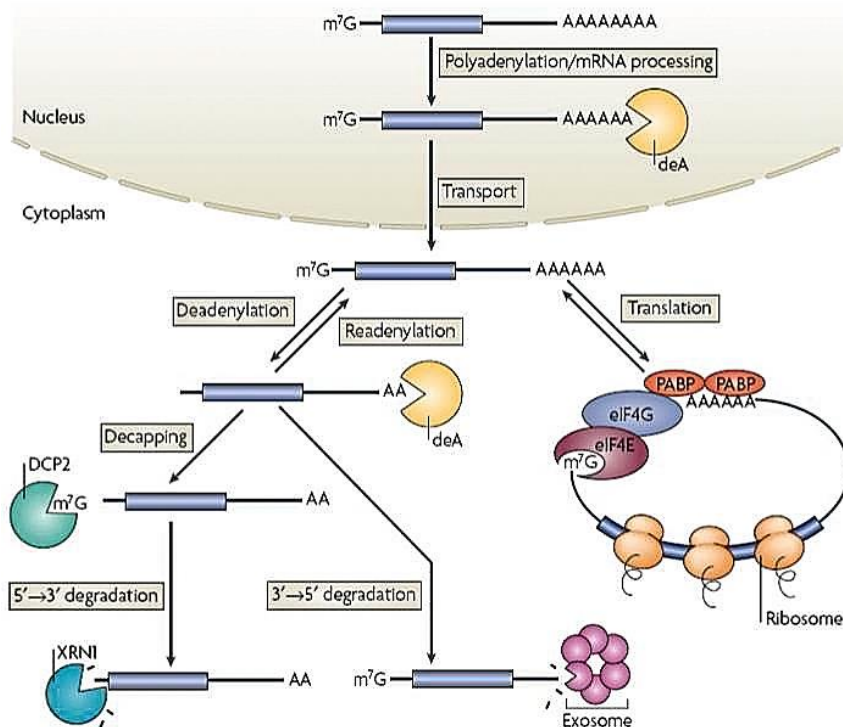


**Figure 1. mRNA Steady-State Levels Reflect a Balance of Synthesis and Degradation of Transcripts**

Mature mRNAs are translocated to the cytoplasm and shuttled through several pathways. Some mRNAs are circularized by protein factors and translated by the ribosome. Other transcripts are degraded by 5'-3' or 3'-5' degradation and some are shuttled to P-bodies (not shown) for later processing. Image from Goldstrohm *et al.* (1).

One of the lesser known pathways of mRNA turnover is miRNA- mediated degradation. It has recently been discovered that miRNAs have roles in targeting mRNA for decay. miRNAs are short, non-coding 20-22 nucleotide (nt) sequences which bind complementary target mRNA sequences. In eukaryotes, miRNAs have the ability to destabilize transcripts and recruit the complexes CCR4-NOT and PAN2-PAN3 (2) to

promote deadenylation. Knockdown of components of the CCR4-NOT complex can impede miRNA-mediated deadenylation and mRNA decay. Knockdown of PAN2-PAN3 only modestly affects miRNA-mediated deadenylation and mRNA decay, indicating that the CCR4-NOT complex is the major deadenylase involved in miRNA-mediated decay.

Another well-known pathway for mRNA turnover is the nonsense-mediated decay (NMD) pathway. Initially, this pathway was believed to be part of an mRNA surveillance system that targeted mRNAs containing premature stop codons. NMD prevents translation of truncated proteins, which could cause deleterious effects in host cells (3,4). Selected normal transcripts are also subject to NMD. Additional research is needed to determine the factors involved in transcript decay regulation by NMD (3,4).

The majority of eukaryotic mRNA transcripts targeted for decay are degraded 3'-5', with the rate-limiting step for 3'-5' mRNA degradation being removal of the poly(A) tail, or deadenylation. The poly(A) tail is protected by stabilizing poly(A)-binding proteins (PABP), which have been shown to protect target transcripts from indiscriminate degradation (5,6). RNA-binding proteins can influence the stability of mRNAs through binding of sequence elements located in 3'-UTRs (7-9) (discussed in further detail in next section). Transcript destabilization by RNA-binding proteins can promote recruitment of factors needed to remove the PABP. The initial degradation of

the poly(A) tail is initiated by Pan2-Pan3, a PABP-dependent poly(A) ribonuclease. The CCR4-NOT complex then completes deadenylation of the transcript. In poly(A)-specific exoribonuclease (PARN)-mediated decay, the exoribonuclease activity of PARN is stimulated by binding to the 3' end of transcripts, and results in removal of the poly(A) tail (8,10).

After removal of the poly(A) tail, the transcript undergoes 3'-5' or 5'-3' directed decay. 3'-5' transcript decay is mediated by the exosome, a complex of proteins consisting of several 3' exoribonucleases (11,12). The residual mRNA cap is hydrolyzed by m7GpppX diphosphatase (also known as Scavenger mRNA-decapping enzyme Dcp5), and an N7 methyl guanosine monophosphate is released by the enzymatic reaction. 5'-3' mRNA decay begins by the removal of the residual 3' mRNA cap by mRNA-decapping enzyme 1A (Dcp1-Dcp2). N7 methyl guanosine diphosphate and 5' monophosphate are released as enzymatic by-products, and the decapped mRNA is degraded by 5'-3' exoribonuclease 1 (XRN1) (12).

### **1.3 Notable 3'-UTR RNA-Binding Proteins and Their Effects on mRNA Stability**

The UTRs of mRNAs have an essential role in the post-transcriptional regulation of transcripts. 5' and 3'-UTRs are responsible for modulating transport of mRNAs out of the nucleus, translation efficiency, subcellular localization, and stability (9). Research has shown that association of RNA binding proteins, otherwise known as *trans*-acting

factors, are essential for regulation of mRNA translation or decay. The focus of this section will be on *trans*-acting factors that influence mRNA stability through *cis*-acting sequences in the 3'-UTR

RNA-binding proteins are often called *trans*-acting because of their abilities to target sequence elements located within RNA and mediate transcript translation or degradation. *Trans*-acting proteins can mediate a stabilizing effect, which promotes transcript translation, or a destabilizing effect, which promotes mRNA deadenylation and decay. Members of the PUF family are classic examples of *trans*-acting proteins which mediate transcript destabilization.

The PUF (from *Pum* in *Drosophila Pumilio* and *EBF* from *Caenorabditis elegans*) family is a group of proteins which recognize *cis*-acting sequences located in the 3'-UTR of transcripts. Members of the PUF family associate with base-specific *cis*-acting elements, called Nanos Response Elements (NREs), of 5-8 nucleotides in length, and usually contain the core sequence UGU (13). The prototypical family member, *Pum*, has been demonstrated to be essential for establishment of proper abdominal segments in *Drosophila* (13). Experiments determined that *Pum* binds to NREs located in the *hunchback* mRNA and promotes deadenylation of *hunchback* transcripts, leading to transcript decay and normal *Drosophila* development (13). Mammals express two distinct PUF proteins which have similar biochemical properties to the invertebrate PUF

proteins. Studies have established that mammalian PUF proteins interact with proteins involved in germ cell development and mRNA translational regulation, suggesting a conserved evolutionary role of this family among different species (13,14).

RNA-binding proteins also can have stabilizing effects on mRNAs as an effective mechanism to increase concentrations of active protein in the cell without expenditure of energy on transcription and exportation of new mRNAs to the cytoplasm. HuR, of the embryonic lethal, abnormal vision (ELAV) family, is one of the best described mRNA stabilizing proteins (15). HuR and other ELAV family members bind to *cis*-acting elements located in the RNA that are uridine-rich (16). The first two RNA-binding domains of HuR bind to U-rich sequence elements in the 3'-UTR, and a third region has been shown to mediate recruitment of proteins essential for 3' adenylation of non-polyadenylated RNA (16). Promotion of adenylation can stabilize and increase transcript steady-state levels and lead to increased concentrations of active protein (16). As mentioned previously, this is an efficient mechanism by which to increase the expression of target proteins without needing to export and transcribe more mRNA. However, stabilization and translation of aberrant transcripts can lead to disease, especially cancer. HuR is found to be upregulated in many cancers. Studies have demonstrated HuR binding and stabilization of the transcripts encoding Cyclin E1, A2, B1, and Epidermal growth factor (EGF) (17), mRNAs with known roles in cancer growth

and proliferation. Researchers are developing methods to reduce HuR-binding activity as a potential target for the development of new chemotherapeutics.

ARE/poly(U)-binding/degradation factor 1 (AUF1), or hnRNP D, is another *trans*-acting RNA-binding protein shown to target AREs. AUF1 has four isoforms expressed differentially in various cell types. Researchers postulate that these different isoforms are expressed in different subcellular compartments, thereby targeting and exerting distinct effects on mRNAs. Previous studies suggested that AUF1 and its isoforms are able to stabilize or destabilize certain transcripts, depending on intracellular conditions, suggesting a role for the AUF1 family members in translational repression and activation (18). AUF1p45, the major AUF1 isomer, is known for destabilization of mRNAs containing ARE-binding sites, and the ability to oligomerize when associated with ARE-binding sites. Oligomerization of multiple AUF1 units may further promote transcript destabilization or serve as a platform essential for the association of other RNA-binding proteins that mediate transcript destabilization (19). This hypothesis was supported by research that demonstrated the binding of the *trans*-acting RNA-binding protein, TTP, a protein with a well-established role in transcript deadenylation, to AUF1 (20). We and others hypothesized that through oligomerization, AUF1p45 can recruit other proteins that can potentiate mRNA destabilization and deadenylation.

## **1.4 Characterization of 3'-UTR Adenosine-Uridine Rich Elements (AREs)**

Sequence elements located in the UTR of mRNA transcripts are essential for translational repression or activation, transcript localization, and degradation. As described earlier, RNA-binding proteins such as HuR and AUF1 rely on these *cis*-acting elements to mediate their roles in mRNA turnover. Some of the most studied *cis*-acting sequence elements are adenosine-uridine rich elements (AREs), often located in the 3'-UTR of mRNA transcripts. AREs have a high content of uridines and adenosines, yet notably, the nonamer sequence of UUAUUUA(U/A)(U/A) has been shown to spatially and temporally control expression of certain mRNAs by promoting destabilization of the transcript and promoting poly(A) removal. The nonamer sequence of UUAUUUA(U/A)(U/A) is found in 5-8% of human mRNAs (21). Transcripts regulated by destabilizing *trans*-acting elements have been demonstrated to undergo rapid deadenylation and degradation in response to intra- and extracellular stimuli. Studies have shown that AREs are prevalent in genes encoding cytokines, mediators of the inflammatory response (22-24). Researchers initially determined that insertion of an ARE from the 3'-UTR of Granulocyte Macrophage-Colony Stimulating Factor (GM-CSF) mRNA, encoding a human inflammatory cytokine, into the 3'-UTR of the  $\beta$ -globin transcript, which contains no AREs in its 3'-UTR, resulted in the destabilization of the  $\beta$ -globin transcript (25). AREs taken from a selection of other labile transcripts did not

confer instability to the  $\beta$ -globin transcript (26). Subsequent studies revealed that destabilization of transcripts through elements located in 3'-UTRs was mediated by rapid deadenylation and ultimate degradation of target transcripts (27).

AREs have been categorized into three classes: class I, class II, and non-AUUUA. Class I AREs are defined by interspersed AUUUA core sequences within a uridine-rich region. Class I AREs are found in the transcripts of the oncogenes *c-fos* and *c-myc*. Class II AREs have two or more of the overlapping nonamer sequences of UUAUUUAUU. Class II AREs are found in the transcripts of the tumor necrosis factor  $\alpha$  (TNF $\alpha$ ) and GM-CSF, two cytokines involved in the mammalian inflammatory response. AREs in the non-AUUUA\_class, or Class III AREs, have a uridine-rich region with no other distinguishing sequence characteristics (28). The *c-jun* transcript 3'-UTR has a class III ARE located in its 3'-UTR. Chen and colleagues reported that each type of ARE has individual characteristics, and that AREs of different classes can regulate recruitment of elements needed for poly(A) shortening and degradation (27) (Figure 2). It was further hypothesized that protein partners must interact with these AREs to confer instability.

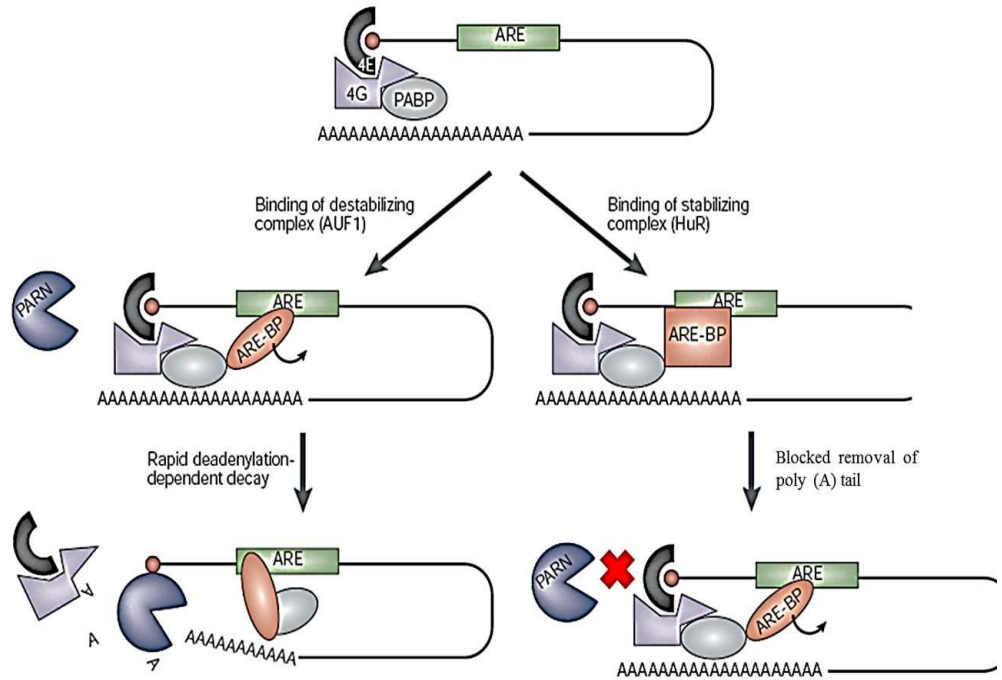


**Figure 2. The Stabilizing and Destabilizing Effects of ARE-binding Proteins on mRNA**

Binding of stabilizing or destabilizing ARE-binding proteins can promote or prevent degradation of an mRNA transcript. An ARE-binding protein (left pathway) promotes release of poly(A)-binding proteins and subsequent removal of the poly(A) tail. A different ARE-binding protein (right pathway) can physically block access to the poly(A) tail and prevents deadenylation. Image adapted from Wilusz *et al.* (33).

## 1.5 The Tristetraprolin Family

One of the most studied groups of ARE-binding proteins are the tandem zinc finger-containing proteins of the tristetraprolin (TTP) family. TTP, the prototypical member of this family, was first identified in 1990 when TTP mRNA was found to be

rapidly induced in response to insulin (29), and, independently, to the tumor-promoting phorbol ester, tetradecanoyl phorbol acetate (TPA) (30). TTP, also known as Tis11 or Nup475, was found to be enriched in proline residues and had a novel tandem CCCH zinc finger domain. Each finger contained the sequence  $CX_8CX_5CX_3H$  (with X representing variable residues) (31,32) and a “lead-in” sequence of (R/K)YKTEL before the first cysteine of each finger (32) (Figure 3).

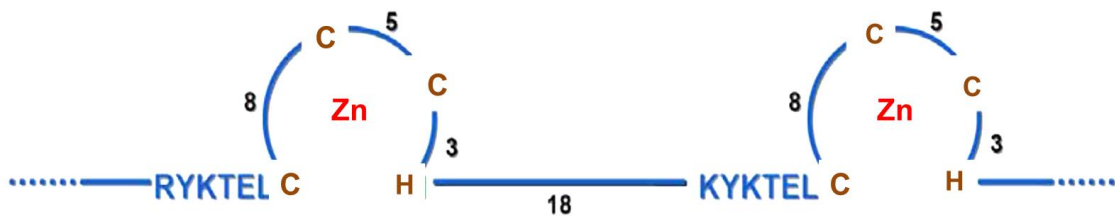


**Figure 3. TTP and its Family Members Contain a Novel Zinc Finger Domain.**

Members of the TTP family have a tandem zinc finger domain containing a “lead-in” sequence of R/KYKTEL and each finger contains the sequence  $CX_8CX_5CX_3H$  with X representing variable residues. A spacer of eighteen residues separates the fingers from each other. The residues colored in brown coordinate to the zinc ion (red).

Nathans and Berg demonstrated that each finger coordinated a zinc ion, but the purpose of the tandem CCCH domain was not known at the time (33,34). A later study determined that the zinc fingers could bind cobalt ions with high affinity. The fingers had greater affinity for zinc ions, similar to affinities reported for zinc ions with known zinc finger proteins (34). Early speculation suggested that because of its rapid induction

in response to stimuli and its novel tandem zinc finger domain, TTP might be involved in DNA binding, and might serve as a transcriptional regulator.

The role of TTP in inflammation was first described in a study of knockout mice reported by the Blackshear group (35). In this study, TTP-deficient mice exhibited a phenotype resembling that seen in mouse models of TNF $\alpha$  overexpression. TTP-deficient mice, similar to mice in TNF $\alpha$  overexpression models, developed cachexia, chronic arthritis, dermatitis, and loss of subcutaneous fat. This syndrome was prevented by treatment of mice with anti-TNF $\alpha$  antibodies (35). A follow-up study by the same group showed that TTP influenced the stability of TNF $\alpha$  mRNA (36). Later studies demonstrated that TTP promoted transcript instability, potentiating transcript deadenylation and degradation by an unknown mechanism (37), whereas TTP deficiency resulted in increased transcript stability. Without TTP, stabilized mRNAs are translated into more active protein than seen in normal TTP-expressing mice. The Blackshear group proposed that the inflammatory syndrome seen in the TTP-deficient mice was due, at least in part, to the lack of TTP-promoted transcript deadenylation and stabilization of TNF $\alpha$  transcripts, among others.

The mouse TTP family also includes three other members: Zfp36 Like 1 (ZFP36L1), Zfp36 Like 2 (ZFP36L2), and Zfp36 Like (ZFP36L3). Studies have determined that ZFP36L1 is necessary for proper chorioallantoic fusion during

embryogenesis (38); ZFP36L2 is involved in coordination of hematopoiesis (39); and ZFP36L3, a rodent-specific and placenta-specific protein, is beneficial for the fertility and fecundity of mice (40). The mammalian TTP family members share significant sequence similarities to TTP, and have been demonstrated to act like TTP in cell transfection studies of RNA binding and decay (37,41). However, various studies have suggested that the other mammalian TTP family members are differentially expressed in various tissues.

TTP proteins are evolutionally conserved, and TTP family members can be found in most groups of eukaryotes. By definition, TTP family members share sequence similarities among their TZF domains. *Drosophila melanogaster* expresses a single TTP family member, called TIS11, which has been shown to bind with high affinity to transcripts containing ARE-binding sites and promote transcript instability (42). Another study reported that overexpression of TIS11 in *D. melanogaster* resulted in reduced eye size, suggesting a potential role in the regulation of transcripts involved in eye development (43). Further roles of TIS11 in *D. melanogaster* physiology and development are still being elucidated.

*Xenopus laevis* expresses four TTP family members. XC3H-1, XC3H-2, and XC3H-3 are the homologues to TTP, Zfp36L1, and Zfp36L2, respectively. The fourth family member, XC3H-4, contains the characteristic tandem zinc finger domain, but also

contains two distantly related zinc fingers. XC3H-4 is only detected in the ovary, oocyte, and embryo. Researchers have hypothesized a role for XC3H-4 in oocyte maturation and/or embryogenesis (44).

Protein binding partners of TTP and other eukaryotic family members are still relatively unknown. Identification of TTP family member binding partners would further help to elucidate the role of TTP in promoting transcript decay. Recent binding studies determined that all human TTP family members contain a C-terminal putative NOT1-binding domain (45). As mentioned in a previous section, the CCR4-NOT complex is hypothesized to be largely responsible for deadenylation of cytoplasmic mRNAs (45,46). The Stoecklin group showed that the C-terminal domain of TTP interacted with NOT1, the major scaffolding core of CCR4-NOT1. Additional data suggested that NOT1 binding is essential for TTP-mediated transcript deadenylation (46). A subsequent paper described the structural basis of TTP-NOT1 recognition through X-ray diffraction studies. The C-terminal domain of TTP was shown to interact with a central domain of NOT1, placing the deadenylase unit of CCR4-NOT complex in proximity to the poly(A) tail, thereby potentially promoting transcript deadenylation (47).

## 1.6 Fungal TTP Family Members

Fungal TTP family members are under extensive study, and have been used as models to understand the activities of these proteins in higher eukaryotes. TTP family members can be found in several members of the *Saccharomycetales* order. The *Saccharomycetales* TTP family members contain the aforementioned conserved TZF domain found in metazoan TTP family members, suggesting a similar biochemical mechanism of binding to AREs. There is no sequence similarity found in the domains outside of the TZF domain, which may be important in the recruitment of certain protein partners needed for regulation of transcript decay. Furthermore, the fungal TTP family members, other than the protein found in a primitive chytrid fungus, *Spizellomyces punctatus*, generally do not have a characteristic NOT1-binding domain. Nonetheless, the fungal TTP family members characterized in *Schizosaccharomyces pombe* and *Saccharomyces cerevisiae* have been shown to promote transcript decay similar to TTP (48,49). Studies have determined that TTP and TTP family members bind mRNAs that contain ARE-binding sites within their 3'-UTRs; however, TTP family members from distantly related species seem to have evolved their own unique sets of target transcripts.

### 1.6.1. *S. pombe*'s TTP family member, Zfs1

*S. pombe*, a member of the fission yeast family, was instrumental in determining the mechanisms of the cell cycle in eukaryotes. *S. pombe* is easily grown and manipulated in a laboratory setting and has one of the smallest genomes in eukaryotes (50). *zfs1*, a gene encoding a member of the TTP family, was first discovered in a screen of multicopy suppressors of sterility caused by overexpressing *pac1*, an RNase III-like dsRNase. Disruption of *zfs1* resulted in a phenotype that had a reduced mating ability and a defect in sporulation as compared to wild-type *S. pombe*. *zfs1* disruption also led to suppression of factors related to mating pheromone signaling (51). The 404-amino acid protein, named Zfs1, is also essential for septum formation if mitosis is blocked, suggesting an additional role in cell division (52). The RNA binding capabilities of Zfs1 were later explored in a paper by the Blackshear group. In microarray experiments, *zfs1*Δ (deficient) *S. pombe* had elevated levels of the mRNA for *arz1* at mean levels of 3.6-fold greater than wild-type. *arz1* transcripts also exhibited a slower rate of decay in *zfs1*Δ as compared to wild-type *S. pombe* (53). The 3'-UTR of the *arz1* (armadillo-repeat containing *zfs1* target 1) transcript contains three UUAUUUAUU nonamer sequences. Mutation of the adenosines within two of the nonamer sequences into guanosines led to protection of *arz1* transcripts from Zfs1-dependent decay (53). Mutations of the core residues, AUUUA, in a single nonamer (UUAUUUAUU) sequence, or attempted

disruption of a single core nonamer by introduction of secondary structure, did not influence the rate of *arz1* transcript decay (53). The binding affinities of probes based on wild-type and mutated *arz1* sequences were determined using electrophoretic mobility shift assays (EMSAs). Recombinantly expressed Maltose Binding Protein (MBP) N-terminally linked to full-length Zfs1 protein bound and upshifted probes containing two UUAUUUAUU nonamers (9-mers), relative to free probe. An RNA oligonucleotide with a mutated 9-mer sequence of UUCUUUCUU resulted in a lower upshifted band as compared to the higher shifted band seen with the probe containing two UUAUUUAUU sequences (53). These data suggested that multiple protein binding events in the 3'-UTR could be a mechanism by which to influence transcript stability. The role of *arz1* in *S. pombe* physiology, and its regulation by Zfs1, are still under investigation.

A later study using mRNA-sequence (mRNA Seq) analysis identified many other Zfs1 mRNA targets. One of these, the *Cbf12* transcript, was shown to be a target of Zfs1 and to be involved in cell-cell adhesion. Overexpression of Cbf12 leads to the adhesion of the *S. pombe* cells to each other, causing them fall out of solution, a phenomenon known as flocculation. The *Cbf12* transcript has several single 7-mer (UAUUUAU) potential TTP family member binding sites located within its 3'-UTR; however, there was only a 1.84-fold increase in transcript levels in the Zfs1 mutants, in the mRNA-Seq results (as compared to *arz1*, which has three potential binding sites and showed a 5.07-

fold increase in the *zfs1Δ* mutant) (49). Studies with the *zfs1Δ* mutant established that the increased flocculation occurred due to increased expression of Cbf12 protein (49). This phenotype was abolished in a double *zfs1Δ cbf12Δ* mutant.

A list of other potential targets from the mRNA-Seq analysis revealed that out of 185 upregulated transcripts, 119 mRNAs had at least one potential 7-mer binding site (49). Many of the transcripts that were significantly upregulated were shown to directly interact with Zfs1, as determined by RNA immunoprecipitation (RIP) assays. Upregulated transcripts containing at least a single 9-mer also exhibited delayed decay rates in *zfs1Δ* mutants as compared to wild-type, suggesting a Zfs1-dependent mechanism (49). These data also suggested that an increased number of potential binding sites within a transcript did not correlate with higher fold changes as reported by mRNA-Seq analysis. This seems to suggest that other protein factors in combination with Zfs1 are essential in promoting transcript selectivity and Zfs1-dependent deadenylation.

### **1.6.2. *S. cerevisiae*'s TTP family members, Cth1 and Cth2**

Modern molecular techniques showed that *S. cerevisiae* underwent a duplication event of its genome (54,55), resulting in expression of two TTP family members. The TZF domains of the TTP family members of *S. cerevisiae* share high sequence similarity, yet these proteins lack any conservation in regions outside of the TZF domains.

One of *S. cerevisiae*'s TTP family members, Cth2 (then called YTIS11), was shown to be rapidly expressed during glucose repression, suggesting a role in the yeast nutritional response pathway. However, disruption of *YTIS11* showed only a cell color change when cells were grown in YPD media with 2.0% glucose (56). A later study published by Thompson and Blackshear determined that *S. cerevisiae* expresses two TTP family members whose genes were named *CTH1* and *CTH2*. Deletion of *CTH1* and *CTH2* genes in *S. cerevisiae* resulted in no obvious phenotype. Overexpression of *CTH1* and *CTH2* attenuated growth, with growth more inhibited when *CTH1* was overexpressed. Expression of a truncated form of Cth1, or deletion of the Cth1 TZF domain, restored normal cellular growth, suggesting a potential compensatory role of Cth2 or another protein (57). The Blackshear group concluded that Cth1 and Cth2 have roles in suppressing cell growth

Critical roles of Cth1 and Cth2 in *S. cerevisiae* physiology were determined by the Thiele and Puig groups in the mid-2000s. In iron-deprived environments, *S. cerevisiae* uses the transcription factors, Aft1 and Aft2, to induce iron regulon expression. The iron regulon encodes proteins essential for heme utilization, iron uptake, and mobilization of intracellular iron stores (58). Research determined that in environments containing normal concentrations of iron, Cth2 could bind to several iron-regulating transcripts containing ARE-binding sites. It was speculated that deadenylases are recruited to the

transcripts associated with Cth2, thereby promoting transcript deadenylation and degradation. In iron-depleted media, *CTH2* is downregulated and transcripts that are normally destabilized are subsequently stabilized. The turnover rate of stabilized transcripts is decreased, thereby increasing their translation and the production of proteins essential in regulation of iron metabolism. *CTH1* only modestly takes part in iron homeostasis, suggesting it plays a role in other molecular pathways (48). A later study concluded that Aft1 and Aft2 induce expression of *CTH1* during iron deprivation. Cth1 then promotes decay of transcripts responsible for iron-dependent mitochondrial processes, such as respiration and amino acid synthesis (59). Furthermore, *CTH1* and *CTH2* transcripts have ARE-binding sites, suggesting self-regulation by Cth1 and Cth2. Cth2 has been shown to promote the decay of *CTH2* and *CTH1*, but Cth1 can only promote the decay of *CTH2* mRNA. Thiele and colleagues hypothesized that auto- and trans-regulation of *CTH1* and *CTH2* allows for a coordinated and tightly controlled response to environmental cellular changes (60).

Studies have shown that the mammalian and fungal TTP family members can bind to sites within AREs and promote destabilization of transcripts. Additional data further demonstrated that the TZF domains of several TTP family members exhibit high-affinity binding to the UUAUUUAUU site (61,62). Despite these findings, it is still poorly understood how these proteins, which lack conservation outside the TZF

domain, have essentially evolved the same biochemical function (Figure 4). Unlike the mammalian TTP family members, with the exception of some primitive chytrid fungi, the fungal TTP family members do not contain a characteristic NOT1 binding site (45), despite expression in *S. cerevisiae* and *S. pombe* of the proteins in the CCR4-NOT complex. It has been postulated that TTP and TTP family members have specifically evolved to target certain transcripts within their respective organisms and, in the case of most fungal TTP family members, can act without the recruitment of CCR4-NOT complex.



## **1.7 The TZF Domain and Its High-Affinity Binding to Target Binding Sites**

The Blackshear lab demonstrated that the TTP TZF domain has a role in mRNA destabilization and decay (41). Mutations of any of the cysteine residues in the first finger to an arginine abrogated binding of TTP to a TNF $\alpha$  probe, which contained several overlapping 9-mer binding sites. Similar mutations in the second finger produced the same result (37). This suggested an essential role for both fingers in binding to ARE-binding site-containing transcripts. Later studies revealed that the TTP TZF domain could bind to ARE sites located within the TNF $\alpha$  mRNA (63). An alignment of the TZF domains from mammals, zebrafish, and fruit flies showed significant sequence conservation of over 50% among the different species (41) (Figure 5), suggesting similar mechanisms of ARE site association.

```

Cth1 (Danio rerio)      RYKTELCSRYAETGTCKYAERCQFAHGLHDLHVPSRHPKYKTELCRTYHTAGYCVYGTRCLFVH
TTP (Homo sapiens)     RYKTELCRTFSESGRCRYGAKCQFAHGLGELRQANRHPKYKTELCCHKFYLQGRCPYGSRCHFIH
DTIS11 (Drosophila melanogaster) RYKTELCRPFEEAGECKYGEKCQFAHGSHELNRNVHRHPKYKTEYCRTFHSVGFPCPYGPRCHFVH
Zfp36L3 (Mus musculus) RYKTELCRPFEEESGICKYGHKCQFAHGYRELRTLSRHPKYKTEPCRTFHSVGFPCPYGTRCHFIH
ZFP36L1 (Homo sapiens) RYKTELCRPFEEENGACKYGDKSQFAHGIHELRLSLTRHPKYKTELCRTFHTIGFCPYGPRCHFIH
ZFP36L2 (Homo sapiens) RYKTELCRPFEEESGTCKYGEKCQFAHGFHELRLSLTRHPKYKTELCRTFHTIGFCPYGPRCHFIH
*****      : * * * : * . : . *****      : * :      ***** * : . : : * * ** * * * : *

```

**Figure 5. Sequence Alignment of the TZF Domains from TTP and other Mammalian and Non-Mammalian TTP Family Members**

The TZF domains of human TTP, ZFP36L1, ZFP36L2, murine ZFP36L3, zebrafish (*Danio rerio*) CTH1, and fruit fly DTIS11 are highly conserved. Identical, conserved, and semi-conserved residues are represented by (\*), (:), and (.), respectively.

Conservation between the TTP TZF domain and these of other family members suggests similar biochemical mechanisms of binding to sites within AREs. The first attempt at a structural characterization of TTP TZF domain was published by the Berg laboratory in 2002. Using nuclear magnetic resonance (NMR) structural techniques, Berg and colleagues attempted to solve the structure of the first zinc finger of the mouse TTP TZF domain; however, to increase protein solubility for NMR experiments, the second finger was mutated such that the zinc binding properties of the second finger were abrogated. They proposed that the first intact finger formed a disk-like novel fold not seen in other metal-binding domains. The three cysteines of the sequence Cx<sub>8</sub>Cx<sub>5</sub>Cx<sub>3</sub>H coordinated the zinc ion, and the secondary interactions of amino acids around the metal center were thought to have a role in organization of the zinc finger (64).

The Wright group subsequently solved a structure for the full-length TZF domain of the human TTP family member ZFP36L2 (TIS11d) using NMR. In this structure, both intact fingers were needed to bind the RNA probe consisting of the 9-mer sequence 5'-UUAUUUAUU-3'. The three cysteines and single histidine in each finger were shown to coordinate the zinc ions found in fingers 1 and 2 (65).

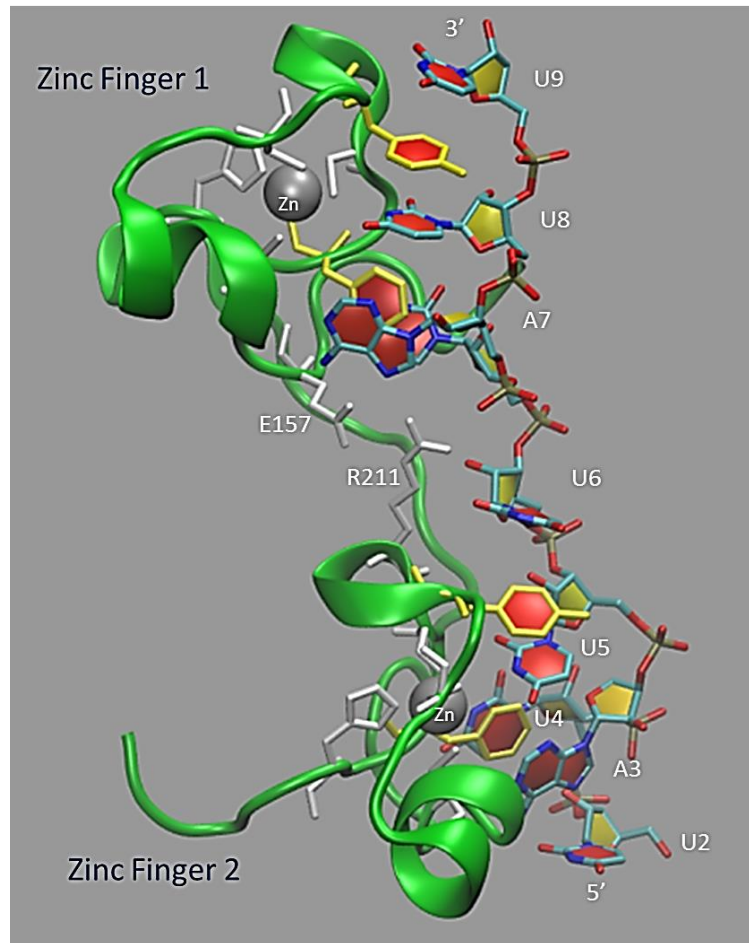


**Figure 6. Structure of the TZF domain of ZFP36L2 associated with a 9-mer RNA containing a single binding site (65)**

The side chains of E157 (Finger 1) and R211 (Finger 2) are shown in white. Zinc atoms (gray spheres) and the zinc coordinating amino acids are displayed.

The Wright structure of the ZFP36L2 TZF domain in complex with the 9-mer established that the second finger bound the 5'-UAUU and the first finger bound the 3'-UAUU nucleotides. The data revealed a possible mechanism by which the protein could scan the oligonucleotide from the 3' to the 5' end to identify binding sites. Several aromatic

residues (namely phenylalanines and tyrosines) formed base stacking interactions with the UAUU nucleotides, probably contributing to the mechanism of high-affinity protein-RNA binding. Additionally, the lead-in sequences, (R/K)YKTEL, found before each finger formed pockets to accommodate the uridine residues and provided stable backbone hydrogen bonding for the RNA probe, reinforcing recognition of certain bases (65) (Figure 6).

Despite high degrees of sequence conservation between TZF domains of different TTP family members, divergence in some of the amino acids can affect localized structural elements. The TZF domains of TTP and ZFP36L2 share 72% sequence identity. A recent study by Lai *et al.*(66) highlighted differences of amino acid composition and structural elements that could influence target binding. Superposition of a model of the TZF domain of TTP and the NMR structure of ZFP36L2 revealed that the fingers of ZFP36L2 are essentially identical to each other when bound to RNA, whereas the zinc fingers of TTP are not. This might be explained by residue differences found in the C-x8-C intervals of the two fingers. The residues found in finger 2 of TTP only allow for one  $\alpha$  helical turn, in comparison to two  $\alpha$  helical turns found in finger 2 of ZFP36L2. Furthermore, mutation of TTP finger 2 residue Y151 to an alanine decreased RNA binding. Y151 was determined to be essential for stabilization of secondary structure, and other residues found in a uridine binding pocket in the

neighboring C-x5-C sequence were shown to be necessary for positioning of the RNA relative to the protein. Additionally, changes in length in the C-x8-C interval were better tolerated by finger 2 than by finger 1 (66). Mutations of residues found in the C-x5-C intervals of either finger reduced binding to an RNA probe containing a validated ARE-binding site. Mutations of the TTP TZF domain could promote destabilization of the binding pockets necessary for the uracil and adenine bases. One of the most important observations of this study is the identification of a potential salt bridge between the R161 in finger 2, and the E107 residue in finger 1. R161 and E107 oriented the two fingers in a conformation that “locked” the protein in a structure that could further stabilize the complex. Disruption of the proposed salt bridge through mutagenesis was shown to compromise the integrity of the TZF domain. Additional data concerning the C-x3-H interval revealed that mutations of the A127 (finger 1) and I165 (finger 2) residues also disrupted association to the ARE-binding site. Furthermore, the alanine was suggested by modeling to indirectly affect the formation of the R161 and E107 salt bridge. As shown with finger 1, changes in the lengths of the intervals C-x5-C or C-x3-H resulted in decreased RNA-binding (66).

Lead-in sequences, which are highly conserved among the mammalian and yeast family members, were found to mediate important positively charged interactions with the RNA backbone. Similar to the R161 and E107 residues that form the salt bridge,

several residues found within the lead-in sequences provided ionic interactions that dictated the relative orientation of the zinc fingers to each other. The eighteen amino acid linker between the two fingers also played a role in the orientation. It was found that shortening or expanding the length of the linker could reduce the binding affinity of the peptide to RNA. The deletion of a single residue in the middle of the linker versus deletion of single a residue found at the beginning of the linker was shown to modestly affect binding affinity (66).

Following the study by the Wright group, it was postulated that, despite sharing common lead-in and  $CX_8CX_5CX_3H$  sequences, non-conserved residues within species-specific TZF domains may have evolved to select certain target sites within AREs, or possibly interactions with other proteins. Mutational studies of other TZF domains could therefore identify residues that would provide critical understanding of target selectivity and specificity between different TTP family members.

### **1.7.1 The TZF Domain is Functionally Conserved**

Sequence alignments (see Figures 4 and 5) have determined high degrees of sequence conservation among the TZF domains of various TTP family members. Despite these findings, not all residues are conserved throughout the TZF domains, suggesting that TZF domains may not be functionally interchangeable among different species. To test the possibility that the TZF domains from distant groups were

interchangeable, the TZF domain from *S. pombe* was replaced with the TZF domains from *Bombyx mori* (silkworm), the yeast *M. guilliermondii*, the plant *Chromolaena odorata* (Christmas Bush), and TTP (*Homo sapiens*), beginning at the residues R(L)YKTE(L/P) and ending in the final histidine in the second zinc finger. Wells *et al.* found that the TZF domains from these evolutionarily very distant species complemented the function of the *S. pombe* Zfs1 TZF domain in regulating target transcript expression and the flocculation phenotype (62). Additionally, the full-length family members from *S. octosporus* (a *Schizosaccharomyces* genus member), *M. guilliermondii*, and TTP (*M. musculus*) were placed in the endogenous *zfs1* locus of *S. pombe*. In this experiment, only the *S. octosporus* full-length TTP family member fully complemented the Zfs1 deficiency. Partial complementation by the full-length TTP family members from *M. guilliermondii* and *M. musculus* resulted in a flocculation phenotype and abnormal target transcript expression (62).

From these data, we concluded that the TZF domains from species as different as those from mammals and plants have the same biochemical function of binding to sites located within AREs. Complete complementation of Zfs1 function in *S. pombe* by the full-length TTP family member from *S. octosporus*, which shares 51% sequence identity to full-length *S. pombe* Zfs1, but not by the more distant yeast *M. guilliermondii*, which shares only 18% sequence identity to full length *S. pombe* Zfs1, suggests that domains

outside of the TZF domain are important for transcript destabilization and recruitment of protein factors involved in mRNA degradation. It remains possible that these domains may also work in tandem with the TZF domain to assist in transcript selectivity and specificity.

### **1.7.2 Characteristics of Target Binding Sites Within AREs**

Previous studies have shown that binding sites located within the AREs of TNF $\alpha$  and GM-CSF transcripts are targeted by TTP (41). Early research determined that binding of TTP and its family members to full-length or partial 3'-UTRs containing binding sites promoted transcript deadenylation and destabilization. However, the minimal target binding sequence needed for high-affinity binding to AREs, and whether multiple targets on a single transcript allowed for multiple binding events, remained unknown. To answer these questions, *in vitro* biochemical methods were used to define target binding sequences and determine their binding affinity to TTP TZF domain.

To conduct these studies, Blackshear and colleagues used a chemically synthesized peptide corresponding to the TZF domain of human TTP (TTP73) (67). Recombinant expression of full-length TTP family members often produces insoluble proteins not suitable for biochemical or structural studies; however, the Blackshear lab has recently expressed and purified several full-length TTP family members (one of which will be the focus of this thesis).

TTP73 contained the core TZF domain from human TTP, but an N-terminal serine was added before the lead-in sequence, and eleven extra residues were added to the C-terminus (when compared to the TTP TZF domain depicted in Figure 5). In EMSAs, the synthetic peptide caused an upward shift of RNA probes consisting of 70 bases or 24 bases of mouse TNF $\alpha$  mRNA containing the proposed target binding sites (bases 1281-1350 and 1309-1332 respectively; GenBank accession number X02611) as compared to free probes. Both sequences shifted in the presence of the TZF domain peptide; however, there were three upshifted complexes using the 70-base probe versus two upshifted complexes seen with the 24-base probe. It had been shown previously that TTP expressed in HEK (Human embryonic kidney) 293 cells could bind to the 24-base probe. Furthermore, Blackshear and colleagues determined that the development of the two upshifted bands was concentration dependent, with the lower band appearing first followed by the second, higher band (67). These data suggested that the phenomenon of multiple occupancy of TTP73 to a single transcript containing several binding sites is concentration dependent. A possibility raised but not studied in that paper was that binding of multiple TTP proteins to a transcript containing several binding sites could be cooperative (67).

It was hypothesized that the unit needed for binding was smaller than 24 bases as two distinct complexes were seen in gel shift assays with the 24-base probe. To test

this hypothesis, a 24-base probe consisting of the sequence

UUUUUUUUUUUUUUUUUU (potential 7-mer binding sites are marked by

underlines or overbars) was assayed to see if the TTP TZF domain produced two

separate upshifted bands. In the next series of studies, the adenosine bases of the core

AUUUA sequences found in the 24-base probe were mutated to cytosine bases in a

series of six probes (Figure 7). Probes 2, 3, and 5 demonstrated a single upshifted band

compared to two upshifted bands seen with probes 1 and 4 (Figure 7). Probes sharing

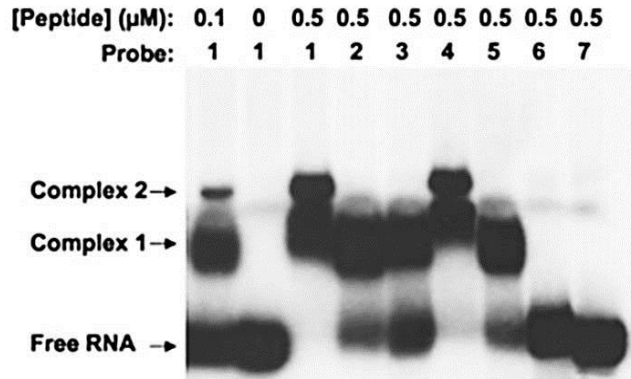
the intact nonamer sequence of UUAUUUAUU bound to the synthetic peptide and

caused an upshift in the EMSA as compared to free probe. An upward shift was not

seen with the UUUAUU (probe 6), suggesting that this sequence is not sufficient for TZF

domain binding. The nonamer sequence provides binding sites for both fingers, as later

established in the NMR structure solved by Hudson *et al.* in 2004 (65).



Probes: 1. UUAUUUAUUUAUUUAUUUAUUUAUU  
 2. UUAUUUAUUUAUUUAUUUCUUUCUU  
 3. UUAUUUAUUUCUUUCUUUCUUUAUU  
 4. UUAUUUAUUUCUUUCUUUAUUUAUU  
 5. UUAUUUAUUUAUUCUUUCUUUAUU  
 6. UUAUUUCUUUCUUUAUUUCUUUAUU  
 7. UUCUUUCUUUCUUUCUUUCUUUCUU

**Figure 7. EMSA Demonstrates the Minimal Binding Sequence Needed for the TTP TZF Domain**

Complex 2 is not found with probes 2, 3, and 5. This suggests that the minimal binding unit needed for both fingers of the TZF domain is the nonamer sequence UUAUUUAUU. Figure adapted from Blackshear *et al.* 2003 (67).

Tandem binding of the TTP TZF domain peptide to two binding sites was present in probes 1 and 4, most likely due to the probes containing two UUAUUUAUU nonamers (67). Blackshear and Wilson concluded from these studies that despite having a high affinity, there appeared to be no cooperativity between the tandem sites (67). The implications of having multiple binding sites within a single RNA probe are still not known, but data presented later in this thesis suggest that multiple ARE-binding sites may affect the steady state concentrations of certain RNA transcripts.

A follow-up study by the Wilson group quantitated the affinities of the TTP TZF domain to RNA probes containing varying binding sites using fluorescence anisotropy (68). Using this biochemical assay, the 13-base sequence of UUUUAUUUAUUUU had a calculated apparent binding affinity ( $K_d$ ) of 3.6 nM to the TTP TZF domain peptide at 24 °C. RNA probes containing two to five internal uridines between the two adenosines could bind to the TZF domain with lower but still high affinities as well. These data suggested that the TTP TZF domain could bind with reasonable affinity to sites different from the optimal sequence of UUUUAUUUAUUUU. Additionally, these reported binding affinities may not represent the binding affinities of other TZF domains or full-length TTP family members.

## 1.8 *Aim of Research*

Research into the interactions of full-length TTP family members with ARE-binding sites is lacking. Many of the studies presented in this introduction relied on overexpression of TTP in cellular lysates, or a synthetic TZF domain peptide, to explore the binding characteristics of TTP and its family members to RNA sequence elements. The aim of this thesis is to study the binding characteristics of the full-length Zfs1, the only TTP family member expressed in *C. albicans*. In this thesis, I will address these questions through the following aims:

1. Determine the binding affinities of full-length Zfs1 with canonical and variant binding sites found within AREs. Additionally, demonstrate if varying ionic conditions affect Zfs1 binding with canonical and variant TTP family member binding sites. (Chapters 2-4)
2. In RNA probes containing multiple TTP family member binding sites, determine if there are multiple binding events between Zfs1 and these target sites. If so, determine if binding cooperativity exists for Zfs1 associating with binding sites. (Chapters 3-4)
3. Explore the possibility of oligomerization of full-length *C. albicans* Zfs1 when bound to RNA probes containing one or two TTP family member binding sites. (Chapter 5)

4. Attempt to elucidate the structural determinants of the Zfs1-RNA complex. In association with this aim, attempt to identify Zfs1 protein binding partners using biochemical techniques. (Chapter 7, Appendix)

Upon analyzing these data, we hope to further understand the selectivity of TTP and its family members for certain ARE-binding sites. Furthermore, the data may provide insights into how these proteins interact with binding sites within AREs on a biochemical level. This information will be influential in revealing the dynamic and complex nature of post-transcriptional regulation by TTP and its family members.

## **2. Post-transcriptional Regulation of Transcript Abundance by a Conserved Member of the Tristetraprolin Family in *C. albicans***

Section adapted from the following paper:

Melissa L. Wells<sup>1</sup>, Onica L. Washington<sup>1</sup>, Stephanie N. Hicks<sup>1</sup>, Clarissa J. Nobile<sup>2</sup>, Nairi Hartooni<sup>2</sup>, Gerald M. Wilson<sup>3</sup>, Beth E. Zucconi<sup>3</sup>, Weichun Huang<sup>4</sup>, Leping Li<sup>4</sup>, David C. Fargo<sup>5</sup>, and Perry J. Blackshear<sup>1,6,#</sup>

<sup>1</sup>Laboratory of Signal Transduction, <sup>4</sup>Biostatistics Branch, <sup>5</sup>Integrative Bioinformatics, National Institute of Environmental Health Sciences, Research Triangle Park, NC 27709, <sup>2</sup>School of Natural Sciences, University of California, Merced, CA 95343, <sup>3</sup>Department of Biochemistry and Molecular Biology, University of Maryland School of Medicine, Baltimore, MD 21201; and <sup>6</sup>Departments of Medicine and Biochemistry, Duke University Medical Center, Durham, NC 27710.

### **2.1 Introduction**

TTP family members (as previously described in the introduction) have been studied in the fungal organisms *Saccharomyces cerevisiae* and *Schizosacchroymyces pombe*. *S. pombe* expresses a single TTP family member called Zfs1, whereas *S. cerevisiae* expresses two TTP family members, Cth1 and Cth2 (56,57). Despite a similar function of binding to ARE-sites within the 3'-UTRs of select transcripts, *S. cerevisiae* Cth1 and Cth2, and *S. pombe* Zfs1, each seems to regulate its own set of transcripts. To further study this

phenomenon, deletion mutants of *ZFS1*, the single TTP family member expressed in *C. albicans*, were evaluated for up-regulated transcripts containing potential TTP family member binding sites.

*C. albicans* and its family members belong to the “CTG clade” of fungi. Members of this clade translate the CTG codon as a serine, not a leucine (58). *C. albicans* has three major forms: yeast, pseudo-hyphae, and hyphae, with the hyphal form being the most virulent form of *C. albicans* (59). *C. albicans* has been shown to cause superficial infections of the mucosal membranes of humans, such as oral thrush. In immunocompromised populations (patients with HIV/ AIDS, patients undergoing chemotherapy, or transplant patients), *Candida* infections can become systemic. Studies have reported mortality rates between 30%-50% in this patient population due to invasive candidiasis (59).

*C. albicans* expresses a single TTP family member that we named *Zfs1* as an orthologue of the *S. pombe* protein. Unlike *Zfs1* found in *S. pombe*, which is 404 amino acid residues in length, *C. albicans* *Zfs1* is one of the smaller TTP family members found in any eukaryote at only 204 amino acid residues. Additionally, *Wells et al.* found that *C. albicans* *Zfs1* does not regulate transcripts for proteins involved in iron metabolism, roles played by *Cth1* and *Cth2* in *S. cerevisiae* (48); however, *ZFS1* expression was up-regulated at the yeast hyphal switch (69), which could be important for *C. albicans*

virulence. Furthermore, *ZFS1* is upregulated at specific times during biofilm formation, suggesting a role in biofilm growth and maturation (70).

Wells *et al.* explored the physiological role of *Zfs1* in *C. albicans* using mutant deletion strains. Two independent deletion strains were constructed to evaluate the effects of *ZFS1* on fungal physiology. The double deletion mutants were viable and showed no growth defects when compared to WT, but there was a slight increase of cells in stationary phase (61). Studies have established that stationary phase cells can increase adherence, virulence, and drug resistance (71,72), and it was reasonable to assume that *Zfs1* would be involved in *C. albicans* virulence. Furthermore, Wells and Blackshear observed an enhancement of biofilm formation in the *zfs1*  $\Delta/\Delta$  mutants as compared to wild type strains (61). *Candida albicans* biofilms have been shown to adhere to medical devices and to be drug resistant (73,74). Studies have linked *Candida albicans* biofilms to high morbidity and mortality rates (73,74). Despite the enhancement of biofilm formation in the *zfs1*  $\Delta/\Delta$  mutant strains, studies have concluded that deletion of *ZFS1* has no effect on *C. albicans* virulence in mice (75).

Wells *et al.* also explored whether *C. albicans* *ZFS1* could be involved in cell-cell adhesion, as in *S. pombe* (49). Deletion of *S. pombe* *ZFS1* resulted in self-aggregation of the cells, or flocculation, upon the addition of calcium (49). *C. albicans* *zfs1*  $\Delta/\Delta$  mutants remained completely suspended in liquid media upon the addition of calcium (61).

These data suggest that, unlike *S. pombe* *ZFS1*, *C. albicans* *ZFS1* is not obviously involved in cell-cell adhesion.

Transcript changes in *C. albicans* were analyzed using mRNA-Seq analysis. Wells *et al.* determined that, of the *C. albicans* transcriptome, 17% of transcripts contain at least one 7-mer potential binding site (UAUUUAU), the minimum TTP binding site. They found that *zfs1*  $\Delta/\Delta$  mutants had only 56 transcripts significantly up-regulated by 2-fold or more as compared to WT strains. Of the 56 transcripts, 44 contained the optimal core sequence UAUUUAU binding site and many of these transcripts contained 9-mer or overlapping binding sites. 156 up-regulated transcripts were identified using a 1.5 fold cutoff, and 113 of these contained the 7-mer binding site UAUUUAU (61).

The question still remained whether or not Zfs1 bound with high affinity to the known optimum binding sequence for the TTP TZF domain. To address this, I recombinantly expressed and purified maltose binding protein (MBP)-tagged full-length Zfs1. MBP-tagged full-length Zfs1 was shown to bind to the RNA sequence element UUUUAUUUAUUUU with low nanomolar affinity (61). The sequence element UUUUAUUUAUUUU has also been reported as the optimal binding site for the TTP TZF domain (67,68). These data suggest a conserved biochemical mechanism of RNA sequence element recognition by TTP and TTP family members.

## **2.2 Materials and Methods**

2'-OH de-protected and purified RNA nucleotides were purchased from Dharmacon, Inc. (Lafayette, CO). RNA oligonucleotides incorporating 5' labeled tags with biotin (Bi) or fluorescein (FL) are indicated by the aforementioned prefixes.

### **2.2.1 Plasmid Construction and Protein Purification of Recombinant MBP-tagged Full-Length Zfs1**

Full-length *C. albicans* Zfs1 (GenBank accession XM\_712044) was cloned into a modified pMALX vector (a gift from Lars Pedersen) (76). Protein was expressed as a maltose-binding protein (MBP) fusion protein linked to the N-terminus of Zfs1 by a 3-alanine linker. Correct insertion of the full-length genes was verified by gene sequencing (Genewiz, Research Triangle Park, NC). The vector was transformed into *E. coli* One Shot® BL21(DE3) cells (ThermoFisher Scientific, Waltham, MA). Protein expression was induced upon the cells reaching an A<sub>600</sub>=0.7-0.9 by the addition of 0.3 mM isopropyl β-D -1-thiogalactopyranoside (IPTG) for 16 hours at 16 °C. Recombinant MBP-Zfs1 was purified from cell lysates using amylose affinity chromatography. Protein was eluted off resin by the addition of buffer (20 mM HEPES (pH 7.6), 300 mM NaCl, 5% glycerol, 10 mM BME, and 25 μM ZnSO<sub>4</sub>) with 70 mM maltose. The eluate was diluted into phenyl column buffer (20 mM HEPES (pH 7.6), 1.0 M NH<sub>4</sub>SO<sub>2</sub>, 5% glycerol, 10 mM BME, and 25 μM ZnSO<sub>4</sub>) in a ratio of 1.0:4.0 (eluate to buffer) and applied onto a HiTrap Phenyl HP column (GE Healthcare Life Sciences, Pittsburg, PA).

A high-salt to low-salt gradient was run and the recombinant protein eluted toward the end of the gradient. Size-exclusion chromatography was done using a buffer of 20 mM HEPES (pH 7.6), 300 mM NaCl, 5% glycerol, 10 mM BME, and 25  $\mu$ M ZnSO<sub>4</sub> and a HiLoad16/600 Superdex column (GE Healthcare Life Sciences, Pittsburg, PA). Protein fractions corresponding to the predicted protein molecular weight of 64000 Da were selected and pooled. Purified protein was concentrated in a final buffer (20 mM HEPES (pH 7.6), 100 mM KCl, 5% glycerol, 25  $\mu$ M ZnSO<sub>4</sub>, 10 mM BME) to 5 mg/mL and checked for purity on SDS-PAGE. Fractions were concentrated using a 10,000 molecular weight cut-off (MWCO) Vivaspin 20 centrifugal filtering device (GE Healthcare). Purified protein was aliquoted into 25  $\mu$ l samples, flash frozen in liquid nitrogen, and then stored at -80 °C for future use.

### **2.2.2 Preparation of RNA Substrates for Biochemical Assays**

5' biotinylated-labeled, 5' fluorescein-labeled, or unlabeled RNA oligonucleotides used in these experiments were purchased from Dharmacon, Inc. (Lafayette, CO). Lyophilized pellets were resuspended in 10 mM Tris (pH 8.0) and stored at -80 °C in aliquots of 35  $\mu$ l. Probes were diluted 1:20 in 10 mM Tris (pH 8.0) and concentration was checked by spectrometry before utilization in fluorescence anisotropy or EMSA.

### **2.2.3 RNA Electrophoretic Mobility Gel Shift (EMSA)**

The protein-RNA complexes were monitored using EMSA as described previously (77). Binding reactions were carried out in binding buffer (20 mM HEPES, pH 7.6, 50 mM KCl, 5% glycerol, 2.5  $\mu\text{g}/\mu\text{l}$  heparin, 50  $\text{ng}/\mu\text{l}$  yeast tRNA, 3.0 mM  $\text{MgSO}_4$ ) containing 3.0 nM of 5' biotinylated RNA and 75 nM of MBP-tagged full-length Zfs1. 20  $\mu\text{l}$  binding reactions were equilibrated at room temperature for 20 mins before running on a 10% Criterion Tris Borate EDTA (TBE) gel (Bio-Rad, Hercules, CA) at 4°C in 0.4X TBE buffer at 190V for 80 mins. The gel was then transferred onto a Biotodyne B Nylon Membrane (Life Technologies, Carlsbad, CA) using 0.4X TBE buffer and run at 90V for 45 mins. The protein-RNA complexes were crosslinked to the membrane using a Stragene UV Stratalinker 1800 UV Crosslinking Chamber (La Jolla, CA). The membrane was probed and developed following the instructions for the Chemiluminescent Nucleic Acid Detection Module Kit (ThermoFisher Scientific, Waltham, MA).

### **2.2.4 Fluorescence Anisotropy**

#### **Determination of apparent dissociation constants using fluorescence anisotropy**

Fluorescence anisotropy experiments were performed as previously described (77). Binding reactions (1.0 mL) were prepared using conditions similar to EMSA experiments (excluding glycerol). The reactions were incubated for 2 mins at room

temperature to ensure equilibrium, and total anisotropy measurements and fluorescence intensities were measured on a Beacon 2000 Variable Temperature Fluorescence Polarization System (Panvera, Madison, WI) containing fluorescein excitation ( $\lambda_{\text{ex}}=490$  nm) and emission ( $\lambda_{\text{em}}=535$  nm) filters. Anisotropy was measured over 1 min and averaged, as this has been shown to be sufficient to reach equilibrium binding (68). Total fluorescence emission was measured to verify that protein binding did not alter the fluorescence quantum yield of fluorescein-labeled RNA probes ((data not shown) (67)).

Total measured anisotropy ( $A_r$ ) was measured over a range of protein concentrations and 0.2 nM or 2.0 nM of FL-5' labelled RNA oligonucleotides (10-fold below known  $K_d$ ). Binding constants were calculated by the nonlinear regression algorithm in PRISM, version 6.0 (GraphPad Software), using Equation 1 (77).

$$A_t = \frac{A_R + A_{PR}K[P]}{1 + K[P]}$$

**Equation 1**

$K$  represents the apparent equilibrium constant ( $K$ ;  $K=1/K_d$ );  $A_R$  and  $A_{pr}$  are the intrinsic anisotropy values of free RNA and the protein-fluorescein-labeled RNA complex, respectively;  $[P]$  is protein concentration. Data are plotted as  $\Delta$ anisotropy, the

change between the anisotropy of the probe alone and the total anisotropy measured at each protein concentration using Microsoft Excel (2010).

## **2.3 Results**

### **2.3.1 Expression and Purification of Recombinant MBP-tagged Full-Length Zfs1**

Full-length TTP and its family members have been difficult to recombinantly express using standard expression hosts, probably because they contain unstructured regions. Unstructured elements can cause protein insolubility or degradation during the purification process. For these reasons, most previous studies have used lysates containing overexpressed TTP or its family members (41,63) for biochemical assays, or TTP family member binding site affinity was determined through the use of a synthetic peptide of the human TTP TZF domain (67). We proposed that the *C. albicans* TTP family member, *Zfs1*, as one of the shortest known TTP family members (204 amino acids), might be more amenable to recombinant expression and purification.

We fused the large carrier protein MBP with *Zfs1* to increase its expression and solubility. Despite having a molecular weight of 42000 Da, MBP can serve as a powerful tool to aid in the process of protein expression and solubility. We were given a pMALx vector (Pedersen lab) expressing an MBP protein modified using surface entropy reduction (SER) (76). Using SER, the Pedersen group was able to mutate large hydrophilic residues with large entropic values to small, non-polar amino acids in an

effort to reduce the total surface entropy of the MBP protein (76). The linker between the MBP tag and the fusion protein was able to be lengthened or shortened to reduce the flexibility between the tag and the fusion, thereby affecting protein expression (76). In our studies, a 3-alanine linker was used to separate MBP and Zfs1 in an attempt to increase protein expression and solubility as well as reduce protein degradation during purification.

To test this strategy using Zfs1, constructs were made using a modified MBP tag N-terminally fused to full-length Zfs1 by a 3-alanine linker. Solubility and expression tests were done with the MBP-Zfs1 and MBP-Zfs1-TZF domain constructs. Soluble protein from both constructs was expressed, using BL21(DE3) competent *E.coli* induced with 0.1 mM IPTG, overnight at 15-17 °C. Expression of these constructs also led to small amounts of MBP being co-purified with fusion protein when using affinity purification. Addition of a final concentration of 0.1%-0.3% glucose (w/v) to media before induction reduced the amount of free MBP expression. *Candida* Zfs1 was also expressed with an MBP tag containing a Tobacco Etch Virus (TEV) cleavage site. However, only small amounts of free, untagged *Candida* Zfs1 could be obtained using the MBP-TEV construct (possibly due to steric hindrance at the TEV cleavage site). The small amount of free, untagged Zfs1 protein obtained was shown to aggregate and elute in the void volume during size exclusion chromatography experiments.

MBP-tagged full-length Zfs1 was purified using affinity, hydrophobic, and size-exclusion chromatography to obtain 85%-90% purified protein. Initially, 2.0-3.0 mg of purified, soluble protein was obtained from 15 liters of media. A method of double selection of high-expressing MBP-tagged full-length Zfs1 colonies was used in later studies to increase expression of the recombinant protein (Chapter 3).

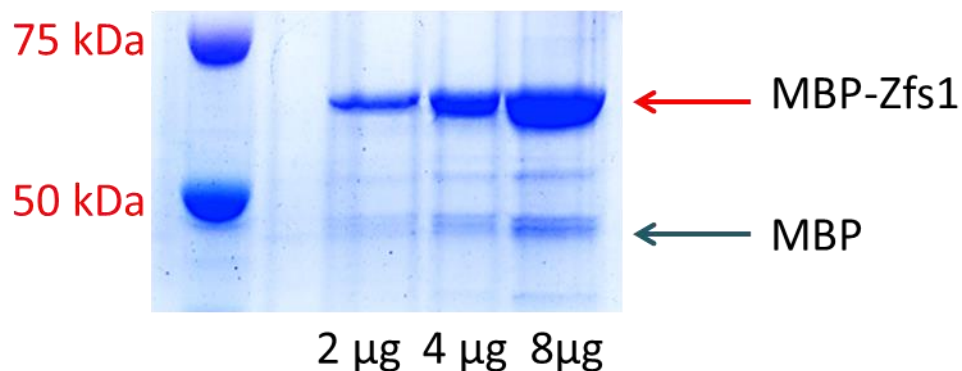


**Figure 8. Purified MBP-tagged Full-Length Zfs1 at Amounts of 2, 4, and 8 µg**

Purified MBP-tagged full-length Zfs1 aliquots were run on a 10-20% Tris-HCl precast gel (Bio-Rad, Hercules, CA) using SDS polyacrylamide gel electrophoresis (PAGE). The red arrow denotes purified MBP-Zfs1 protein (64 kDa) and the blue arrow denotes free MBP (42 kDa).

### **2.3.2 Characteristics of Binding of MBP-tagged Full-Length Zfs1 to an RNA Oligonucleotide Containing a Single Binding Site**

Previous studies have shown high affinity binding between a 73-amino acid synthetic peptide comprising TTP TZF domain, termed TTP73, and RNA targets containing AREs (68). Specifically, the human peptide bound to the optimum TTP binding sequence UUAUUUAUU with a binding affinity of 3.2 nM at 24 °C (68).

Deviations from this optimum sequence decreased the binding affinities of the TTP TZF domain peptide for RNA probes (68). To determine whether the *C. albicans* TTP family member could bind to similar RNA sequences with similar affinity, we recombinantly expressed MBP-tagged full-length Zfs1 in *Escherichia coli* as described above. The purified protein was then utilized for binding measurements to a similar RNA oligonucleotide using fluorescence anisotropy under steady-state conditions. For these studies we used the 13-base fluorescein-labeled RNA probe (5'-FL-UUUUAUUUAUUU-3'; FL-ARE13) and the purified *C. albicans* Zfs1 full-length protein with an MBP tag fused to the N-terminus (68). Strikingly, similar to the human TTP73 peptide, the purified full-length MBP-tagged Zfs1 fusion protein bound with a  $K_d$  of 1.8 nM at 24 °C to the FL-ARE13 probe, with a stoichiometry of 1:1 for the protein-RNA complex (Figure 9). I observed essentially no binding of the purified MBP-Zfs1 to the control poly(U) probe (5'-FL-UUUUUUUUUUUUUU-3').

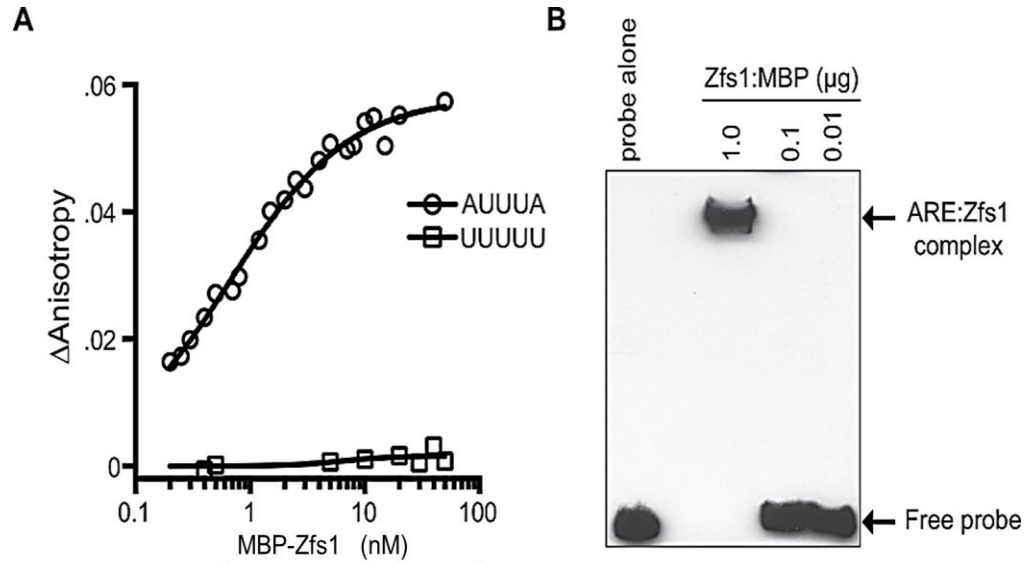


**Figure 9. Measurement of MBP-Zfs1 RNA-Binding Affinity Using Fluorescence Anisotropy**

**A.** Binding reactions containing the 13-base fluorescein-labeled RNA target (5'-FL-UUUUAUUUAUUUU-3'; FL-ARE13) or the control poly(U) probe (5'-FL-UUUUUUUUUUUUU-3') and a titration of purified MBP-Zfs1 were mixed and fluorescence polarization and intensity were monitored. A nonlinear regression algorithm in PRISM was used to calculate Zfs1-dependent changes in anisotropy.  $\Delta$ Anisotropy was calculated as anisotropy for probe alone subtracted from total anisotropy measured at each protein concentration.

**B.** Increasing concentrations of purified MBP-Zfs1 or no protein (probe alone) were used in a gel shift analysis with a 5' biotin-labeled TNF $\alpha$  ARE probe. Arrows to the right indicate migration positions of the ARE probe and the MBP-Zfs1ARE probe complex.

No fluorescence quenching was observed over the course of the experiments

(data not shown). We also performed gel shift analyses using varying concentrations of purified MBP-Zfs1 and a TNF $\alpha$  ARE-based RNA probe (20). Incubation of 1.0  $\mu$ g of the purified MBP-Zfs1 fusion protein with the probe resulted in the complete shifting of the

protein into a single band complex, whereas no shift was detectable at lower protein concentrations.

These data demonstrate that the optimum binding site found in the studies of human TTP, UUUUAUUUAUUUU, is also a high-affinity binding site for full-length *C. albicans* Zfs1 (61,68). It is still not known if UUUUAUUUAUUUU is the optimal ARE-binding site for MBP-Zfs1. Further studies with modified oligonucleotides will be necessary to determine the optimal binding site of MBP-Zfs1 and if target site sequence specificity is similar between the mammalian and fungal TTP family members.

## **2.4 Discussion**

Through utilization of a modified pMALx vector we cloned, expressed, and purified Zfs1, the full-length TTP family member found in *C. albicans*. Full-length Zfs1 was expressed as a fusion protein linked N-terminally by a 3-alanine linker to a modified MBP molecule. Expression of MBP-tagged full-length Zfs1 (MBP-Zfs1) increased the solubility of Zfs1 and enhanced protein purification through the use of affinity chromatography and other biochemical purification methods. 2.0-3.0 mg of MBP-Zfs1 were typically purified from 10 liters of culture; however, this was not enough protein to facilitate further investigations of the binding of MBP-Zfs1 with RNA sequence elements. Therefore, later chapters describe methods developed to increase

expression of MBP-Zfs1 and the MBP-Zfs1 TZF domain fusions for use in future experiments.

The TTP family members expressed in *S. pombe* and *S. cerevisiae* have been shown to regulate transcripts containing ARE-binding sites (48,53), suggesting a biochemical mechanism similar to that found in the mammalian TTP family members. Using fluorescence anisotropy assays, *Candida* MBP-Zfs1 bound the sequence of UUUUAUUUAUUUU with similar affinity to that of the TTP TZF domain peptide (TTP73) (68). These data suggest that, despite sequence differences between the TTP TZF domain peptide and fungal TTP family members of the “CTG” clade, these widely separated TTP family members have evolved a similar biochemical mechanism of association to ARE-binding sites. Recent studies by the Blackshear group have also demonstrated high affinity binding of the TZF domains from the TTP family members found in the yeast *Meyerozyma guilliermondii* and the chytrid fungus *Spizellomyces punctatus* to the probe containing the sequence UUUUAUUUAUUUU (62). They further showed that the TZF domains from distant species, including plants, could complement the function of the TZF domain of *S. pombe* Zfs1 in vivo (62). These data demonstrate that the TZF domains from very different species have retained the ability to bind similar sites within AREs located in the 3'-UTR of transcripts. Additionally, the data presented here indicates that a full-length TTP family member can bind with similar

high affinity to an RNA site previously seen for TZF domains from different species. We conclude from the data presented here that the TZF domains are responsible for high affinity binding to sites within AREs; however domains outside the TZF domain could still be important in recruitment of protein binding partners essential for mRNA decay.

Future experiments will be needed to validate the UUAUUUAUU sequence as the optimal ARE-binding site for MBP-Zfs1. In the chapters that follow, I will determine the binding affinities of MBP-Zfs1 to variant ARE-binding sites using fluorescence anisotropy. These studies may further our understanding of Zfs1-mediated transcript decay, and the need to include non-canonical binding sites in mRNA-Seq analyses to determine potential new TTP family member transcript targets.

### **3. Full-length *C. albicans* Tristetraprolin Family Member, Zfs1, Binds to Non-Canonical AREs**

#### **3.1 Introduction**

Tristetraprolin (TTP), a *trans*-acting RNA-binding protein and the prototypical family member of a group of tandem CCCH zinc finger proteins, has been demonstrated to destabilize and promote transcript deadenylation and degradation (as previously discussed in the introduction) (37,41,78-80). Studies have demonstrated that association of TTP with ARE-binding sites is mediated through the tandem CCCH zinc finger domain (TZF domain) (41,63,81). To help elucidate the binding selectivity of the TTP TZF domain, a synthetic TTP peptide named TTP73 was created to examine the binding of the TTP TZF domain with RNA sequence elements having the core AUUUA sequence. The TTP TZF domain bound to the sequence UUAUUUAUU with a binding affinity of 3.2 nM at 24 °C (68). Strikingly, the TZF domains of TTP family members share high degrees of sequence conservation, which suggests that they have similar biochemical mechanisms of targeting and association to ARE-binding sites. To test this hypothesis, binding of the recombinant TZF domain peptide of the *S. pombe* TTP family member, Zfs1, was examined with fluorescence anisotropy using a 13-base fluorescein-labeled RNA oligonucleotide having the sequence 5'-FL-UUUUAUUUAUUUU-3' (FL-ARE 13). The Zfs1 TZF domain of *S. pombe* bound with high affinity ( $1.2 \pm 0.1$  nM;

binding constant measured at 24 °C) to the probe (62), demonstrating that the *S. pombe* Zfs1 TZF domain associated with the optimum ARE-binding site of TTP with an affinity similar to that determined for the TTP TZF domain (68).

Additional studies determined the binding affinities of the TTP TZF domain peptide with non-canonical TTP family member binding sites. The binding of the human TTP TZF domain peptide was examined using fluorescein-labeled RNA oligonucleotides that contained expanding or decreasing poly(U) sequences between the two adenosines. The human TTP TZF domain (TTP73) bound with highest affinity to the FL-ARE13 probe, but high-affinity binding was also measured with the probes FL-5'-UUUUAUUUUAUUUU-3' (FL-ARE14) and FL-5'-UUUUAUUUUUAUUUU-3' (FL-ARE15) ( $K_{as}$ =6.4 nM and 17 nM, respectively at 24 °C) (68). Conversely, binding affinities decreased with a decreased number of uridines within the AUUUA core, as in the probe FL-5'-UUUUAUAUUUU-3' (FL-ARE11), or FL-5'-UUUUAUUAUUUU-3' (FL-ARE12), which had measured binding affinities of 160 nM and 18 nM, respectively, to the TTP TZF domain synthetic peptide (binding constants measured at 24 °C) (68). These data were obtained with the TZF domain peptide; the binding characteristics of a full-length TTP family member to variant ARE-binding sites are not known. To address this question, I used fluorescent anisotropy to determine the binding affinities of non-

canonical ARE-binding sites to the full-length *C. albicans* TTP family member, Zfs1, fused to MBP.

*C. albicans* expresses a single TTP family member (204 amino acid residues in length) called Zfs1. *C. albicans* *zfs1* $\Delta/\Delta$  mutants are viable and only exhibited a slight increase in biofilm formation compared to wild-type. There was also upregulation of transcripts containing one or more copies of the 7-mer sequence UAUUUUAU in *zfs1* $\Delta/\Delta$  mutants, which suggests that there is targeting of these transcripts by Zfs1 (61). I recombinantly expressed and purified the full-length Zfs1, using a vector encoding an N-terminal maltose-binding protein (MBP) for use in affinity chromatography (as demonstrated in Chapter 2). I found that MBP-tagged full-length Zfs1 could bind with  $K_d$  of 1.8 nM at 24 °C to the RNA oligonucleotide FL-ARE13 (61), a high-affinity association similar to that described for this oligonucleotide to the TTP TZF domain (68). Utilizing purified MBP-Zfs1, I determined the binding affinities of a full-length TTP family member to probes containing single ARE sites containing varying numbers of uridines between two adenosines. I concluded that the FL-ARE13 sequence is the optimum ARE-binding site for full-length Zfs1, *in vitro*, but that varying intracellular conditions could influence Zfs1 selectivity of transcripts containing variant binding sites. These data suggest the possibility that the association of TTP family members with non-

canonical binding sites within AREs can destabilize target transcripts containing these sites, and possibly promote transcript deadenylation and decay *in vivo*.

## **3.2 Materials and Methods**

2'-OH de-protected and purified RNA nucleotides were purchased from Dharmacon, Inc. (Lafayette, CO) as described in section 2.2.

### **3.2.1 Plasmid Construction and Protein Purification**

Full length *C. albicans* Zfs1 (GenBank accession XM\_712044) was cloned and expressed as previously described in section 2.2.1.

#### **3.2.1.A. Double selection of high-expressing clones for optimal protein expression**

Full length *C. albicans* Zfs1 (GenBank accession XM\_712044) was cloned as previously described in section 3.2.1. Correct insertion of the full length genes was verified by sequencing (Genewiz, Research Triangle Park, NC). The vector was then transformed into One Shot® BL21(DE3) cells as instructed per protocol (ThermoFisher Scientific, Waltham, MA). Cells were spread on a selection plate (100 µg/µl ampicillin) and incubated overnight at 37 °C. Four colonies were resuspended into liquid cultures containing 0.3 mM ampicillin. Cultures were allowed to shake at 37 °C until a maximum optical density (OD) of 0.6 was obtained. 1 mL samples were taken from each culture and stored at 4 °C. Cultures were then induced with 0.3 mM IPTG and incubated overnight at 16 °C. The following day, cells were lysed and checked for

protein expression using SDS-PAGE. The 1 mL sample obtained from the highest expressing colonies from the previous day was diluted and spread on a selection plate. Double selection was repeated as previously described (with another 1 mL sample being stored at 4 °C). Samples were checked again for protein expression using SDS-PAGE. The 1 mL samples (stored previously at 4 °C) identified as being from the highest expressing colony after the second round of selection were aliquoted into four 250 µl samples and mixed 1:1 with 50% v/v glycerol. The samples were then labeled and stored at -80 °C for future use.

### **3.2.2 Preparation of RNA Substrates for Biochemical Assays**

5' biotinylated or unlabeled RNA oligonucleotides used in experiments were purchased and prepared as previously mentioned in section 2.2.2.

### **3.2.3 RNA Electrophoretic Mobility Gel Shift (EMSA)**

The protein-RNA complexes were monitored using EMSA as previously described (77) and as written in section 2.2.1, with the exception that the binding buffer contained 200 mM KCl.

### **3.2.4 Fluorescence Anisotropy**

#### **Determination of apparent dissociation constants using fluorescence anisotropy**

Fluorescence anisotropy experiments were performed as previously described (77). Binding reactions (1.0 mL) were prepared using conditions similar to EMSA

experiments (excluding glycerol). Experiments were conducted with the indicated amounts of KCl to examine the effects of ionic strength on the protein-RNA dissociation constants. Reactions were incubated for 2 mins at room temperature to ensure equilibrium was reached before total anisotropy measurements and fluorescence intensities were measured on a Beacon 2000 Variable Temperature Fluorescence Polarization System (Panvera, Madison, WI) containing fluorescein excitation ( $\lambda_{ex}=490$  nm) and emission ( $\lambda_{em}=535$  nm) filters. Anisotropy was measured over 1 min and averaged, as this has been shown to be sufficient to reach equilibrium binding (68). Total fluorescence emission was measured to verify that protein binding did not alter the fluorescence quantum yield of fluorescein-labeled RNA probes ((data not shown) (67)).

Total measured anisotropy ( $A_t$ ) was measured over a range of protein concentrations and 0.2 nM or 2.0 nM of FL 5' labelled RNA oligonucleotides. Binding constants were calculated by the nonlinear regression algorithm in PRISM, version 6.0 (GraphPad Software) using Equation 1 (77).

$$A_t = \frac{A_R + A_{PR}K[P]}{1 + K[P]} \quad \text{Equation 1}$$

Where  $K$  represents the apparent equilibrium constant ( $K; K=1/K_d$ );  $A_R$  and  $A_{pr}$  are the intrinsic anisotropy values of free RNA and the protein-fluorescein-labeled RNA

complex, respectively; and  $[P]$  is protein concentration. Data are plotted as  $\Delta$ anisotropy, the change between the anisotropy of the probe alone and the total anisotropy measured at each protein concentration, using Microsoft Excel (2010).

### **3.3 Results**

#### **3.3.1 Binding Affinities of MBP-Zfs1 to Non-Canonical TTP Family Member Binding Sites are Affected by Buffer Ionic Salt Concentrations**

The Wilson group showed that the synthetic TTP TZF domain peptide (TTP73) could bind to fluorescein-labeled RNA probes containing variant Class I ARE-binding sites with reasonably high affinities (68). TTP73 bound to the optimal sequence of FL-5'-UUUUAUUUAUUUU-3' (FL-ARE13) with a  $K_d$  of 3.2 nM at 24 °C (measured in 100 mM KCl). The synthetic peptide was further shown to bind to the fluorescein probes having the sequences of FL-5'-UUUUAUUUAUUUU-3' (FL-ARE12), FL-5'-UUUUAUUUUUAUUUU-3' (FL-ARE14), and FL-5'-UUUUAUUUUUAUUUU (FL-ARE15) with  $K_d < 100$  nM (68) (Table 1). The TTP73 peptide could bind the probes FL-5'-UUUUAUAUUUU-3' (FL-ARE11) and FL-5'-UUUUUUUUUUU-3' (poly(U)) with considerably lower affinity (Table 1). These data established that the synthetic TTP TZF domain peptide could bind to variant ARE sequences containing two to five internal uridines within the AUUUA core with low nanomolar affinity, suggesting that

transcripts containing these variant ARE sites could be potential targets of TTP-mediated transcript decay *in vivo*.

However, it was possible that the binding affinities of a TZF domain peptide to non-canonical ARE sites could be different from the binding affinities of a full-length TTP family member protein to these same sites. To address this question, I determined the binding affinities of the full-length *C. albicans* TTP family member, Zfs1, to the same variant AREs using fluorescence anisotropy. I also wanted to explore the effects of ionic strength on the binding affinities of the MBP-Zfs1-RNA complex to variant Class I AREs.

**Table 1. Equilibrium Binding of MBP-Zfs1 to Variant Class I AREs as Compared to the TTP TZF domain Synthetic Peptide (TTP73) (68)**

RNA probes	RNA probes (Abbreviated titles)	K <sub>a</sub> of MBP-Zfs1 at 25 ° C in 50 mM KCl	K <sub>a</sub> of MBP-Zfs1 at 25 ° C in 150 mM KCl	K <sub>a</sub> of TTP73 at 25 ° C in 100 mM KCl (from ref. 74)
5' FL-UUUUUUUUUUU 3'	Poly(U)	>1000	>1000	280 nM
5' FL-UUUUAUAUUUU 3'	FL-ARE11	677.0 ± 145.5 nM	>1000.0 nM	160 nM
5' FL-UUUUAUUUUUU 3'	FL-ARE12	60.2 ± 7.0 nM	604.7 ± 146.6 nM	18 nM
5' FL-UUUUAUUUUUU 3'	FL-ARE13	1.2 ± 0.1 nM	9.4 ± 1.7 nM	3.2 nM
5' FL-UUUUAUUUUUU 3'	FL-ARE14	1.8 ± 0.2 nM	141.7 ± 22.6 nM	6.4 nM
5' FL-UUUUAUUUUUU 3'	FL-ARE15	5.9 ± 1.7 nM	264.6 ± 28.7 nM	17 nM

All fluorescence anisotropy measurements were made at 25 °C in salt concentrations denoted in Table 1. An average of three independent experiments were measured for each probe in each salt concentration. Values are mean ± standard deviation.

In 50 mM KCl, MBP-Zfs1 bound to the RNA probes FL-ARE13, FL-ARE14, and FL-ARE15 with steady state dissociation constants of  $1.2 \pm 0.1$  nM,  $1.8 \pm 0.2$  nM, and  $5.9 \pm 1.7$  nM, respectively (Table 1). MBP-Zfs1 also associated with the sequence FL-ARE12 with an affinity of  $60.2 \pm 7.0$  nM, which was nearly 60-fold lower than the binding affinities of the FL-ARE13 and FL-ARE14 RNA oligonucleotides and 10-fold lower than the binding affinity of FL-ARE15. The poly(U) and FL-ARE11 RNA probes exhibited weak or no binding affinity for MBP-Zfs1, with  $K_{as}$  of  $677.0 \pm 145.5$  nM and  $>1000$  nM, respectively.

In 150 mM KCl, MBP-Zfs1 showed a weaker binding affinity for all RNA oligonucleotides. FL-ARE13 remained the optimum binding site ( $9.2 \pm 1.7$  nM). At higher KCl concentrations, MBP-Zfs1 had moderate affinity for the probes FL-ARE14 and FL-ARE15 ( $141.7 \pm 22.6$  nM and  $264.6 \pm 28.7$  nM, respectively). Likewise, there was a weakened interaction between FL-ARE12 and MBP-Zfs1. The binding affinity of FL-ARE12 to MBP-Zfs1 was measured at  $604.7 \pm 146.6$  nM, 10-fold weaker than the dissociation constant measured of FL-ARE12 in 50 mM KCl, suggesting that at this ionic strength, FL-ARE12 is not a likely TTP family member binding site *in vivo*. The RNA oligonucleotides poly(U) and FL-ARE11 were determined to have micromolar affinity with MBP-Zfs1 at high salt and, like FL-ARE12, are not considered to be likely ARE binding sites with MBP-Zfs1 *in vivo*.

### **3.4 Discussion**

Several experimental techniques have suggested that UUAUUUAUU is the optimal binding sequence of TTP73, a synthetic peptide of the TTP TZF domain (68). Fluorescent anisotropy experiments further determined that TTP73 could bind with reasonably high affinity to oligoribonucleotides having two, four, or five uridines within the core ARE sequence of AUUUA (68). TTP73 bound to the poly(U) probe with an affinity of 280 nM and to the FL-ARE11 probe with an affinity of 160 nM at equilibrium conditions.

In this study, I determined the steady-state binding constants of a full-length TTP family member to optimal and non-canonical ARE sites. I demonstrated, using fluorescence anisotropy experiments, that the optimal ARE-binding site for MBP-Zfs1 is UUUUAUUUAUUUU. It seems likely that the MBP-Zfs1 TZF domain forms base-stacking interactions with the RNA, as seen within the solved structure of the ZFP36L2 TZF domain bound to UUAUUUAUU (65), and that the biochemical mechanisms of binding are similar. I further investigated the salt dependence of the binding affinities of the MBP-Zfs1-RNA complex. RNA is highly negatively charged, and cations in solution can neutralize the negatively charged phosphate backbone, potentially stabilizing RNA secondary structure (82). Measurements of the binding affinities of the TTP73 peptide with ARE-containing probes were taken in solutions of 100 mM KCl, a

non-physiological salt concentration used by Brewer and Wilson (68). To improve upon these earlier experiments, I measured the binding affinities of MBP-Zfs1 to AREs in 50 and 150 mM KCl. In 50 mM KCl, MBP-Zfs1 associated with reasonably high affinity to the probes FL-ARE12, FL-ARE13, FL-ARE14, and FL-ARE15, whereas it bound to the RNA oligonucleotides FL-ARE11 and poly(U) bound to MBP-Zfs1 with lower affinity. In a more physiological salt concentration of 150 mM KCl, MBP-Zfs1 still demonstrated high affinities for the probes FL-ARE13, FL-ARE14, and FL-ARE15. FL-ARE11 and poly(U) bound with low affinity to MBP-Zfs1, suggesting that they are not physiologically relevant ARE-binding sites. Additionally, FL-ARE12 bound with lower affinity to MBP-Zfs1 in 150 mM KCl than the other probes. These data suggest that electrostatic interactions are involved in the MBP-Zfs1-RNA association, as shown by the decreased binding affinities of MBP-Zfs1 to all RNA probes in 150 mM KCl than the others. However, the stronger forces of hydrogen bonding and pi stacking are likely to be essential for the high-affinity, stable protein-RNA interaction. It is possible that changing intracellular conditions mediate TTP family member selectivity for ARE sites. The eukaryotic cell is highly compartmentalized and it has been reported that both TTP family member proteins and mRNA can be shuttled among different compartments (83). Additionally, ions can be sequestered and stored in varying parts of the cell (84). These factors suggest that the cellular location of transcripts containing potential TTP family

member binding sites may regulate Zfs1-mediated decay. The data presented here illustrate that MBP-Zfs1 binds to FL-ARE13, FL-ARE14, and FL-ARE15 with high affinities in both low and high salt conditions, suggesting that transcripts containing these sequences could be targeted for Zfs1-mediated decay independent of ionic cellular conditions. On the other hand, the binding affinities of MBP-Zfs1 to the sequences of FL-ARE11 and FL-ARE12 are markedly decreased in higher salt concentrations. Taken together, these studies suggest including FL-ARE13, FL-ARE14, and FL-ARE15 sequences in screens for binding partners.

## **4. Characteristics of Binding of MBP-tagged, *Candida albicans* Full-Length Zfs1 to RNA Probes Containing Double and Overlapping ARE-Binding Sites.**

### **4.1 Introduction**

Post-transcriptional regulation of gene expression at the levels of mRNA stability and translation are effective mechanisms of controlling active amounts of protein within the eukaryotic cell. Control of mRNA stability through RNA sequences located in the 3'-UTR has been demonstrated to promote translation or degradation of transcripts. Among the best-known RNA sequence elements are adenosine-uridine rich elements (AREs). In conjunction with RNA-binding proteins, AREs have been shown to promote transcript destabilization. However, the associations of RNA-binding proteins like tristetraprolin (TTP) to AREs containing multiple overlapping binding sites have not been well defined. The studies described in this chapter investigated tandem and high-affinity binding of a full-length TTP family member to RNA probes containing adjacent and overlapping potential binding sites. These data expand our understanding of TTP family member selectivity for overlapping binding sites.

It has been estimated that 5.0-8.0% of the human transcriptome contains AREs containing potential 9-mer binding sites. AREs have been categorized into three classes: I, II, and III. Class I AREs are described as having 1 to 3 copies of the core AUUUA

motif scattered within the 3'-UTR, and represent 70% of all AREs within the human transcriptome (85). Class II AREs have at least two copies of the 9-mer sequence UUAUUUAU(U/A)(U/A). Class III AREs are defined as having uridine-rich regions; however, the exact features that make them targets of *trans*-acting RNA-binding proteins are not well understood (28).

Transcripts encoding cytokines were the first known targets of TTP- mediated decay. Cytokines are small, non-structural proteins that mediate the inflammatory response in higher eukaryotes (86). Although present in small amounts, these peptides and proteins are released by lymphocytes and monocytes in response to induction signals (86). Tumor necrosis factor alpha (TNF $\alpha$ ) and granulocyte-macrophage colony-stimulating factor (GM-CSF) are two cytokines with well-defined roles in the inflammatory cascade response. TNF $\alpha$ , released from white blood cells, recruits other white blood cells to sites of injury, promotes cellular apoptosis, and is pyrogenic (87). Chronic overexpression of TNF $\alpha$  has been implicated in rheumatoid arthritis, ankylosing spondylitis, Crohn's disease, and other diseases (88). The Blackshear lab first demonstrated that TTP-deficient mice developed a wasting syndrome along with loss of adipose tissue, dermatitis, conjunctivitis, and erosive arthritis. The phenotype of the TTP-deficient mice could be prevented by treatment with a TNF $\alpha$  antibody (35), suggesting that TTP regulated the production of TNF $\alpha$ . Later experiments determined

that the half-life of TNF $\alpha$  mRNA in TTP-deficient cells was significantly increased compared to wild-type. This increase in TNF $\alpha$  transcript stability, and ultimately protein levels, likely contributed to the wasting syndrome seen in TTP-deficient mice. In a subsequent study, the 3'-UTR of TNF $\alpha$  was placed 3' of a known stable transcript,  $\beta$ -globin, and co-transfected into cells expressing TTP.  $\beta$ -globin mRNA accumulation was inhibited, suggesting that elements in the 3'-UTR, in association with TTP, mediated transcript degradation (36).

GM-CSF, another cytokine protein, induces differentiation, proliferation, and activation of cells involved in the immune response; additionally, GM-CSF is a myeloproliferative agent used for myeloid reconstitution in transplant patients (89). Blackshear and colleagues established that TTP-deficient mice had myeloid hyperplasia, indicating that TTP may regulate proteins and/or transcripts involved in myeloid development (35,90). The TTP-deficient mice had an accumulation of GM-CSF mRNA, resulting from increased transcript stability, and producing an increased synthesis of protein. Additional studies demonstrated that placing the ARE from the 3'-UTR of GM-CSF into to a normally stable transcript (78) conferred instability, providing evidence that these RNA sequence elements, in conjunction with TTP, regulate GM-CSF transcript turnover.

Studies done by Carballo *et al.* demonstrated that the Class II AREs found in the TNF $\alpha$  and GM-CSF transcripts confer instability and promote TTP-mediated decay (36). Other validated targets of TTP-mediated deadenylation and decay, including transcripts encoding Interleukins 2 and 3 (IL-2 and IL-3) and immediate early response 3 (91), a protein with possible involvement in the control of blood pressure, also contain class II AREs within their 3'-UTRs. However, the role of multiple, overlapping binding sites in mediating TTP activity is not known. It was proposed by the Blackshear group that these adjacent and/or overlapping sites might provide additional binding sites for TTP, in some way making the transcript more susceptible to deadenylation and decay. For example, the transcripts of TNF $\alpha$  and GM-CSF have 5 and 3 neighboring or overlapping UUAUUUAUU (9-mer) sequence elements, respectively. It remained unclear whether or not TTP could bind overlapping RNA sequence. The TTP73 peptide, a synthetic TTP TZF domain construct, bound the partial TNF $\alpha$  3'-UTR sequence, UUAUUUAUUUUAUUUAUUUAUU (WT) (potential 7-mer binding sites are marked by underlines or overbars), and caused an upshift of the protein-RNA complex compared to free RNA alone using EMSAs (67). Strikingly, there appeared to be generation of two protein-RNA complexes with this probe. The binding characteristics of TTP73 bound to the mutant probes, UUAUUUAUUUUCUUCUUAUU (probe 1) and UUAUUUCUUCUUUAUUUCUUAUU (probe 0) (potential 7-mer binding sites are

underlined), were compared to WT in that paper. EMSA revealed that probe 1 produced a single, lower band compared to the WT probe described above, whereas probe 0 was not detectably shifted. From these data, Blackshear *et al.* concluded that the WT probe allowed two binding events, but the location of the binding sites in the WT probe was unclear. Additionally, overlapping sites have been shown to serve as ARE-binding sites for multiple TTP73 binding events. However, overlapping sites (or two tandem 9-mer sequences) must be separated by two uridine bases (67).

The Blackshear group later determined that a single 9-mer conferred instability to a known stable transcript, but the presence of two 9-mer sequences further destabilized the transcript. For these studies, a portion 3'-UTR of the mouse MARCKS-like protein (MLP) was replaced with part of the 3'-UTR of TNF $\alpha$  containing a single 7-mer binding site (UUAUUUAUUUCUUCUUUCUUUAUU), two slightly overlapping 7-mer binding sites (UUAUUUAUUUAUUUAUUUCUUCUU), or two 7-mer binding sites separated by eight bases (UUAUUUAUUUCUUCUUUAUUUAUU). Transcripts containing two AUUUA core sequences separated by eight bases, or two overlapping 7-mer AREs, were deadenylated 3-fold more in the presence of TTP than in its absence, suggesting that increasing the number of ARE-binding sites increases susceptibility of transcripts to TTP-mediated deadenylation (92). These data were further validated using a real-time PCR assay of mRNA levels, which demonstrated that TTP co-

expressed with MLP transcripts containing either two 9-mer binding sites separated by six bases, or two overlapping 7-mer binding sites, in their 3'-UTRs, showed a 4- to 5-fold decrease in MLP mRNA accumulation compared to the MLP transcript containing no ARE-binding sites in its 3'-UTR (92).

The main objective of the studies described in this chapter was to determine the spacing required between two 9-mer binding sites to allow for tandem binding of the full-length *C. albicans* TTP family member Zfs1, and determine whether two binding events affected the binding affinities of MBP-Zfs1 for the RNA, as measured by fluorescence anisotropy studies. Our data suggest that MBP-Zfs1 tandemly binds two adjacent AUUUA core sequences with a 2-uridine spacer between the adenosines. MBP-Zfs1 bound with high-affinity to these adjacent sites in several ionic strength conditions. There was no evidence of cooperativity when comparing one binding event to two. *In vivo* data will be needed to establish the role of such tandem binding events in Zfs1-mediated transcript decay. Nonetheless, the data presented here have broadened our understanding of TTP family member association with neighboring 9-mer sites.

## **4.2 Materials and Methods**

2'-OH de-protected and purified RNA nucleotides were purchased from Dharmacon, Inc. (Lafayette, CO) as previously described in section 2.2.

### 4.2.1 Preparation of RNA Substrates for Biochemical Assays

5' biotinylated or unlabeled RNA oligonucleotides used in experiments were purchased and prepared as previously mentioned in section 2.2.2.

### 4.2.2 Plasmid Construction and Protein Purification

Full length *C. albicans* Zfs1 (GenBank accession XM\_712044) expressed and purified as described in section 2. 2.1. The purified protein was aliquoted into 25  $\mu$ l samples, flash frozen in liquid nitrogen, and stored at -80 °C for future use.

### 4.2.3 RNA Electrophoretic Mobility Gel Shift (EMSA)

Protein-RNA complexes were monitored using EMSA as described in (77) and as written in section 3.2.3.

#### 4.2.3.A. EMSA quantification

Background fluorescent intensity units of the binding of MBP-Zfs1 to the poly(U) probe, as calculated by Odyssey® CLx, were subtracted from the fluorescence intensity units of the probe-protein complexes. Values were calculated using Equation 2.

$$(X/(X + Y)) * 100 = \% \text{ fraction bound}$$

Equation 2

Where X represents the fluorescence intensity units of one binding event (after subtracting the background from the same band in the poly(U) probe lane) and Y

represents the fluorescence intensity units of the second binding event (after subtracting from the background from the same band in the poly(U) probe lane).

#### **4.2.4 Fluorescence Anisotropy**

##### **Determination of apparent dissociation constants using fluorescence anisotropy**

Fluorescence anisotropy experiments were performed as previously described (77) and as written in section 3.2.4. Hill coefficients were calculated using PRISM (GraphPad Software).

### **4.3 Results**

#### **4.3.1 Transition from One to Two Binding Events of MBP-Zfs1 to RNA Oligonucleotides Containing TTP Family Member Binding Sites Determined by EMSAs**

Previous studies determined that the TTP73 peptide could bind twice to a single probe containing two overlapping 9-mer ARE-binding sites in which the 5' and 3' adenosines of each site were separated by two uridines (67). In our studies, we first wanted to determine if this phenomenon could be reproduced using a full-length TTP family member protein. For this series of experiments, we utilized a HEPES (4-(2-hydroxyethyl)-1-piperazineethanesulfonic acid) buffer containing 200 mM KCl to more accurately reflect the intracellular environment of *C. albicans* (93). A series of probes were created (Table 2) to determine the transition from one to two binding events of MBP-Zfs1 to a single RNA oligonucleotide.

**Table 2. Biotinylated Probes Containing One, Overlapping, and Two Separated ARE Sites**

Probe number	Sequence (5→3)
1	5' Bi-UUUUUUUUUUUUUUUUUUUUUUUUUUUUUUU 3'
2	5' Bi-UUUU <u>UAUUUAU</u> UUUUUUUUUUUUUUUUUUUU 3'
3	5' Bi-UUUU <u>UAUUUA</u> UUUUUUUUUUUUUUUUUUUU 3'
4	5' Bi-UUUU <u>UAUUUAU</u> AUUUUUUUUUUUUUUUUUU 3'
5	5' Bi-UUUU <u>UAUUUAUU</u> AUUUUUUUUUUUUUUUU 3'
6	5' Bi-UUUU <u>UAUUUAUUU</u> AUUUUUUUUUUUUUU 3'
7	5' Bi-UUUU <u>UAUUUAUUUA</u> UUUUUUUUUUUUUU 3'
8	5' Bi-UUUU <u>UAUUUAU</u> AUUUAUUUUUUUUUUUU 3'
9	5' Bi-UUUU <u>UAUUUAUU</u> AUUUAUUUUUUUUUU 3'
10	5' Bi-UUUU <u>UAUUUAUUUAUU</u> UUUUUUUUUUUU 3'
11	5' Bi-UUUU <u>UAUUUAUUUU</u> AUUUAUUUUUUUU 3'
12	5' Bi-UUUU <u>UAUUUAUUUUUU</u> AUUUAUUUUUU 3'
13	5' Bi-UUUU <u>UAUUUAUUUUUU</u> UAUUUAUUUUUU 3'
14	5' Bi-UUUUUUUUUUUUUUUUUUU <u>UAUUUAUU</u> UUUU 3'

Potential binding sites are underlined or overlined.

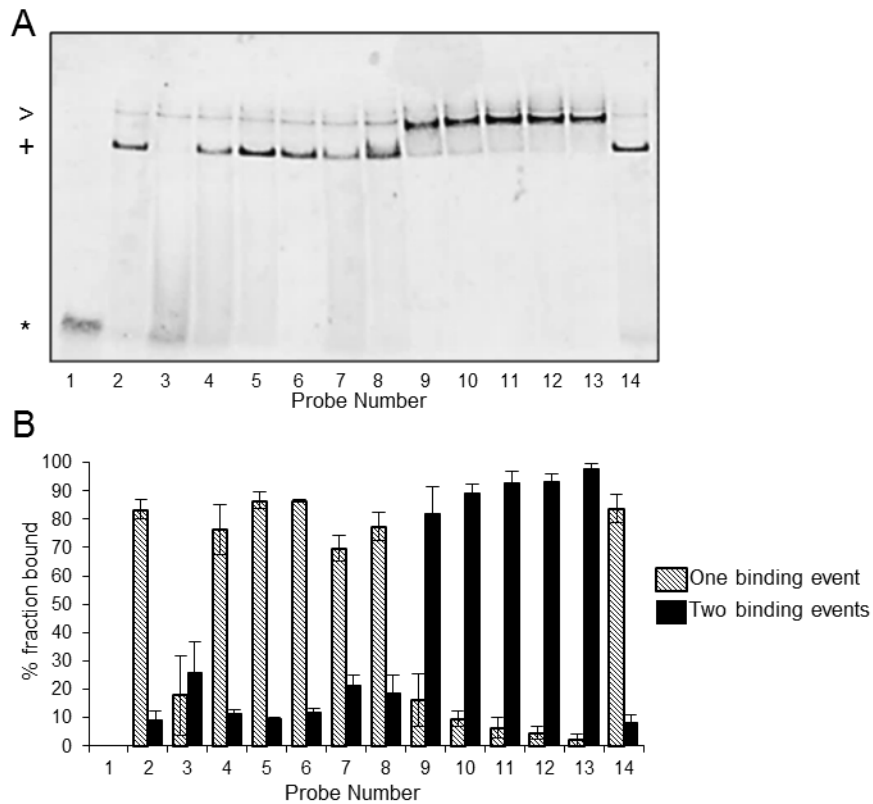


**Figure 10. EMSA Demonstrates Transition from Single to Tandem Binding Events of MBP-Zfsf1 to ARE-Binding Sites Containing Overlapping UUAUUUAUU (9-mer) Sequences**

Binding and EMSA reactions were carried out as described in “Materials and Methods”. **A.** Migration of free probe (\*), one protein binding event to a single probe (+), and two binding events to a single probe containing two target sites (>). Reactions were carried out with a final probe concentration of 3 nM.

**B.** Fluorescent intensities of bands were quantified as described in section 4.2.3.A. The one-site protein binding events are shown with dashed bars and the two-site binding events are shown as solid black bars. Normalized values were calculated using equation 2 located in “Materials and Methods” (Chapter 4).

The transition from one to two binding events of MBP-Zfs1 to a single RNA probe was visualized using EMSA (Figure 10). The transition from one to two binding events first occurred in the transition from Probe 8 to Probe 9, the latter of which had two 7-mers separated by no uridines (Figure 10). Two adjacent 7-mer binding sites did not show 2-site binding, but 7-mer binding sites separated by 1 uridine or more did. Probes 3, 7, and 8 contained a single binding site, as shown using EMSA. However, there appeared to be much less binding between the protein and probe 3 and somewhat less binding to probes 7 and 8 than with, e.g., Probe 2.

I then determined the binding affinities of MBP-Zfs1 for RNA probes containing a single, overlapping, or separate binding sites using fluorescence anisotropy. I established that MBP-tagged full-length Zfs1 bound to all of the RNA oligonucleotides (Table 3) with relatively high affinity, with exception of the RNA probe UUUUAUUUAAUUUUUUUUUUUUUUUUUUUU (probe 3), which bound to MBP-Zfs1 with an affinity of  $78.1 \pm 6.3$  nM in 200 mM KCl at 24 °C. In the salt conditions of 50 and 150 mM KCl at 24 °C, MBP-Zfs1 bound to probe 3 with somewhat higher affinities (Table 4). Despite having lower apparent affinity for Probes 7 and 8 in EMSA, MBP-Zfs1 was found to bind with relatively high affinity to these probes in 50, 150, and 200 mM KCl at 24 °C.

Another question posed was whether TTP family members exhibited cooperative binding to RNA probes containing multiple overlapping or adjacent sites. Blackshear *et al.* found no evidence of positive cooperativity in the binding of TTP73 to overlapping 7-mer sequences in which the adenosines were separated by no uridines (67).

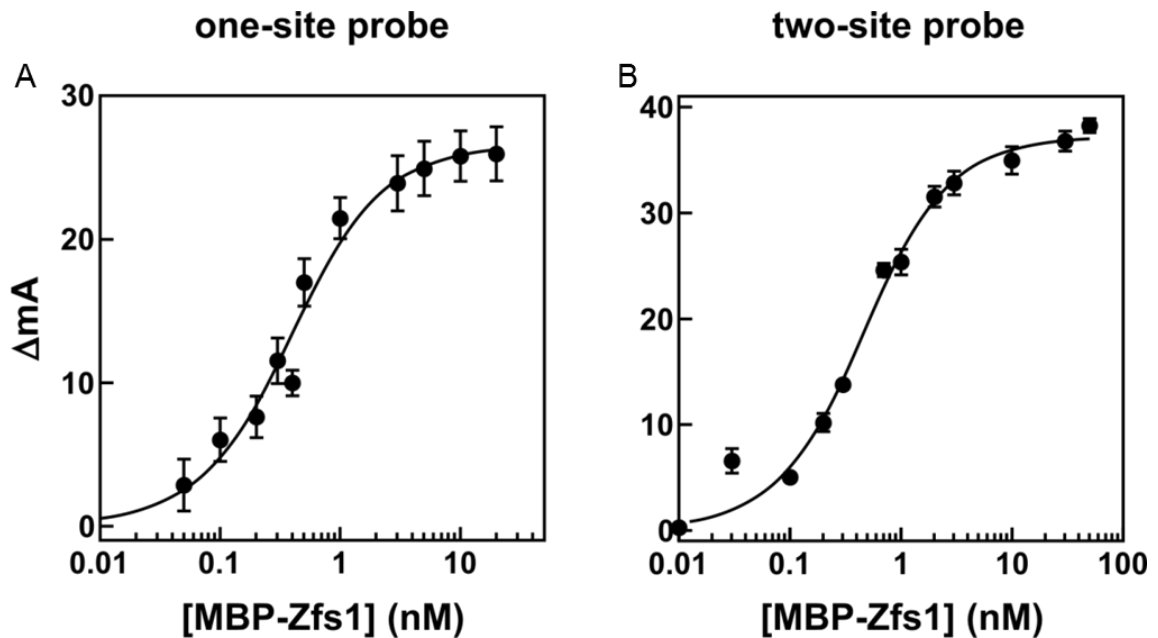


**Figure 11. Fluorescent Anisotropy Studies Reveals No Cooperative Binding of MBP-Zfs1 to Probes Containing One or Two Binding Sites.** Binding studies were done as described in section 2.2.4, using 50 mM KCl. Plots were created by Dr. Gerald Wilson (University of Maryland School of Medicine, Baltimore, MD).

**Table 3. Binding Constants and Hill Coefficients of MBP-Zfs1 bound to RNA containing a single or two binding sites.**

Probe Name	Probe Sequence	Hill Coefficient
One-Site	FL-5'-UUUU <u>AUUUA</u> UUUUUUUUUUUUUUUUUU-3'	1.2
Two-Site	FL-5'-UUUU <u>AUUUA</u> UUUUUUU <u>AUUUA</u> UUUUUU-3'	0.9

Hill Coefficients were calculated in PRISM, version 6.0 (GraphPad Software). Potential 7-mer binding sites are underlined.

Fluorescent anisotropy measurements suggested no cooperativity of binding by MBP-Zfs1 to overlapping 7-mers separated by no uridines or two AUUUA core sequences separated by seven uridines (or two 7-mer binding sites separated by 5 uridines). When binding of MBP-Zfs1 to a probe containing a single site was compared to binding of the protein to a probe containing two widely separated sites, no detectable second inflection point could be seen, suggesting that there was no cooperativity between the binding of two MBP-Zfs1 molecules to the two-site probe (Figure 10). Using PRISM (GraphPad Software), the data further showed that the binding of MBP-Zfs1 to the one-site probe and two-site probe had Hill Coefficients of 1.2 and 0.9, respectively, indicating that there was no cooperativity between the protein and RNA probes containing one or two binding sites.

Surprisingly, fluorescent anisotropy measurements showed that MBP-Zfs1 had similar affinities for probes 7, 8, and 9, even though probe 9 had two separate ARE-binding sites in 200 mM KCl (Table 4). MBP-Zfs1 also had similar binding affinities for probes 2 and 13 in 200 mM KCl (Table 4). We also demonstrated that the binding affinities of MBP-Zfs1 to RNA oligonucleotides increased with decreasing salt concentrations (Table 4), as described for MBP-Zfs1 interactions to variant binding sites (Chapter 3).

**Table 4. Equilibrium Binding Constants MBP-Zfs1 to RNA Oligonucleotides Containing One, Overlapping, and Two Separated ARE Sites**

Probe Number	RNA probe sequence	Number of ARE-binding sites	Apparent $K_d$ measured at 25 °C in 50 mM KCl	Apparent $K_d$ measured at 25 °C in 150 mM KCl	Apparent $K_d$ measured at 25 °C in 200 mM KCl
2	5' FL -UUUU <u>UAUUUAU</u> UUUUUUUUUUUUUUUUUU 3'	1	1.3 ± 0.1 nM	2.9 ± 0.3 nM	13.6 ± 3.2 nM
3	5' FL- UUUU <u>UAUUUA</u> AUUUUUUUUUUUUUUUUUU 3'	1	5.7 ± 0.6 nM	23.9 ± 2.3 nM	78.1 ± 6.3 nM
7	5' FL-UUUU <u>UAUUUA</u> AUUUUUUUUUUUUUUUU 3'	1	3.1 ± 0.4 nM	23.5 ± 0.6 nM	32.0 ± 3.5 nM
8	5' FL-UUUU <u>UAUUUA</u> UAUUUUUUUUUUUUUU 3'	1	ND*	12.5 ± 1.9 nM	32.5 ± 2.0 nM
9	5' FL-UUUU <u>UAUUUA</u> UUUUUUUUUUUUUUUU 3'	2	ND*	5.0 ± 0.3 nM	35.2 ± 2.8 nM
13	5' FL-UUUU <u>UAUUUA</u> UUUUUU <u>UAUUUA</u> UUUUUU 3'	2	1.0 ± 0.1 nM	ND*	10.6 ± 1.4 nM

Values shown are mean ± standard deviation (N=3 in each case). Potential binding sites are underlined. \*ND = not determined

## 4.4 Discussion

AREs located within the 3'-UTR of transcripts have been shown to promote transcript deadenylation and degradation, mediated by *trans*-acting RNA-binding proteins. Previous research has reported that the *trans*-acting RNA-binding protein TTP binds with high affinity to sites containing the 9-mer sequence UUAUUUAUU (37,92). Association to this RNA sequence element promotes transcript destabilization and recruitment of deadenylases (46,47). The TTP TZF domain forms stable, high-affinity associations to these sites through pi base stacking and hydrogen bond interactions (65). However, few data existed to describe the interactions between full-length TTP family members and multiple binding sites.

Two well-known transcripts targeted by TTP for decay, TNF $\alpha$  and GM-CSF, contain multiple overlapping and neighboring 7-mer sequences located within the 3'-UTRs of their respective mRNAs. Little is known about how much distance is needed between overlapping and neighboring binding sites for multiple binding of TTP and its family members. Additionally, the affinities of a full-length TTP family member for overlapping binding sites were previously unknown. Using EMSAs, we show here that the full-length TTP family member protein expressed in *C. albicans*, Zfs1, exhibited tandem binding to an RNA oligonucleotide having the sequence 5'-



interactions play a role in the MBP-TTP-RNA association. However, stronger interactions, as previously mentioned, are thought to be essential for stabilization and high-affinity binding of the protein-RNA complex. Even though MBP-Zfs1 does not exhibit cooperative binding to RNA probes containing multiple sites, we speculate that multiple sites may be essential for maintaining high-affinity associations in a range of intracellular ionic conditions. This could be a regulatory mechanism by which to tightly control the decay rates and steady-state levels of certain transcripts. Two or more ARE-binding sites within a single transcript could increase transcript instability and promote rapid deadenylase recruitment. This hypothesis is supported by previous research that reported that the addition of an additional 9-mer to a 3'-UTR already containing a single 9-mer increased transcript destabilization (92). Conversely, as *C. albicans* Zfs1 deadenylase binding sites have not yet been identified, tandem binding of Zfs1 to a single transcript could serve as a platform for the association of factors, which in turn could promote deadenylase recruitment and transcript destabilization.

## **5. Evidence for Binding of Two Molecules of MBP-Zfs1 to Oligonucleotides Containing a Single 9-mer Binding Site**

### **5.1 Introduction**

mRNA turnover has been demonstrated to be regulated, in part, by *cis*-acting elements located in the 3'-UTR. *Cis*-acting elements mediate mRNA stability or instability through the binding of *trans*-acting RNA-binding proteins. The RNA-binding protein tristetraprolin (TTP) and its family members have been reported to associate with *cis*-acting elements and promote transcript instability. However, there is little information to support the formation of TTP oligomers or its family members in solution. My studies have identified possible oligomerization of a full-length TTP family member in the presence of a RNA probe containing a *cis*-acting binding element. These results introduce a potential novel attribute of TTP family members.

HuR (Human antigen R) has been shown to stabilize transcripts of cytokines, growth factors, and other factors through binding of AREs located in the 3'-UTRs of mRNAs (15,94). Additionally, the overexpression of HuR has been linked to stabilization of transcripts with known roles in cancer proliferation and growth (15). The N-terminal domains (RRM1 and RRM2) of HuR have been shown to bind elements in the 3'-UTRs of mRNAs, while the C-terminal domain (RRM3) has been shown to bind

the poly(A) tail and mediate 3'-end adenosyl modifications. More recent data have suggested that the RRM3 is also involved in HuR dimerization. Scheiba and colleagues determined that dimerization of HuR is mediated by a stretch of residues located on an  $\alpha$  helix found in the C-terminus of RRM3. The mutation of a single tryptophan residue in this domain abrogated dimerization, as shown in nuclear magnetic resonance (NMR) and analytical ultracentrifugation (AU) experiments (95). Additional data indicated that RRM3 binds with higher affinity to Class III AREs (uridine rich) than to Class I AREs (RNA sequences of AUUUA) (95). However, this study did not demonstrate binding of the HuR dimer to RNA oligonucleotides containing AREs. Further studies will be needed to determine if dimerization is a regulatory mechanism to enhance transcript stability in this case.

The *trans*-acting RNA-binding protein AUF1 (AU-rich element RNA-binding protein 1) forms tetramers in the presence of ARE-binding sites. Previous studies have shown that AUF1 binds to ARE-binding sites and stimulates transcript destabilization (18). Dimerization of AUF1 is mediated through interactions of an N-terminal alanine-rich domain and a short glutamine-rich region at the C-terminus. Mutagenesis of residues in these two regions impaired AUF1 dimerization (96). Later, Wilson and Brewer determined that dimeric AUF1 sequentially associates with transcripts containing ARE-binding sites and forms a tetramer (19). Researchers have speculated

that the tetramer functions to not only destabilize transcripts, but to serve as a platform for the binding of other proteins involved in transcript destabilization and degradation. This hypothesis was supported by a study from Kedar *et al.*, who determined that AUF1 associates with TTP, a protein with a well-established role in transcript destabilization (20). Additional studies have reported the binding of AUF1 to other proteins involved in mRNA degradation (18).

These data suggest that oligomerization may be a common characteristic of *trans*-acting binding proteins as a mechanism to enhance targeting and association to ARE-binding sites and other protein factors. A secondary binding event of MBP-Zfs1 to a 27-base RNA oligonucleotide containing a single 9-mer binding site was suggested using EMSA in Chapter 4 (Figure 9). The goal of this chapter was to elucidate the nature of the possible second protein binding event demonstrated in previous EMSAs. I present evidence here that the secondary binding event is not an artifact of our biochemical assays, but an interaction that is first preceded by the association of an MBP-Zfs1 protein to the ARE-binding site. This suggests that the binding of the free MBP-Zfs1 is mediated by the bound MBP-Zfs1 and RNA bases not involved in ARE-dependent binding. Finally, I discuss the implications of Zfs1 oligomerization in the role of ARE selectivity and transcript turnover.

## **5.2 Materials and Methods**

2'-OH de-protected and purified RNA nucleotides were purchased from Dharmacon, Inc. (Lafayette, CO) as previously described in section 2.2.

### **5.2.1 Expression and Purification of MBP-tagged Full-Length Zfs1**

Full length *C. albicans* Zfs1 (GenBank accession XM\_712044) was cloned and expressed as previously described in section 2.2.1.

### **5.2.2 RNA Electrophoretic Mobility Gel Shift (EMSA)**

The protein-RNA complexes were monitored using EMSA as described in (77) and as written in section 3.2.3.

### **5.2.3 Analytical Gel Filtration**

Purified MBP-Zfs1 was prepared as described in section 5.2.2. A 9.0 mg/mL sample of MBP-Zfs1 in 30  $\mu$ l was diluted 600-fold in dilution buffer (20 mM HEPES pH 7.6, 150 mM KCl, 5% glycerol, 10 mM  $\beta$ ME, and 25  $\mu$ M ZnSO<sub>4</sub>). 200  $\mu$ l of diluted MBP-Zfs1 was aliquoted into four 1 mL microcentrifuge tubes. 27-mer or 13-mer RNA oligonucleotides containing a single ARE-binding site of interest were added in the following protein: RNA molar ratios: 1:0, 1:1.2, 4:1, or 0:1. The protein and RNA was allowed to associate on ice for 30 mins before applying to a calibrated Superdex 200 10/300 column (GE Healthcare Life Sciences, Pittsburg, PA). The elution volumes of free RNA, protein-RNA complex, as indicated by specific wavelengths (protein absorbance

measured at  $\lambda = 280$  nm and RNA absorbance measured at  $\lambda = 260$ ) and free protein were compared to a series of protein size standards to determine the molecular weight.

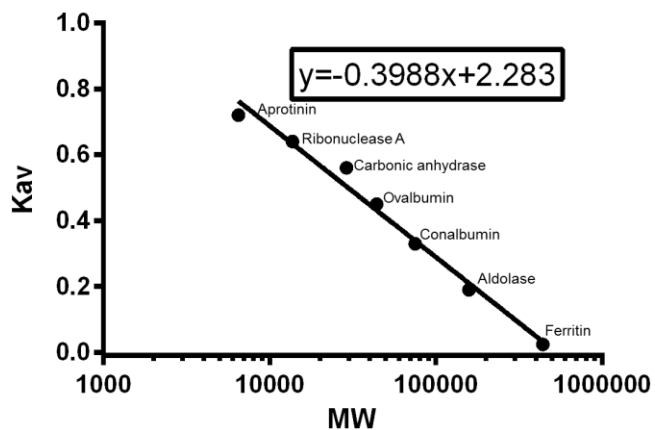


**Figure 12. Calibration Curve of Superdex 200 10/30 Using Standard Proteins**

The protein standards used for column calibration were Aprotinin (6.5 kDa), Ribonuclease A (13700 Da), Carbonic anhydrase (29000 Da), Ovalbumin (44000 Da), Conalbumin (75000 Da), Aldolase (158000 Da), and Ferritin (440000 Da). Blue Dextran 2000 was used to calculate the void volume of the column.

$$K_{av} = \frac{V_e - V_o}{V_c - V_o} \quad \text{Equation 3}$$

$V_e$  = Elution volume

$V_o$  = Void volume (calculated value for Superdex 200 10/300 = 8.1 mLs)

$V_c$  = Column volume (calculated value for Superdex 200 10/300 = 24.0 mLs)

To calculate molecular weights, the elution volume ( $V_e$ ) of a selected peak was placed into Equation 3 to solve for  $K_{av}$ . Calculated  $K_{av}$  value for a single peak was

used in the equation noted in Figure 11 to solve for  $x$  (logarithmic molecular weight of unknown protein).

#### **5.2.4 Size Exclusion Chromatography Coupled to Multi-Angle Light Scattering (SEC-MALS)**

Purified MBP-Zfs1 was prepared as described in section 5.2.2. An aliquot of MBP-Zfs1 concentrated to 9.0 mg/mL in 30  $\mu$ l was diluted to 1.0 mg/mL in dilution buffer (20 mM HEPES pH 7.6, 150 mM KCl, 5% glycerol, 10 mM  $\beta$ ME, and 25  $\mu$ M ZnSO<sub>4</sub>). 100  $\mu$ l of diluted MBP-Zfs1 was aliquoted into 1 mL microcentrifuge tubes. 27-mer or 13-mer RNA oligonucleotides containing an ARE-binding site of interest were added in the following protein: RNA molar ratios: 1:0, 1:1.2, 4:1, or 0:1. The protein-RNA complex was equilibrated on ice for 30 mins before applying onto a calibrated Superdex 200 10/300 column (GE Healthcare Life Sciences, Pittsburg, PA) coupled to a mini Dawn TREOS Multi-Angle Light Scattering Detector (Wyatt Technologies, Santa Barbara, CA) followed by an Optilab T-rEX Refractometer (Wyatt Technologies, Santa Barbara, CA). Molecular weights were calculated in ASTRA software (Wyatt Technologies, Santa Barbara, CA).

## **5.3 Results**

### **5.3.1 The Binding of MBP-Zfs1 to a 27-mer Oligonucleotide Containing One ARE-Binding Site and a 13-mer Oligonucleotide Containing One ARE-Binding Site Generates Two Protein: RNA Complexes**

There are few available data on oligomerization of full-length TTP family members. Our initial studies with MBP-Zfs1 suggested 1:1 or 2:1 (protein: RNA) molar ratios in the presence of RNA probes with one or two ARE-binding sites using fluorescent anisotropy experiments (data not shown). In gel shift experiments using 3.2 nM of a biotinylated 27-mer oligonucleotide incorporating a single ARE-binding site (5'-Bi-UUUUAUUUAUUUUUUUUUUUUUUUUUU-3'), I detected the generation of two upshifted bands as the MBP-Zfs1 concentration increased. The lower band (Figure 13A, complex I) was hypothesized to be the 1:1 MBP-Zfs1:RNA complex (Chapter 4). This lower complex only appeared at protein concentrations lower than 30 nM (data not shown). Complex I is formed by the initial high-affinity association of the MBP-Zfs1 TZF domain to the ARE-binding site. At protein concentrations of 100 nM and above, however, the lower band completely disappeared and an upshifted, more prominent band (Complex II) appeared. In gel shift assays of the MBP-Zfs1-13-mer RNA oligonucleotide (5' Bi-UUUUAUUUAUUUU-3'), also with a single ARE-binding site, two similarly upshifted bands were detected. Notably, there was no disappearance of the lower band at higher protein concentrations, which was likely due to the generation

of two major protein:RNA species (Figure 12B). MBP-Zfs1 did not appear to bind to a RNA oligonucleotide having a poly(U) sequence of 27 bases (Figure 14).

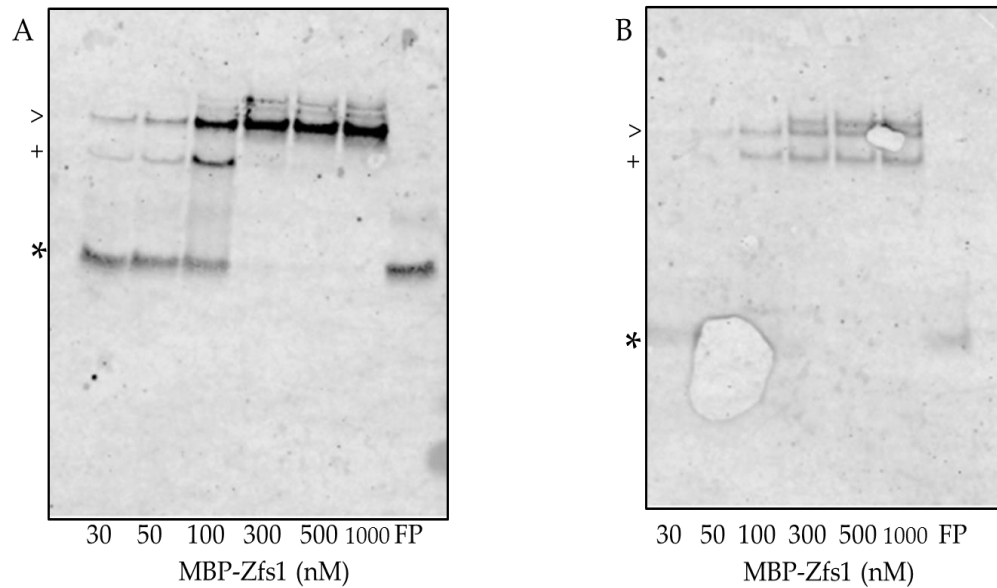


**Figure 13. Detection of Multiple MBP-Zfs1:RNA Species Using EMSAs**

Binding and EMSA reactions were carried out as described in “Materials and Methods”(Chapter 5). Migration of free probe (\*), one protein binding event to a single probe (+, Complex I), and two binding events to a single probe containing one target site (>, Complex II). Reactions were carried out with the final probe concentration at 3.0 nM.

**A.** MBP-Zfs1 binding to the 27-mer oligonucleotide having a single ARE-binding site (5' Bi-UUUUAUUUAUUUUUUUUUUUUUUUUUUUU-3').

**B.** MBP-Zfs1 binding to the 13-mer oligonucleotide having a single ARE-binding site (5' Bi-UUUUAUUUAUUUU).

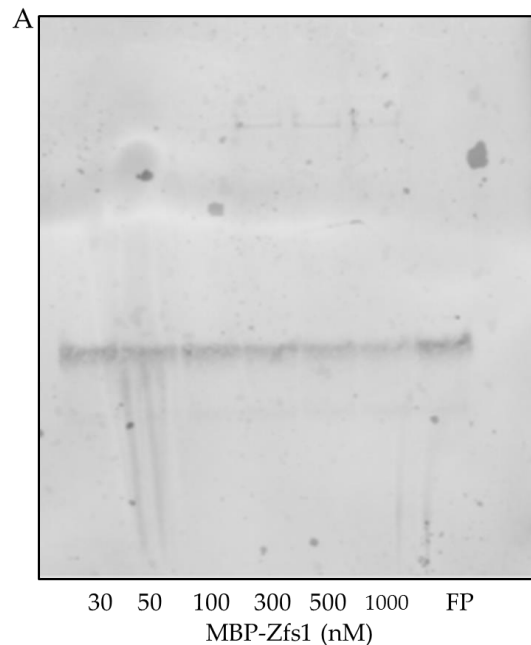


**Figure 14. MBP-Zfs1 Does Not Bind to a 27-mer RNA Oligonucleotide Containing a Poly(U) Sequence**

### **5.3.2 Size Exclusion Chromatography and SEC-MALS Assays Report Dimerization of MBP-Zfs1 in the Presence of a 27-mer RNA Oligonucleotide Containing a Single ARE-Binding Site**

The presence of Complex II seen in EMSAs (Figure 13) was surprising and suggested the possibility that the Zfs1 may form a dimer when associated to mRNAs with single ARE binding sites. I performed size exclusion chromatography (SEC) to determine if MBP-Zfs1 formed oligomers in solution in the absence of added RNA. We further examined whether or not oligomerization occurred only when an ARE-binding site was present. Initial SEC experiments revealed that MBP-Zfs1 was a monomer (64,000 Da) in solution in the absence of added RNA. To determine the oligomerization

state of MBP-Zfs1, MBP-Zfs1 was incubated with RNA oligonucleotides that were 13 or 27 bases in length and contained a single 9-mer ARE-binding site. The 27-base RNA probe containing two ARE-binding sites (probe 13 in Chapter 4, Table 2) served as a control. In this control, a single eluted peak was seen from the sample containing MBP-Zfs1 and the 27-mer RNA probe with two binding sites in a protein: RNA ratio of 4.0:1.5 (Figure 15, Peak 1). The single peak corresponded in size to two MBP-Zfs1 molecules bound to the two ARE-binding sites found within the RNA probe, i.e., the SEC calculated molecular weight was reported to be 159,000 Da, close to the expected molecular weight of 136,000 Da (two MBP-Zfs1 molecules: 128,000 Da and one 27-mer: 8,000 Da). MBP-Zfs1 was also incubated in protein: RNA ratios of 4.0:1.0 and 1.0: 1.3 with the 13-mer oligonucleotide. The protein: RNA complexes eluted at approximately 13.60-13.85 mL, corresponding to molecular weights between 66,000Da and 72,000 Da (Figure 16, Peaks 1 and 2). The calculated molecular weight of the MBP-Zfs1: 13-mer complex is 68,000 Da. This result was expected, since a single molecule of MBP-Zfs1 has an apparent molecular weight of 64,000 Da, whereas the molecular weight of the 13-mer RNA is only calculated to be 4,000 Da. There was no evidence for higher order oligomerization in this experiment, since a peak was not detectable at elution volumes nearer to 11.00 mL or 12.00 mL (Figure 17).

When MBP-Zfs1 was in excess to the 27-mer oligonucleotide with a single ARE site (Protein : RNA ratio of 4:1), the eluted protein came off earlier than when an equimolar ratio of protein and RNA was used (Figure 17, Peak 1). The shifted peak eluted at a calculated molecular weight of 98,000 Da, placing it between the eluted peaks of MBP-Zfs1: 27-mer two ARE site probe complex and the peak of the equimolar MBP-Zfs1: 27-mer one ARE site complex. Another peak eluted at 14.01 mL and was calculated to have a molecular weight of 61,000 Da. This peak most likely corresponded to apo MBP-Zfs1, as it corresponded more prominently with the 280 nm wavelength (Figure 17). RNA absorbance was also monitored at 260 nm wavelength to determine bound and free RNA substrate (data not shown).

The molecular weights of protein-RNA complexes could be inaccurate using SEC; therefore, we used SEC coupled to multi-angle light scattering (MALS) to more accurately measure the protein: RNA oligomerization state and molecular weights of the protein: RNA complexes. 1.0 mg/ml of MBP-Zfs1 was incubated with 13-mer and 27-mer RNA oligonucleotides, as previously mentioned. The results from SEC-MALS analyses (Table 5) were similar to the reported molecular weights calculated using SEC alone. Remarkably, MBP-Zfs1 bound to the 27-mer RNA probe with a single ARE site (protein: RNA ratio of 4.0:1.0) eluted between the peaks of MBP-Zfs1 bound to the 27-mer RNA probe with two single ARE sites and the protein in the absence of RNA. The

results suggest that there are transient protein-protein and protein-RNA interactions not associated with binding of the MBP-Zfs1 to the binding site. However, these data also suggest that the possible secondary interactions between the free protein and the protein: RNA complex are transient and only occur in the presence of a single binding site containing an oligonucleotide that is 27 bases in length. Furthermore, this phenomenon was only observed when the MBP-Zfs1 was in 4-fold or more excess to RNA containing a binding site.

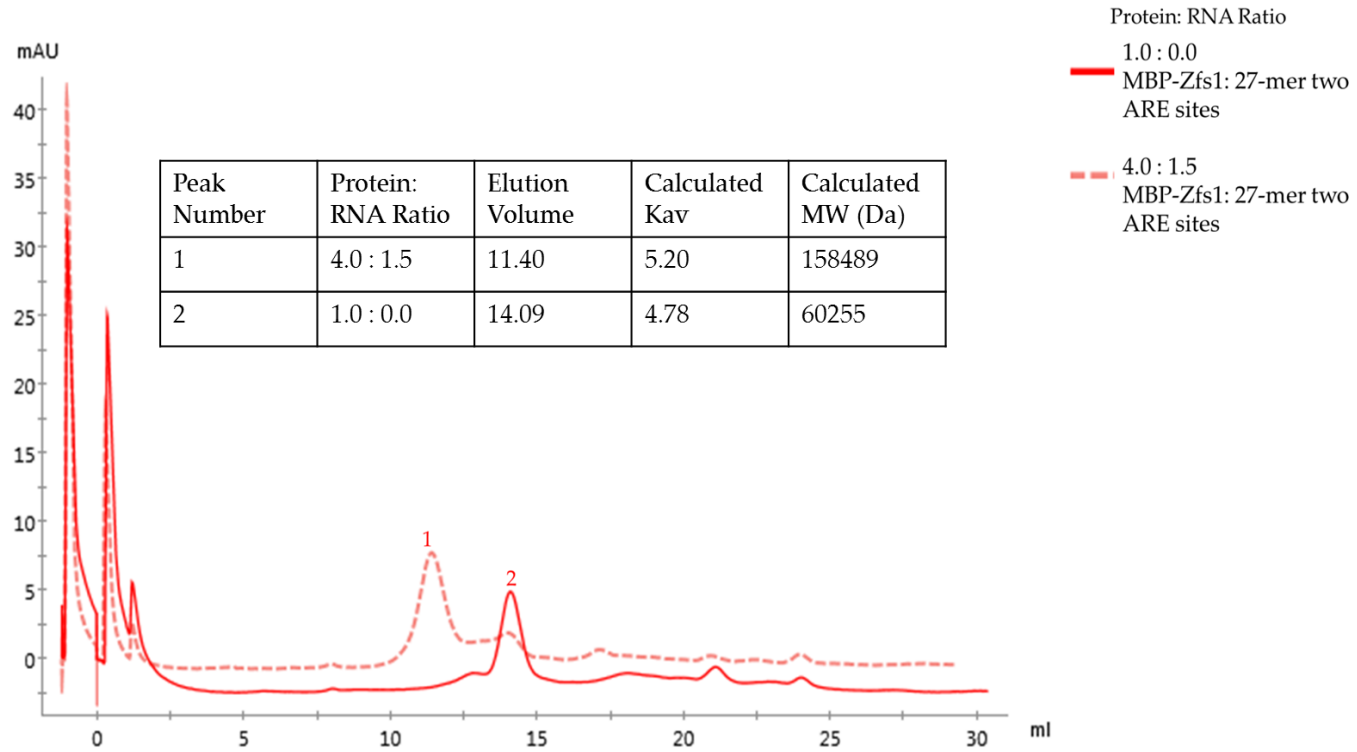


**Figure 15. Size Exclusion Chromatography of MBP-Zfs1 Bound to 5'- UUUUAUUUAUUUUUUUAUUUAUUUUUUU-3' (27-mer two ARE sites) Probe**

Protein absorbance was measured at the wavelength 280 nm. RNA absorbance at the wavelength 260 nm was not shown.

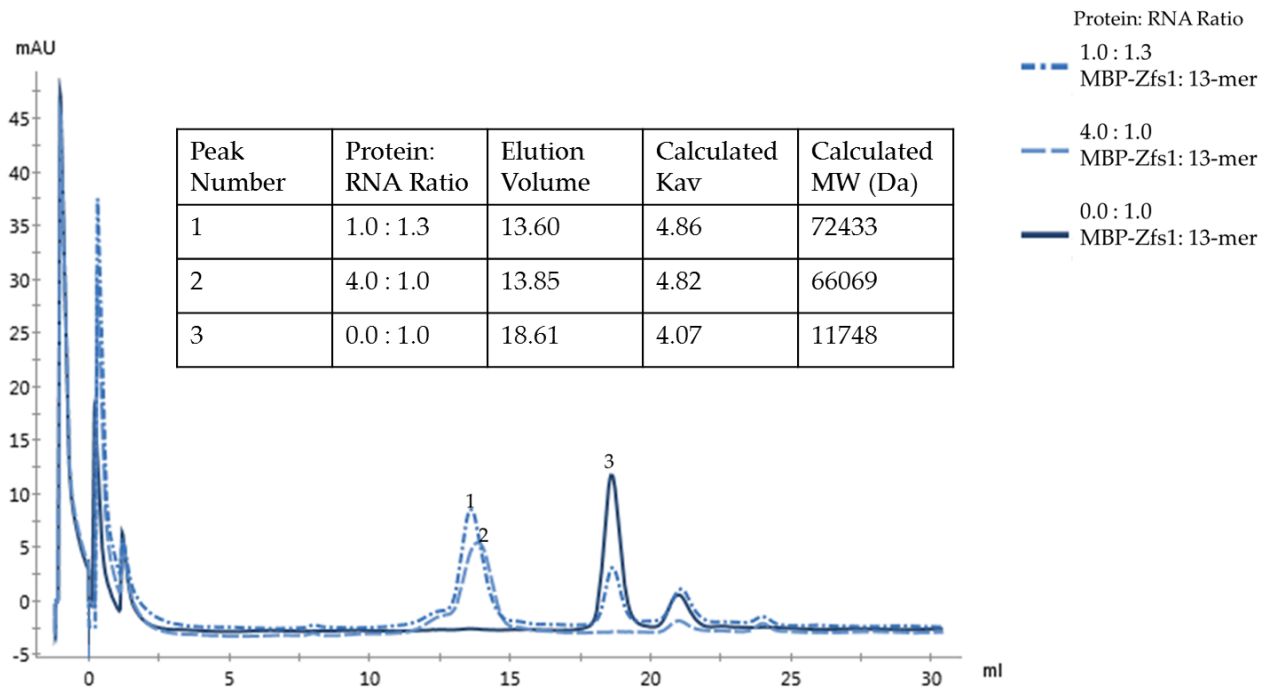


**Figure 16. Size Exclusion Chromatography of MBP-Zfs1 Bound to 5'-UUUUAUUUAUUUU-3' (13-mer) Probe**

Protein absorbance was measured at the wavelength 280 nm. RNA absorbance at the wavelength 260 nm was not shown.

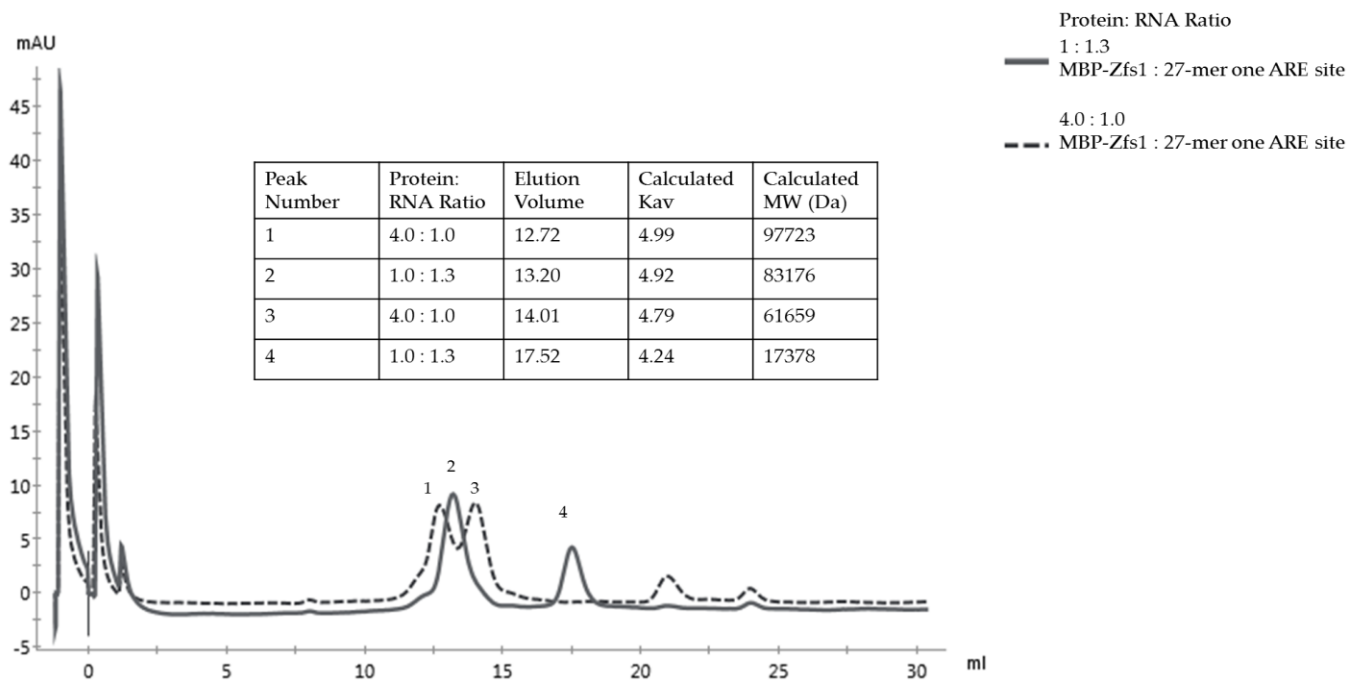


**Figure 17. Size Exclusion Chromatography of MBP-Zfs1 Bound to 5'- UUUUAUUUAUUUUUUUUUUUUUUUUUUUUU-3' (27-mer one ARE site) Probe**

Protein absorbance was measured at the wavelength 280 nm. RNA absorbance at the wavelength 260 nm was not shown.

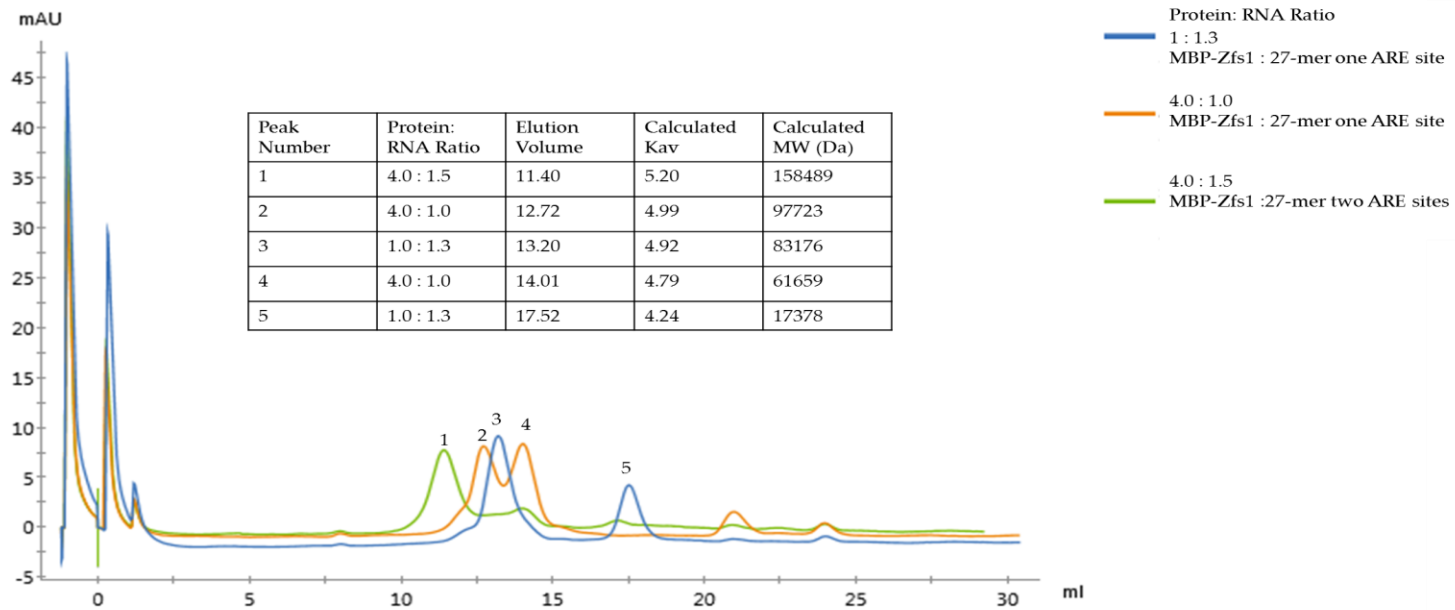


**Figure 18. Size Exclusion Chromatography Overlay of MBP-Zfs1 Associations to 5'-UUUUAUUUAUUUUUUUUUUUUUUUUUUUUUUUU-3' (27-mer one ARE site) Probe, 5'-UUUUAUUUAUUUUUUUAUUUAUUUUUUUU-3' (27-mer two ARE sites) Probe, and 5'-UUUUAUUUAUUUU-3' (13-mer one ARE site) Probe.**

Protein absorbance was measured at the wavelength 280 nm. RNA absorbance at the wavelength 260 nm was not shown.

**Table 5. SEC-MALS Calculated Molecular Weights of Protein-RNA Complexes**

RNA Probe	Protein : RNA Molar Ratio	SEC calculated Molecular weight (Da)
None	1.0 : 0.0	70700
27-mer two ARE sites	4.0 : 1.5	123600
27-mer one ARE site	4.0 : 1.0	104000
13-mer one ARE site	1.0 : 1.3	59800

## **5.4 Discussion**

The primary goal of this study was to determine the oligomerization state of MBP-Zfs1 when bound to an ARE-containing substrate. Although the mechanistic basis for protein oligomerization of MBP-Zfs1 to ARE substrates remains unknown, our observations suggest that oligomerization must be preceded by association of MBP-Zfs1 to the ARE-binding site, as we did not see oligomerization of the protein in the presence of a poly(U) probe (Figure 14) or in our SEC experiments (Figures 15, 16, 17). In EMSAs, two separate protein-RNA complexes were observed with probes that were 13 and 27 bases in length and contained a single ARE site. The lower molecular weight bands (Complex I of Figures 13A and 13B) were attributed to the binding of a single MBP-Zfs1

protein to the sequence UUAUUUAUU. We postulated that Complex II (Figures 13A and 13B) was most likely due to two proteins bound to a single RNA oligonucleotide. There exists the possibility that this event could be promoted by the gel matrix mediating a “caging effect” around the proteins and RNA, producing a biochemical artifact associated with this method. Using the solution-based methods of SEC and SEC-MALS, I observed evidence for oligomerization of MBP-Zfs1 to a 27-base RNA oligonucleotide with a single ARE site. These data suggest that protein oligomerization was mediated and stabilized by the bound MBP-Zfs1 protein and bases that were not part of the ARE site. Nonetheless, this event was not seen with the 13-mer RNA oligonucleotide containing a single 9-mer ARE-binding site, suggesting that an oligomer formed with MBP-Zfs1 when bound to this probe is not stable in solution. Without the stabilization effect of bases outside the ARE-binding site, the 13-mer only promoted protein-protein interactions that were not strong enough to hold the complex together in solution but may have been sustained by the “caging effect” of the gel matrix.

Similar results with AUF1 were published by Zucconi and Wilson, who reported that AUF1, an ARE-binding protein, only oligomerized to ARE-containing RNA substrates having 30 or more bases (97). *C. albicans* does not express AUF1, and it is possible that Zfs1 has evolved a similar mechanism of forming higher order structures when bound to transcripts containing ARE-binding sites. Previous researchers have

speculated that oligomerization of AUF1 could serve as a platform for the association of other proteins essential for transcript deadenylation and degradation. It is possible that Zfs1 may have a similar *in vivo* mechanism. Furthermore, oligomerization may be essential for the binding of Zfs1 protein partners.

More experiments are needed to determine the minimum probe length needed for RNA-dependent Zfs1 oligomerization. Most fungal 3'-UTRs are reported to be between 50-200 nucleotides (98). My data suggest that MBP-Zfs1 binds as a monomer to the smaller 13-mer RNA oligonucleotide containing a single ARE-binding site (Chapters 2-4) (61). We hypothesize that, since the longer 27-mer RNA oligonucleotides are more representative of *in vivo* 3'-UTRs, oligomerization of Zfs1 in the presence of an ARE-binding site is plausible. As mentioned previously, oligomerization of Zfs1 could serve as a platform for the association of other proteins. Additionally, Zfs1 oligomerization may be a mechanism to disrupt RNA secondary structure, perpetuate mRNA instability, and maintain local concentrations of Zfs1 in the vicinity of ARE-containing transcripts. More *in vivo* data are needed to validate our hypotheses, but our data support the idea that Zfs1- and TTP family member-mediated decay may rely not only on ARE-binding sites, but on flanking RNA regions and local intracellular conditions.

## 6. Conclusion

Post-transcriptional regulation of gene expression through transcript stability has expanded the central dogma that DNA is transcribed into RNA, which is then translated into active protein. *Trans*-acting proteins, in association with *cis*-acting RNA sequence elements, have been reported to promote translation and degradation of mRNAs, thereby regulating the amounts and types of proteins which are expressed in response to cellular cues. Tristetraprolin, one of the best-known *trans*-acting RNA-binding proteins, has been reported to target transcripts containing 3'-UTR AREs and promote mRNA deadenylation. My thesis has explored the binding characteristics of the single full-length TTP family member found in *C. albicans*, as a model system to study the mechanisms by which all TTP family members interact with ARE sites. Data presented in this thesis indicate that the binding of a TTP family member to an ARE-binding site could be influenced by changing intracellular conditions. Furthermore, RNA sequence elements outside of the ARE-binding site, and protein domains apart from the TZF domain, may play roles in ARE selectivity and protein oligomerization. Previous studies have reported that most target mRNAs were not conserved among widely different organisms (49,61). Using MBP-Zfs1, future studies could elucidate the mechanism of Zfs1 oligomerization, and whether or not oligomerization is observed

with other full-length TTP family members. Studies should also investigate how varying intracellular conditions (pH and buffer ionic strength) affect the selectivity of other full-length TTP family members for ARE sites. The work presented here suggests that Zfs1 and other TTP family members are complex players in an even more complex system. However, it is becoming increasingly clear that TTP family member transcript decay is mediated through elements located within the TTP proteins and in RNA sequence elements outside of the ARE-binding site. This collection of knowledge will enhance our understanding of the expression of proteins in response to intra-and extracellular cues.

## Appendix

### **7. Crystallographic Determination of the *Candida albicans* Zfs1-RNA complex and the use of Biochemical Studies to Help Elucidate Zfs1 Protein Partners**

#### **7.1 Introduction**

The cytoplasmic mRNAs code for proteins essential for cellular survival. The turnover rate of transcripts must be regulated in normal homeostatic conditions and in response to intra- and extracellular stimuli. *Cis*-acting elements located in the 3' untranslated region (UTR) of mRNAs are important determinants of mRNA stability and the binding of *trans*-acting binding proteins can mediate transcript translation and degradation. Yet, there are still mechanistic details involved in the process of transcript selectivity, TTP family member-protein interactions, and structural changes that occur during RNA sequence element binding that are not completely understood.

One of the best understood families of *trans*-acting RNA binding proteins is the tristetraprolin (TTP) family. TTP and its family members bind to adenosine-uridine rich elements (AREs) located in the 3'-UTR of transcripts. The binding of TTP to AREs then promotes transcript destabilization through the recruitment of deadenylases. Previous studies have demonstrated the binding of a C-terminal domain of TTP to NOT1, a core domain of the major mammalian deadenylase CCR4-NOT complex (45-47). While many

metazoan TTP family members have an apparent C-terminal NOT1 binding domain, most fungal TTP family members do not, suggesting that fungal organisms have evolved mechanisms of ARE-mediated transcript decay through the recruitment of protein factors that may be different from those of their metazoan counterparts. The mechanisms by which fungal TTP family members interact with the deadenylation machinery and other proteins of their respective cells are not known, and warrant further investigation.

Structural characterization of the TTP family members has been a major challenge because many contain intrinsically disordered regions. This has hindered the purification of full-length TTP family members for biochemical and structural assays. Previous structural studies have only been able to characterize the tandem CCCH zinc finger domain (TZF domain) (64,65), the region responsible for high-affinity RNA-binding. To date, there has been no structural characterization of a full-length TTP family member bound to an RNA sequence element. The elucidation of such a structure would give insight into how domains outside the TZF domain participate in ARE-binding and selectivity.

The *C. albicans* TTP family member Zfs1 can bind AREs like TTP itself, through its TZF domain (61,68). The studies presented in this thesis suggest that full-length *Candida* Zfs1 could be used to further enhance our understanding of the structural

characteristics of TTP family members bound to RNA sequence elements, and aid in the determination of conserved and novel protein factors essential in TTP family member-mediated decay. The studies highlighted in this chapter are exploratory experiments I have conducted to begin to investigate the most difficult questions related to TTP- and TTP family member-mediated decay.

## **7.2 Materials and methods**

### **7.2.1 Expression and Purification of MBP tagged Full-Length Zfs1 and MBP tagged Zfs1 TZF domain**

#### **7.2.1.A. Plasmid construction and protein purification of MBP tagged full-length Zfs1**

Full length *C. albicans* Zfs1 (GenBank accession XM\_712044) was cloned and expressed as described in section 2.2.1.

#### **7.2.1.B. Plasmid construction and purification of *C. albicans* MBP-Zfs1-TZF domain**

The tandem zinc finger domain of *C. albicans* Zfs1 (GenBank accession XM\_712044) was cloned into a modified pMALX vector (a gift from Lars Pedersen, (76)). The TZF domain peptide was expressed as an MBP fusion linked to the N-terminus of the Zfs1 TZF domain by a three alanine linker. Correct insertion of the appropriate sequences was verified by sequencing (Genewiz, Research Triangle Park, NC). The vector was transformed into *E. coli* One Shot® BL21(DE3) cells (ThermoFisher Scientific, Waltham, MA). Peptide expression was induced when the cells reached an A<sub>600</sub>=0.7-0.9 by the addition of 0.3 mM isopropyl β-D -1-thiogalactopyranoside (IPTG) for 16 hours at

16 °C. Recombinant MBP-Zfs1 TZF domain was purified from cell lysates using amylose affinity chromatography. The peptide was eluted off resin by the addition of buffer (20 mM HEPES (pH 7.6), 300 mM NaCl, 5% glycerol, 10 mM BME, and 25  $\mu$ M ZnSO<sub>4</sub>) that included 70 mM maltose. The eluate was diluted into phenyl column buffer (20 mM HEPES (pH 7.6), 1.0 M NH<sub>4</sub>SO<sub>2</sub>, 5% glycerol, 10 mM BME, and 25  $\mu$ M ZnSO<sub>4</sub>) in a ratio of 1.0:4.0 (eluate to buffer) and applied onto a HiTrap Phenyl HP column (GE Healthcare Life Sciences, Pittsburg, PA). A high salt to low salt gradient was run, and the recombinant peptide eluted at the end of the gradient. Size exclusion chromatography (HiLoad16/600 Superdex column, GE Healthcare Life Sciences, Pittsburg, PA) using a buffer consisting of 20 mM HEPES (pH 7.6), 300 mM NaCl, 5% glycerol, 10 mM BME, and 25  $\mu$ M ZnSO<sub>4</sub> was used to select fractions corresponding to the correct peptide molecular weight of 55000 Da. Purified protein was concentrated in a final buffer (20 mM HEPES (pH 7.6), 100 mM KCl, 5% glycerol, 25  $\mu$ M ZnSO<sub>4</sub>, 10 mM BME) to 5 mg/mL and checked for purity on SDS-PAGE. Fractions were concentrated using a 10,000 MWCO Vivaspin 20 centrifugal filtering device (GE Healthcare). Purified peptide was aliquoted into 25  $\mu$ l samples, flash frozen in liquid nitrogen, and then stored at -80 °C for future use.

### 7.2.1.C. Plasmid construction and protein purification of 6xHis-Zfs1

Full-length *C. albicans* Zfs1 (GenBank accession XM\_712044) was cloned into a modified pET 20/30 vector. Zfs1 was expressed as a fusion protein linked to an N-terminal 6xHistidine tag (6xHis). Correct insertion of the appropriate sequences was verified by sequencing (Genewiz, Research Triangle Park, NC). The vector was transformed into *E. coli* One Shot® BL21(DE3) cells (ThermoFisher Scientific, Waltham, MA). Protein expression was induced when the cells reached an A<sub>600</sub>=0.7-0.9 by the addition of 0.3 mM IPTG for 16 hours at 16 °C. Recombinant 6xHis-Zfs1 was purified from cell lysates in binding buffer (20 mM HEPES pH 7.6, 300 mM NaCl, 5% glycerol, and 5.0 mM Imidazole) and applied to a HisTrap HP column (GE Healthcare Life Sciences, Pittsburg, PA). A low to high imidazole gradient was run and the recombinant protein eluted in the middle of the gradient. Size exclusion chromatography (HiLoad16/600 Superdex column, GE Healthcare Life Sciences, Pittsburg, PA) using a buffer of consisting of 20 mM HEPES (pH 7.6), 300 mM NaCl, 5% glycerol, 10 mM BME, and 25 μM ZnSO<sub>4</sub> was used to select fractions corresponding to the correct protein molecular weight of 21000 Da. Purified protein was concentrated in a final buffer (20 mM HEPES (pH 7.6), 100 mM KCl, 5% glycerol, 25 μM ZnSO<sub>4</sub>, 10 mM BME) to a protein concentration of 3.0 mg/mL and checked for purity on SDS-PAGE. Purified protein was

aliquoted into 25  $\mu$ l samples, flash frozen in liquid nitrogen, and then stored at -80 °C for future use.

### **7.2.2 Setup of Protein Crystallization Experiments**

Initial screening for crystallization conditions was carried out in 96-well sitting-drop plates using Index, Crystal Screen I and II, Additive Screen, and Natrix (Hampton Research, CA) or PACT premier (Molecular Dimensions, FL). 9.0 mg/mL of purified MBP-Zfs1 or MBP-Zfs1-TZF domain protein was mixed with an oligonucleotide (either a 9-mer, 13-mer, or 27-mer two site) in a molar ratio of 1.0:1.1 (protein: RNA) and incubated on ice for 30 mins before tray setup. A Mosquito Crystal robot (TTP Labtech, Cambridge, MA) was used to set up drops containing 200 nl of protein to 200 nl of reservoir solution (in a reservoir volume of 100  $\mu$ l). Screens were incubated at 4 °C or 22 °C and monitored for crystal growth. 24-well sitting and hanging plates were used to screen for promising conditions and to increase the volume of drops (1  $\mu$ l protein to 1  $\mu$ l reservoir solution).

### **7.2.3 Production and Testing of Antibodies to 6xHis-Zfs1**

6xHis-Zs1 was purified as described above (Chapter 6.2.1.C). 1200  $\mu$ g of purified protein was mixed with 5x SDS loading buffer and boiled for 10 mins before loading on 10-20% Tris-HCL gels (Bio-Rad, Hercules, CA). 200 ng of protein was loaded per well and gel were run at 200 V for 60 mins. The gels were developed using Coomassie blue

staining solution and destained overnight in destaining solution (40% v/v methanol, 10% v/v acetic acid, and brought to 1 liter using distilled H<sub>2</sub>O). Bands representing 6xHis-Zfs1 were excised and shipped on ice to Harlan laboratories (now Envigo, Indianapolis, IN, US). Gel slices were digested and injected into New Zealand White rabbits using a two rabbit 70-day protocol. After 70 days, 10 mL of antisera from each rabbit was shipped to the Blackshear lab to be tested using protein immunoblot assays against purified MBP-Zfs1, 6xHisZfs1, and *C. albicans* wild type (WT) as well as *zfs1*Δ/Δ clarified lysates.

Protein immunoblot assays (western blots) were done as previously described (99). Blots were probed with rabbit antisera (1:10000 dilution) followed by anti-rabbit IgG, HRP-linked antibody (1:100000 dilution; Cell Signaling Technology, Danvers, MA) as the secondary antibody. Protein blots were developed using WesternBright Sirius (Advansta, Menlo Park, CA), imaged by X-ray film, and developed using a Konica film processor.

#### **7.2.4 Pull-Down Assays using MBP-Zfs1 and *C. albicans* Clarified Lysates**

*C. albicans* WT cells were provided by Dr. Melissa Wells (National Institute of Environmental Health Sciences (NIEHS), Research Triangle Park, NC). WT cells were plated on yeast extract peptone dextrose (YPD) plates and incubated at 30 °C for three days. After three days, single colonies from both plates were used to inoculate 50 mL

liquid YPD cultures. Cells were outgrown to an optical density of 0.7 and pelleted for 15 mins at 2000g. Cells were then “beadbeat” in binding buffer (20 mM HEPES pH 7.6, 200 mM KCl, 5% glycerol, and 10 mM  $\beta$ ME) for 10 cycles of 1 min on disrupter followed by a 1 min rest period on ice. Cellular lysates were centrifuged at 5000g for 20 mins at 4 °C. Protein concentrations of clarified lysates were checked using spectrophotometric determination. Lysates were stored at 4 °C before pull-down experiments.

Two 500 ng aliquots of MBP and two 500 ng aliquots of MBP-Zfs1 were incubated with 50  $\mu$ l of washed amylose resin for two hours at 4 °C. All four samples were washed with three times the column volume of binding buffer and then 7.50 ng of clarified WT lysate (previously stored at 4 °C) was added to each. Samples were rotated end over end for three hours at 4 °C. Resin was gently pelleted at 200g for 2 mins and supernatant was pipetted and stored at 4 °C. Resin was washed with 5x or 10x column volumes with binding buffer. 100  $\mu$ l of SDS sample buffer was added to resin and samples were boiled for 10 mins at 90 °C. Samples were run on a 10-20% Tris HCL gel (Bio-Rad, Hercules, CA) using SDS-PAGE. Results of pull-down assays (including supernatants) were checked using Coomassie blue and silver gel staining techniques.

## **7.3 Results**

### **7.3.1 Crystallization Trials of MBP-Zfs1 and MBP-Zfs1-TZF domain**

To date, structural biologists have been able to study only the secondary structure of the ZFP36L2 TZF domain bound to a 9-mer oligonucleotide (65). These studies provided important insights into the structure of the highly conserved TZF domain and the mechanism of high-affinity binding to RNA sequences elements. Research has not shown whether domains outside of the TZF domain participate in transcript selectivity or whether changes mediated by TZF domain RNA-binding affect secondary structures located in neighboring RNA domains. Data outlined in this thesis suggest that these outside regions could influence the binding affinities of full-length Zfs1 for AREs (Chapters 2, 3, 4, and 5), and provide impetus for further research into full-length TTP family member.

I screened more than 500 different crystallization conditions at 4 °C and 22 °C in the hopes of obtaining protein crystals of full-length MBP-Zfs1 and MBP-Zfs1-TZF domain for diffraction studies. Unfortunately, these conditions mostly produced precipitated protein, phase separation, and birefringent precipitate (possibly microcrystals) (Figure 19).

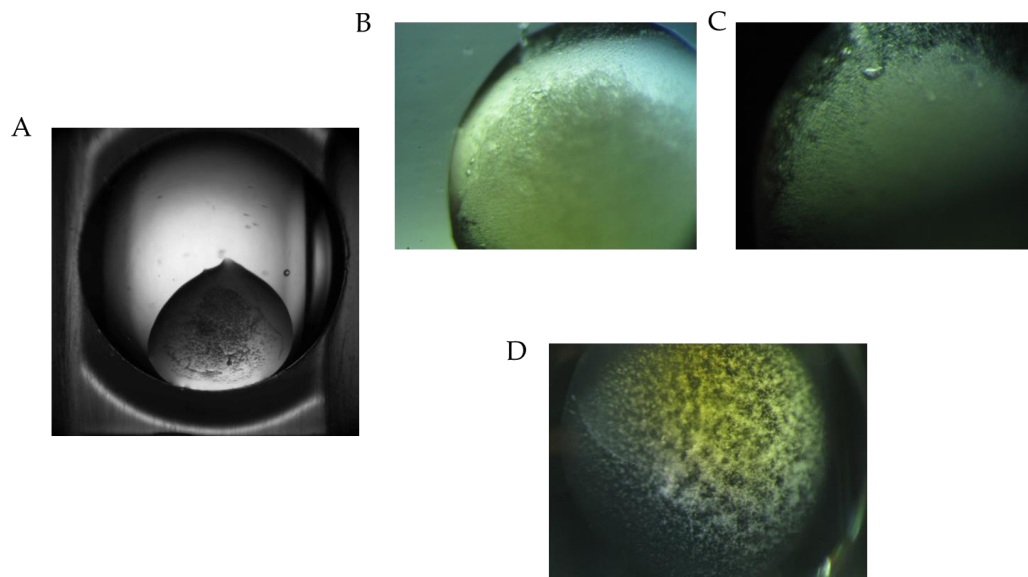


**Figure 19. Representative figures of outcomes of crystallization experiments using MBP-tagged full-length Zfs1 and MBP-tagged Zfs1-TZF domain**

- A. Droplet contains denatured protein which has precipitated out of solution.
- B. Close-up of precipitated, denatured protein.
- C. Possible phase separation or malformed microcrystals in droplet.
- D. Birefringent precipitate as seen using polarized light microscopy.

Out of the conditions screened, only two produced crystals that could be mounted and checked for diffraction quality. The first crystals of MBP-tagged full-length Zfs1 bound to the one site 9-mer oligonucleotide were seen in a condition from the PACT screen (Hampton Research, CA) consisting of 0.2 M sodium sulfate, 0.1 Bis-tris propane pH 8.5, and 20% w/v Peg 3350. The highly birefringent crystals were determined to be salt crystals after analysis with a home X-ray source (Figure 20A). A protein crystal of MBP-Zfs1-TZF domain bound to the one site 9-mer oligonucleotide was grown in the

condition of 0.5 M ammonium sulfate, 1.0 M lithium sulfate, 0.1 M sodium citrate tribasic dehydrate pH 5.6 (crystal II screen, Hampton Research, CA). This crystal appeared to be a protein crystal (birefringent and crushable), yet it had no diffraction when analyzed on the home X-ray source (Figure 20B).

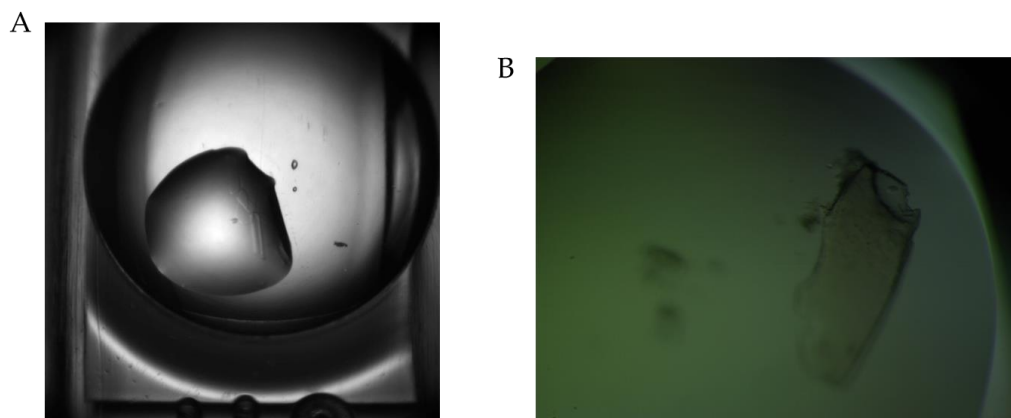


**Figure 20. Crystallization Experiments with MBP-tagged Full-Length Zfs1 and MBP-Zfs1-TZF domain**

- A.** Salt crystal formed of MBP-Zfs1 in complex with 9-mer RNA probe containing a single ARE site in a condition consisting of 0.2 M sodium sulfate, 0.1 Bis-tris propane pH 8.5, and 20% w/v Peg 3350.
- B.** A non-diffracting crystal of MBP-Zfs1-TZF domain in complex with the 9-mer oligonucleotide containing a single ARE site.

### 7.3.2 Determination of Zfs1 Protein Partners

The determination of the binding partners for TTP and its family member proteins has been a long-term goal of our laboratory. To date, TTP has been shown to

bind to NOT1 through a binding site located in the C-terminus of TTP (47). It has been postulated that the interaction between TTP and NOT1 is essential for the recruitment of the CCR4-NOT1 deadenylase complex to the poly(A) tail of transcripts containing TTP family member binding sites. Although most fungal TTP family members lack a NOT1 binding domain, numerous studies have reported that Zfs1 (*S. pombe*) (49,53) and Cth1 and Cth2 (*S. cerevisiae*) (48) are involved in the destabilization and degradation of target transcripts containing ARE sites. Puig and colleagues demonstrated the association of Cth2 to DEAD box Dhh1 helicase, suggesting that fungal TTP family members are involved in the recruitment of proteins necessary for RNA unwinding (100). This might be used as a mechanism for increasing RNA accessibility to proteins involved in transcript destabilization and decay. Using pull-down experiments, I wanted to capture protein interactions between MBP-Zfs1 and protein factors found in *C. albicans* lysates in an effort to further elucidate how Zfs1 works in coordination with other proteins to promote transcript deadenylation and decay. Purified MBP-Zfs1 protein was incubated with WT *C. albicans* lysates. Using the MBP tag to our advantage, we pulled down Zfs1 bound to potential partners using affinity chromatography. Samples were washed in 5x or 10x column volumes in binding buffer (see “Materials and Methods” section 6.2.4) to disrupt non-specific interactions (Figure 21). We analyzed the proteins remaining on the affinity resin using SDS-PAGE and later Matrix-Assisted Laser Desorption/Ionization

(MALDI) Time Of Flight (TOF) (data not shown). However, this project was discontinued as the MBP tag seemed to associate and interfere with possible Zfs1 protein partners, thus skewing our pull-down assay results.

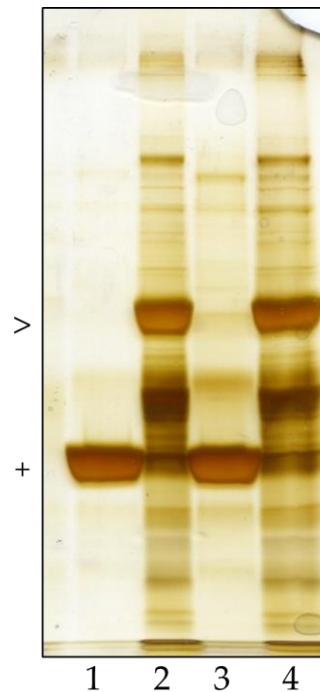


**Figure 21. Representative Silver Stained Gel of Pull-Down Experiments Using *C. albicans* Clarified Lysates and Purified MBP and MBP-Zfs1 Protein**

Pull-down assays were done as previously described in “Materials and Methods” (Chapter 5). In lanes 1 and 3, MBP (+) was used to pull down protein partners out of clarified *C. albicans* lysates. Samples were washed in 5x or 10x column volumes in binding buffer, respectively. Lanes 1 and 3 served as experimental controls. MBP-Zfs1 (>) was used in lanes 2 and 4 to pull down protein partners out of clarified *C. albicans* lysates. Samples were washed in 5x or 10x column volumes in binding buffer, respectively. Gels were analyzed using MALDI-TOF mass spectrometry (data not shown).

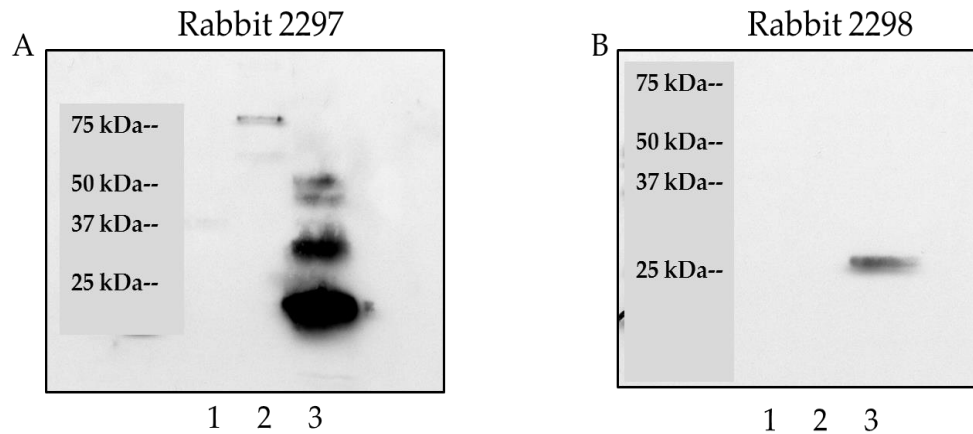


**Figure 22. 6xHis-Zfs1 Antibodies Detect Purified 6xHis-Zfs1 and MBP-Zfs1.**

Western blots were probed and imaged as reported in Chapter 5. Lane 1 represents MBP alone control. Purified MBP-Zfs1 (Lane 2) and 6xHis-Zfs1 protein (Lane 3) were detected by the primary Zfs1 antibody (1:10000 dilution). Expected molecular weights of proteins used: MBP (42000 Da), MBP-Zfs1 (64000 Da), and 6xHisZfs1 (25000 Da). Anti-sera from **A. Rabbit 2297** and **B. Rabbit 2298** were used in the assays.

In addition to using purified MBP-Zfs1 for the attempted identification of Zfs1 protein partners, I used MBP-Zfs1 in the production of antibodies. Antibodies to MBP-Zfs1 have the potential to be used in co-immunoprecipitation assays to identify Zfs1 protein partners. However, MBP was determined to be very antigenic and our initial antibodies reacted to purified MBP as well as to MBP-Zfs1. Consequently, we constructed a vector expressing full-length Zfs1 tagged at the N-terminus with 6 histidine residues (6x). The 6xHis tag was not as antigenic as the MBP tag and 6xHis-Zfs1 antibodies recognized MBP-Zfs1 and 6xHis-Zfs1 but not MBP (Figure 22). The 6xHis-Zfs1 antibodies were then used to detect endogenous Zfs1 in lysates of WT and

*zfs1Δ/Δ C. albicans* strains. Unfortunately, the antibody failed to detect endogenous Zfs1 (24000 Da) (Figures 23A and 23B).

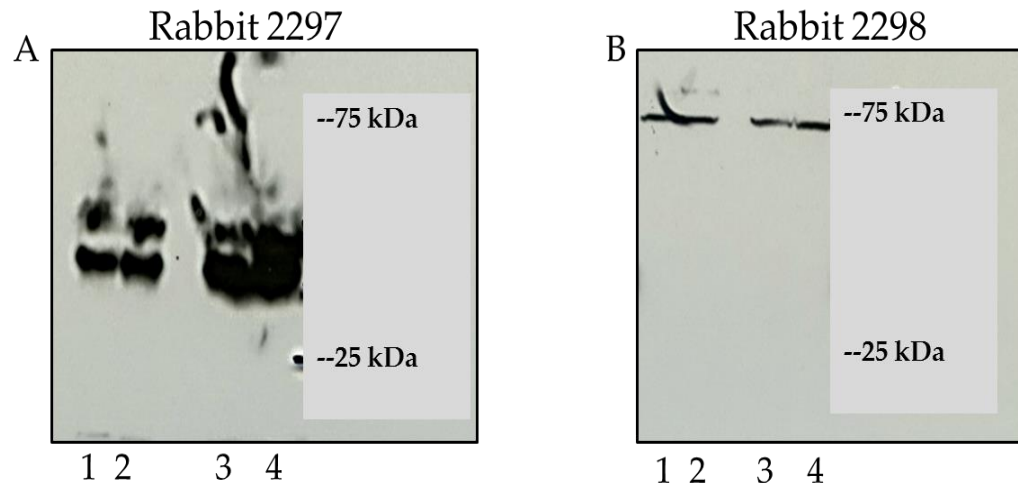


**Figure 23. 6xHis-Zfs1 Antibodies Failed to Detect Endogenous Zfs1 in *C. albicans* lysates.**

Clarified WT and *zfs1Δ/Δ* lysates were prepared for western blot analysis. 20  $\mu$ l (lane 1) and 5  $\mu$ l (lane 3) of clarified WT lysates and 20  $\mu$ l (lane 3) and 5  $\mu$ l (lane 4) of clarified *zfs1Δ/Δ* lysates were probed with 6xHis-Zfs1 antibodies (1:10000 dilution). Expected molecular weight of endogenous Zfs1 is 24000 Da. Anti-sera from **A. Rabbit 2297** and **B. Rabbit 2298** were used in the assays.

## **7.4 Discussion**

The primary goal of these experiments was to answer longstanding questions regarding the structural characteristics of a full-length TTP family member.

Additionally, in an effort to elucidate the mechanism by which Zfs1 mediates transcript deadenylation and degradation, we wanted to identify Zfs1 protein partners through several biochemical techniques. Despite not answering these questions outright, we

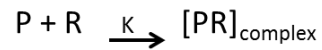
have determined which biochemical techniques have not been useful in probing the biochemical and structural properties of Zfs1. For example, our inability to crystallize full-length Zfs1 with and without RNA suggests that Zfs1 has an inherent amount of secondary structure disorder. The amount of disorder within Zfs1 makes the formation of contacts essential for the formation of crystalline structure improbable. Using nuclear magnetic resonance (NMR), small angle X-ray scattering (SAXS), and cryo-electron microscopy (Cryo-EM), the structural characterization of Zfs1 and other TTP family members can be explored. The listed structural techniques are solution based, avoiding the need for screening of conditions favorable for the formation of a Zfs1 protein crystal. Aside from needed structural data, my current work highlights novel full-length TTP family member ARE associations.

Although the 6xHis-Zfs1 antibodies failed to detect endogenous Zfs1, they can potentially be used in co-immunoprecipitation assays to determine Zfs1 binding proteins. The optimization of our pull-down assays through the addition of RNA substrates containing ARE-binding sites could mimic the oligomerization event reported in *in vitro* experiments and facilitate the binding of Zfs1 protein partners. The optimized pull-down assay, in conjunction with the 6xHis-Zfs1 antibodies, can be utilized to capture novel Zfs1 protein partners.

Although these experiments did not succeed, we have laid the foundation for a better understanding of a full-length TTP family member. Future studies should be pursued using the biochemical techniques mentioned above to finally elucidate structural characteristics of Zfs1 and other full-length TTP family members bound to RNA substrates containing ARE-binding sites. Likewise, the optimization of pull-down assays with the use of the 6xHis-Zfs1 antibodies could be essential in the discovery of Zfs1 protein partners and elucidation of factors involved in Zfs1-mediated transcript decay.

## 8. Deviation of Equation 1 (Chapter 3)

P=Protein  
R=RNA  
K=Equilibrium Constant  
A=Anisotropy  
F=Fractional Concentration



$$PR = K[P][R]$$

$$R_{\text{total}} = R_{\text{Free}} + PR$$

$$\Sigma A_{\text{Total}} = \Sigma A_{\text{individual species}} * F_{\text{individual species}}$$

$$R_{\text{total}} = R_{\text{Free}} + K[P][R]$$

$$A_{\text{Total}} = A_R \frac{[R_{\text{Free}}]}{R_{\text{Total}}} + A_{PR} \frac{[PR]_{\text{complex}}}{R_{\text{Total}}}$$

$$\frac{R_{\text{Free}}}{R_{\text{total}}} = \frac{1}{1 + K[P]}$$

$$A_{\text{Total}} = A_R \frac{[R_{\text{Free}}]}{R_{\text{total}}} + A_{PR} \frac{[P][R]}{R_{\text{total}}}$$

$$A_{\text{total}} = \frac{A_R + A_{PR}[P][R]}{1 + K[P]}$$

## References

1. Goldstrohm, A. C., and Wickens, M. (2008) Multifunctional deadenylase complexes diversify mRNA control. *Nat Rev Mol Cell Biol* **9**, 337-344
2. Iwakawa, H. O., and Tomari, Y. (2015) The Functions of MicroRNAs: mRNA Decay and Translational Repression. *Trends Cell Biol* **25**, 651-665
3. Huang, L., and Wilkinson, M. F. (2012) Regulation of nonsense-mediated mRNA decay. *Wiley Interdiscip Rev RNA* **3**, 807-828
4. Popp, M. W., and Maquat, L. E. (2013) Organizing principles of mammalian nonsense-mediated mRNA decay. *Annu Rev Genet* **47**, 139-165
5. Bernstein, P., Peltz, S. W., and Ross, J. (1989) The poly(A)-poly(A)-binding protein complex is a major determinant of mRNA stability in vitro. *Mol Cell Biol* **9**, 659-670
6. Burd, C. G., Matunis, E. L., and Dreyfuss, G. (1991) The multiple RNA-binding domains of the mRNA poly(A)-binding protein have different RNA-binding activities. *Mol Cell Biol* **11**, 3419-3424
7. Ross, J. (1995) mRNA stability in mammalian cells. *Microbiol Rev* **59**, 423-450
8. Wu, X., and Brewer, G. (2012) The regulation of mRNA stability in mammalian cells: 2.0. *Gene* **500**, 10-21
9. Mignone, F., Gissi, C., Liuni, S., and Pesole, G. (2002) Untranslated regions of mRNAs. *Genome Biol* **3**, REVIEWS0004

10. Lee, J. E., Lee, J. Y., Trembly, J., Wilusz, J., Tian, B., and Wilusz, C. J. (2012) The PARN deadenylase targets a discrete set of mRNAs for decay and regulates cell motility in mouse myoblasts. *PLoS Genet* **8**, e1002901
11. Chlebowski, A., Lubas, M., Jensen, T. H., and Dziembowski, A. (2013) RNA decay machines: the exosome. *Biochim Biophys Acta* **1829**, 552-560
12. Siwaszek, A., Ukleja, M., and Dziembowski, A. (2014) Proteins involved in the degradation of cytoplasmic mRNA in the major eukaryotic model systems. *RNA Biol* **11**, 1122-1136
13. Spassov, D. S., and Jurecic, R. (2003) The PUF family of RNA-binding proteins: does evolutionarily conserved structure equal conserved function? *IUBMB Life* **55**, 359-366
14. Filipovska, A., and Rackham, O. (2012) Modular recognition of nucleic acids by PUF, TALE and PPR proteins. *Mol Biosyst* **8**, 699-708
15. Govindaraju, S., and Lee, B. S. (2013) Adaptive and maladaptive expression of the mRNA regulatory protein HuR. *World J Biol Chem* **4**, 111-118
16. Barker, A., Epis, M. R., Porter, C. J., Hopkins, B. R., Wilce, M. C., Wilce, J. A., Giles, K. M., and Leedman, P. J. (2012) Sequence requirements for RNA binding by HuR and AUF1. *J Biochem* **151**, 423-437
17. Abdelmohsen, K., and Gorospe, M. (2010) Posttranscriptional regulation of cancer traits by HuR. *Wiley Interdiscip Rev RNA* **1**, 214-229
18. Gratacos, F. M., and Brewer, G. (2010) The role of AUF1 in regulated mRNA decay. *Wiley Interdiscip Rev RNA* **1**, 457-473

19. Wilson, G. M., Sun, Y., Lu, H., and Brewer, G. (1999) Assembly of AUF1 oligomers on U-rich RNA targets by sequential dimer association. *J Biol Chem* **274**, 33374-33381
20. Kedar, V. P., Zucconi, B. E., Wilson, G. M., and Blackshear, P. J. (2012) Direct binding of specific AUF1 isoforms to tandem zinc finger domains of tristetraprolin (TTP) family proteins. *J Biol Chem* **287**, 5459-5471
21. Bakheet, T., Williams, B. R., and Khabar, K. S. (2003) ARED 2.0: an update of AU-rich element mRNA database. *Nucleic Acids Res* **31**, 421-423
22. Gillis, P., and Malter, J. S. (1991) The adenosine-uridine binding factor recognizes the AU-rich elements of cytokine, lymphokine, and oncogene mRNAs. *J Biol Chem* **266**, 3172-3177
23. Iwai, Y., Bickel, M., Pluznik, D. H., and Cohen, R. B. (1991) Identification of sequences within the murine granulocyte-macrophage colony-stimulating factor mRNA 3'-untranslated region that mediate mRNA stabilization induced by mitogen treatment of EL-4 thymoma cells. *J Biol Chem* **266**, 17959-17965
24. Shyu, A. B., Belasco, J. G., and Greenberg, M. E. (1991) Two distinct destabilizing elements in the c-fos message trigger deadenylation as a first step in rapid mRNA decay. *Genes Dev* **5**, 221-231
25. Shaw, G., and Kamen, R. (1986) A conserved AU sequence from the 3' untranslated region of GM-CSF mRNA mediates selective mRNA degradation. *Cell* **46**, 659-667
26. Chen, C. Y., and Shyu, A. B. (1994) Selective degradation of early-response-gene mRNAs: functional analyses of sequence features of the AU-rich elements. *Mol Cell Biol* **14**, 8471-8482

27. Chen, C. Y., Chen, T. M., and Shyu, A. B. (1994) Interplay of two functionally and structurally distinct domains of the c-fos AU-rich element specifies its mRNA-destabilizing function. *Mol Cell Biol* **14**, 416-426
28. Chen, C. Y., and Shyu, A. B. (1995) AU-rich elements: characterization and importance in mRNA degradation. *Trends Biochem Sci* **20**, 465-470
29. Lai, W. S., Stumpo, D. J., and Blackshear, P. J. (1990) Rapid insulin-stimulated accumulation of an mRNA encoding a proline-rich protein. *J Biol Chem* **265**, 16556-16563
30. Varnum, B. C., Lim, R. W., Kujubu, D. A., Luner, S. J., Kaufman, S. E., Greenberger, J. S., Gasson, J. C., and Herschman, H. R. (1989) Granulocyte-macrophage colony-stimulating factor and tetradecanoyl phorbol acetate induce a distinct, restricted subset of primary-response TIS genes in both proliferating and terminally differentiated myeloid cells. *Mol Cell Biol* **9**, 3580-3583
31. Taylor, G. A., Lai, W. S., Oakey, R. J., Seldin, M. F., Shows, T. B., Eddy, R. L., Jr., and Blackshear, P. J. (1991) The human TTP protein: sequence, alignment with related proteins, and chromosomal localization of the mouse and human genes. *Nucleic Acids Res* **19**, 3454
32. Varnum, B. C., Ma, Q. F., Chi, T. H., Fletcher, B., and Herschman, H. R. (1991) The TIS11 primary response gene is a member of a gene family that encodes proteins with a highly conserved sequence containing an unusual Cys-His repeat. *Mol Cell Biol* **11**, 1754-1758
33. DuBois, R. N., McLane, M. W., Ryder, K., Lau, L. F., and Nathans, D. (1990) A growth factor-inducible nuclear protein with a novel cysteine/histidine repetitive sequence. *J Biol Chem* **265**, 19185-19191
34. Worthington, M. T., Amann, B. T., Nathans, D., and Berg, J. M. (1996) Metal binding properties and secondary structure of the zinc-binding domain of Nup475. *Proc Natl Acad Sci U S A* **93**, 13754-13759

35. Taylor, G. A., Carballo, E., Lee, D. M., Lai, W. S., Thompson, M. J., Patel, D. D., Schenkman, D. I., Gilkeson, G. S., Broxmeyer, H. E., Haynes, B. F., and Blakeshear, P. J. (1996) A pathogenetic role for TNF alpha in the syndrome of cachexia, arthritis, and autoimmunity resulting from tristetraprolin (TTP) deficiency. *Immunity* **4**, 445-454
36. Carballo, E., Lai, W. S., and Blakeshear, P. J. (1998) Feedback inhibition of macrophage tumor necrosis factor-alpha production by tristetraprolin. *Science* **281**, 1001-1005
37. Lai, W. S., Carballo, E., Strum, J. R., Kennington, E. A., Phillips, R. S., and Blakeshear, P. J. (1999) Evidence that tristetraprolin binds to AU-rich elements and promotes the deadenylation and destabilization of tumor necrosis factor alpha mRNA. *Mol Cell Biol* **19**, 4311-4323
38. Stumpo, D. J., Byrd, N. A., Phillips, R. S., Ghosh, S., Maronpot, R. R., Castranio, T., Meyers, E. N., Mishina, Y., and Blakeshear, P. J. (2004) Chorioallantoic fusion defects and embryonic lethality resulting from disruption of Zfp36L1, a gene encoding a CCCH tandem zinc finger protein of the Tristetraprolin family. *Mol Cell Biol* **24**, 6445-6455
39. Stumpo, D. J., Broxmeyer, H. E., Ward, T., Cooper, S., Hangoc, G., Chung, Y. J., Shelley, W. C., Richfield, E. K., Ray, M. K., Yoder, M. C., Aplan, P. D., and Blakeshear, P. J. (2009) Targeted disruption of Zfp36l2, encoding a CCCH tandem zinc finger RNA-binding protein, results in defective hematopoiesis. *Blood* **114**, 2401-2410
40. Blakeshear, P. J., Phillips, R. S., Ghosh, S., Ramos, S. B., Richfield, E. K., and Lai, W. S. (2005) Zfp36l3, a rodent X chromosome gene encoding a placenta-specific member of the Tristetraprolin family of CCCH tandem zinc finger proteins. *Biol Reprod* **73**, 297-307
41. Lai, W. S., Carballo, E., Thorn, J. M., Kennington, E. A., and Blakeshear, P. J. (2000) Interactions of CCCH zinc finger proteins with mRNA. Binding of

tristetraprolin-related zinc finger proteins to Au-rich elements and destabilization of mRNA. *J Biol Chem* **275**, 17827-17837

42. Choi, Y. J., Lai, W. S., Fedic, R., Stumpo, D. J., Huang, W., Li, L., Perera, L., Brewer, B. Y., Wilson, G. M., Mason, J. M., and Blackshear, P. J. (2014) The *Drosophila* Tis11 protein and its effects on mRNA expression in flies. *J Biol Chem* **289**, 35042-35060
43. Yeh, P. A., Yang, W. H., Chiang, P. Y., Wang, S. C., Chang, M. S., and Chang, C. J. (2012) *Drosophila* eyes absent is a novel mRNA target of the tristetraprolin (TTP) protein DTIS11. *Int J Biol Sci* **8**, 606-619
44. De, J., Lai, W. S., Thorn, J. M., Goldsworthy, S. M., Liu, X., Blackwell, T. K., and Blackshear, P. J. (1999) Identification of four CCCH zinc finger proteins in *Xenopus*, including a novel vertebrate protein with four zinc fingers and severely restricted expression. *Gene* **228**, 133-145
45. Blackshear, P. J., and Perera, L. (2014) Phylogenetic distribution and evolution of the linked RNA-binding and NOT1-binding domains in the tristetraprolin family of tandem CCCH zinc finger proteins. *J Interferon Cytokine Res* **34**, 297-306
46. Sandler, H., Kreth, J., Timmers, H. T., and Stoecklin, G. (2011) Not1 mediates recruitment of the deadenylase Caf1 to mRNAs targeted for degradation by tristetraprolin. *Nucleic Acids Res* **39**, 4373-4386
47. Fabian, M. R., Frank, F., Rouya, C., Siddiqui, N., Lai, W. S., Karetnikov, A., Blackshear, P. J., Nagar, B., and Sonenberg, N. (2013) Structural basis for the recruitment of the human CCR4-NOT deadenylase complex by tristetraprolin. *Nat Struct Mol Biol* **20**, 735-739
48. Puig, S., Askeland, E., and Thiele, D. J. (2005) Coordinated remodeling of cellular metabolism during iron deficiency through targeted mRNA degradation. *Cell* **120**, 99-110

49. Wells, M. L., Huang, W., Li, L., Gerrish, K. E., Fargo, D. C., Oszolak, F., and Blackshear, P. J. (2012) Posttranscriptional regulation of cell-cell interaction protein-encoding transcripts by Zfs1p in *Schizosaccharomyces pombe*. *Mol Cell Biol* **32**, 4206-4214
50. Sunnerhagen, P. (2002) Prospects for functional genomics in *Schizosaccharomyces pombe*. *Curr Genet* **42**, 73-84
51. Kanoh, J., Sugimoto, A., and Yamamoto, M. (1995) *Schizosaccharomyces pombe* zfs1+ encoding a zinc-finger protein functions in the mating pheromone recognition pathway. *Mol Biol Cell* **6**, 1185-1195
52. Beltraminelli, N., Murone, M., and Simanis, V. (1999) The *S. pombe* zfs1 gene is required to prevent septation if mitotic progression is inhibited. *J Cell Sci* **112 Pt 18**, 3103-3114
53. Cuthbertson, B. J., Liao, Y., Birnbaumer, L., and Blackshear, P. J. (2008) Characterization of zfs1 as an mRNA-binding and -destabilizing protein in *Schizosaccharomyces pombe*. *J Biol Chem* **283**, 2586-2594
54. Wolfe, K. H., and Shields, D. C. (1997) Molecular evidence for an ancient duplication of the entire yeast genome. *Nature* **387**, 708-713
55. Kellis, M., Birren, B. W., and Lander, E. S. (2004) Proof and evolutionary analysis of ancient genome duplication in the yeast *Saccharomyces cerevisiae*. *Nature* **428**, 617-624
56. Ma, Q., and Herschman, H. R. (1995) The yeast homologue YTIS11, of the mammalian TIS11 gene family is a non-essential, glucose repressible gene. *Oncogene* **10**, 487-494
57. Thompson, M. J., Lai, W. S., Taylor, G. A., and Blackshear, P. J. (1996) Cloning and characterization of two yeast genes encoding members of the CCCH class of

zinc finger proteins: zinc finger-mediated impairment of cell growth. *Gene* **174**, 225-233

58. Rutherford, J. C., Ojeda, L., Balk, J., Muhlenhoff, U., Lill, R., and Winge, D. R. (2005) Activation of the iron regulon by the yeast Aft1/Aft2 transcription factors depends on mitochondrial but not cytosolic iron-sulfur protein biogenesis. *J Biol Chem* **280**, 10135-10140
59. Puig, S., Vergara, S. V., and Thiele, D. J. (2008) Cooperation of two mRNA-binding proteins drives metabolic adaptation to iron deficiency. *Cell Metab* **7**, 555-564
60. Martinez-Pastor, M., Vergara, S. V., Puig, S., and Thiele, D. J. (2013) Negative feedback regulation of the yeast CTH1 and CTH2 mRNA binding proteins is required for adaptation to iron deficiency and iron supplementation. *Mol Cell Biol* **33**, 2178-2187
61. Wells, M. L., Washington, O. L., Hicks, S. N., Nobile, C. J., Hartooni, N., Wilson, G. M., Zucconi, B. E., Huang, W., Li, L., Fargo, D. C., and Blackshear, P. J. (2015) Post-transcriptional regulation of transcript abundance by a conserved member of the tristetraprolin family in *Candida albicans*. *Mol Microbiol* **95**, 1036-1053
62. Wells, M. L., Hicks, S. N., Perera, L., and Blackshear, P. J. (2015) Functional equivalence of an evolutionarily conserved RNA binding module. *J Biol Chem*
63. Lai, W. S., and Blackshear, P. J. (2001) Interactions of CCCH zinc finger proteins with mRNA: tristetraprolin-mediated AU-rich element-dependent mRNA degradation can occur in the absence of a poly(A) tail. *J Biol Chem* **276**, 23144-23154
64. Amann, B. T., Worthington, M. T., and Berg, J. M. (2003) A Cys3His zinc-binding domain from Nup475/tristetraprolin: a novel fold with a disklike structure. *Biochemistry* **42**, 217-221

65. Hudson, B. P., Martinez-Yamout, M. A., Dyson, H. J., and Wright, P. E. (2004) Recognition of the mRNA AU-rich element by the zinc finger domain of TIS11d. *Nat Struct Mol Biol* **11**, 257-264
66. Lai, W. S., Perera, L., Hicks, S. N., and Blackshear, P. J. (2013) Mutational and structural analysis of the tandem zinc finger domain of tristetraprolin. *J Biol Chem*
67. Blackshear, P. J., Lai, W. S., Kennington, E. A., Brewer, G., Wilson, G. M., Guan, X., and Zhou, P. (2003) Characteristics of the interaction of a synthetic human tristetraprolin tandem zinc finger peptide with AU-rich element-containing RNA substrates. *J Biol Chem* **278**, 19947-19955
68. Brewer, B. Y., Malicka, J., Blackshear, P. J., and Wilson, G. M. (2004) RNA sequence elements required for high affinity binding by the zinc finger domain of tristetraprolin: conformational changes coupled to the bipartite nature of Au-rich mRNA-destabilizing motifs. *J Biol Chem* **279**, 27870-27877
69. Nantel, A., Dignard, D., Bachewich, C., H Marcus, D., Marcil, A., Bouin, A. P., Sensen, C. W., Hogues, H., van het Hoog, M., Gordon, P., Rigby, T., Benoit, F., Tessier, D. C., Thomas, D. Y., and Whiteway, M. (2002) Transcription profiling of *Candida albicans* cells undergoing the yeast-to-hyphal transition. *Mol Biol Cell* **13**, 3452-3465
70. Bonhomme, J., Chauvel, M., Goyard, S., Roux, P., Rossignol, T., and d'Enfert, C. (2011) Contribution of the glycolytic flux and hypoxia adaptation to efficient biofilm formation by *Candida albicans*. *Mol Microbiol* **80**, 995-1013
71. McCourtie, J., and Douglas, L. J. (1984) Relationship between cell surface composition, adherence, and virulence of *Candida albicans*. *Infection and Immunity* **45**, 6-12
72. Mayer, F. L., Wilson, D., and Hube, B. (2013) *Candida albicans* pathogenicity mechanisms. *Virulence* **4**, 119-128

73. Fox, E. P., Bui, C. K., Nett, J. E., Hartooni, N., Mui, M. C., Andes, D. R., Nobile, C. J., and Johnson, A. D. (2015) An expanded regulatory network temporally controls *Candida albicans* biofilm formation. *Mol Microbiol* **96**, 1226-1239
74. Nobile, C. J., and Johnson, A. D. (2015) *Candida albicans* Biofilms and Human Disease. *Annu Rev Microbiol* **69**, 71-92
75. Noble, S. M., French, S., Kohn, L. A., Chen, V., and Johnson, A. D. (2010) Systematic screens of a *Candida albicans* homozygous deletion library decouple morphogenetic switching and pathogenicity. *Nat Genet* **42**, 590-598
76. Moon, A. F., Mueller, G. A., Zhong, X., and Pedersen, L. C. (2010) A synergistic approach to protein crystallization: combination of a fixed-arm carrier with surface entropy reduction. *Protein Sci* **19**, 901-913
77. Wilson, G. M., Sutphen, K., Chuang, K., and Brewer, G. (2001) Folding of A+U-rich RNA elements modulates AUF1 binding. Potential roles in regulation of mRNA turnover. *J Biol Chem* **276**, 8695-8704
78. Carballo, E., Lai, W. S., and Blackshear, P. J. (2000) Evidence that tristetraprolin is a physiological regulator of granulocyte-macrophage colony-stimulating factor messenger RNA deadenylation and stability. *Blood* **95**, 1891-1899
79. Blackshear, P. J. (2002) Tristetraprolin and other CCCH tandem zinc-finger proteins in the regulation of mRNA turnover. *Biochem Soc Trans* **30**, 945-952
80. Lai, W. S., Kennington, E. A., and Blackshear, P. J. (2003) Tristetraprolin and its family members can promote the cell-free deadenylation of AU-rich element-containing mRNAs by poly(A) ribonuclease. *Mol Cell Biol* **23**, 3798-3812
81. Lai, W. S., Kennington, E. A., and Blackshear, P. J. (2002) Interactions of CCCH zinc finger proteins with mRNA: non-binding tristetraprolin mutants exert an

inhibitory effect on degradation of AU-rich element-containing mRNAs. *J Biol Chem* **277**, 9606-9613

82. Day-Storms, J. J., Niranjanakumari, S., and Fierke, C. A. (2004) Ionic interactions between PRNA and P protein in *Bacillus subtilis* RNase P characterized using a magnetocapture-based assay. *RNA* **10**, 1595-1608
83. Gabaldón, T., and Pittis, A. A. (2015) Origin and evolution of metabolic sub-cellular compartmentalization in eukaryotes. *Biochimie* **119**, 262-268
84. Go, Y. M., and Jones, D. P. (2008) Redox compartmentalization in eukaryotic cells. *Biochim Biophys Acta* **1780**, 1273-1290
85. Bakheet, T., Williams, B. R., and Khabar, K. S. (2006) ARED 3.0: the large and diverse AU-rich transcriptome. *Nucleic Acids Res* **34**, D111-114
86. Haddad, J. J. (2002) Cytokines and related receptor-mediated signaling pathways. *Biochem Biophys Res Commun* **297**, 700-713
87. Locksley, R. M., Killeen, N., and Lenardo, M. J. (2001) The TNF and TNF receptor superfamilies: integrating mammalian biology. *Cell* **104**, 487-501
88. Bradley, J. R. (2008) TNF-mediated inflammatory disease. *J Pathol* **214**, 149-160
89. Francisco-Cruz, A., Aguilar-Santelises, M., Ramos-Espinosa, O., Mata-Espinosa, D., Marquina-Castillo, B., Barrios-Payan, J., and Hernandez-Pando, R. (2014) Granulocyte-macrophage colony-stimulating factor: not just another haematopoietic growth factor. *Med Oncol* **31**, 774
90. Carballo, E., Gilkeson, G. S., and Blackshear, P. J. (1997) Bone marrow transplantation reproduces the tristetraprolin-deficiency syndrome in recombination activating gene-2 (-/-) mice. Evidence that monocyte/macrophage

progenitors may be responsible for TNFalpha overproduction. *J Clin Invest* **100**, 986-995

91. Lai, W. S., Parker, J. S., Grissom, S. F., Stumpo, D. J., and Blakeshear, P. J. (2006) Novel mRNA targets for tristetraprolin (TTP) identified by global analysis of stabilized transcripts in TTP-deficient fibroblasts. *Mol Cell Biol* **26**, 9196-9208
92. Lai, W. S., Carrick, D. M., and Blakeshear, P. J. (2005) Influence of nonameric AU-rich tristetraprolin-binding sites on mRNA deadenylation and turnover. *J Biol Chem* **280**, 34365-34377
93. Arino, J., Ramos, J., and Sychrova, H. (2010) Alkali metal cation transport and homeostasis in yeasts. *Microbiol Mol Biol Rev* **74**, 95-120
94. Kotta-Loizou, I., Giaginis, C., and Theocharis, S. (2014) Clinical significance of HuR expression in human malignancy. *Med Oncol* **31**, 161
95. Scheiba, R. M., de Opakua, A. I., Diaz-Quintana, A., Cruz-Gallardo, I., Martinez-Cruz, L. A., Martinez-Chantar, M. L., Blanco, F. J., and Diaz-Moreno, I. (2014) The C-terminal RNA binding motif of HuR is a multi-functional domain leading to HuR oligomerization and binding to U-rich RNA targets. *RNA Biol* **11**, 1250-1261
96. DeMaria, C. T., Sun, Y., Wagner, B. J., Long, L., and Brewer, G. A. (1997) Structural determination in AUF1 required for high affinity binding to A + U-rich elements. *Nucleic Acids Symp Ser*, 12-14
97. Zucconi, B. E., Ballin, J. D., Brewer, B. Y., Ross, C. R., Huang, J., Toth, E. A., and Wilson, G. M. (2010) Alternatively expressed domains of AU-rich element RNA-binding protein 1 (AUF1) regulate RNA-binding affinity, RNA-induced protein oligomerization, and the local conformation of bound RNA ligands. *J Biol Chem* **285**, 39127-39139

98. Kebaara, B. W., and Atkin, A. L. (2009) Long 3'-UTRs target wild-type mRNAs for nonsense-mediated mRNA decay in *Saccharomyces cerevisiae*. *Nucleic Acids Res* **37**, 2771-2778
99. Burnette, W. N. (1981) "Western Blotting": Electrophoretic transfer of proteins from sodium dodecyl sulfate-polyacrylamide gels to unmodified nitrocellulose and radiographic detection with antibody and radioiodinated protein A. *Analytical Biochemistry* **112**, 195-203
100. Pedro-Segura, E., Vergara, S. V., Rodriguez-Navarro, S., Parker, R., Thiele, D. J., and Puig, S. (2008) The Cth2 ARE-binding protein recruits the Dhh1 helicase to promote the decay of succinate dehydrogenase SDH4 mRNA in response to iron deficiency. *J Biol Chem* **283**, 28527-28535

## Biography

### Onica Leigh Washington

Onica Leigh Washington was born to Charles and Onetha Washington on December 27, 1985 in Charleston, SC. In 2004, she started her undergraduate career at the College of Charleston, Charleston, SC. In 2008, she graduated from the College of Charleston with a Bachelor of Science in Biochemistry and a Bachelor of Arts in Chemistry. She entered the Medical University of South Carolina to obtain a doctorate of medicine. However, she decided to put her medical career on hold and seek a doctorate in Biochemistry. In August 2010, she matriculated to Duke and joined the Blackshear lab in October of 2012.

#### **Publications:**

Wells ML, Washington OL, Hicks SN, Nobile CJ, Hartooni N, Wilson GM, Zucconi BE, Huang W, Li L, Fargo DC, Blackshear PJ. Post-transcriptional regulation of transcript abundance by a conserved member of the tristetraproline family in *C. albicans*. *Mol Microbiol.* 2015 Mar; 95(6):1036-53. doi: 10.1111/mmi.12913. Epub 2015 Jan 30.